Technical University of Crete

School of Mineral Resource Engineering

Master Thesis

Postgraduate Program in Petroleum Engineering

Critical evaluation of wax appearance temperature (WAT), wax disappearance temperature (WDT) and comparison with various thermodynamic models' predictions

Author

Predrag Mirkovic

Supervisor:

Prof. Nikolaos Pasadakis

Scientific Advisors:

Prof. Bahman Tohidi

Dr. Ramin Mousavi

Examination Committee:

1. Prof. Nikolaos Pasadakis

2. Dr. Dimitris Marinakis

3. Prof. Bahman Tohidi

This thesis is submitted in fulfillment of the requirements for the Master's degree of Petroleum Engineering in the School of Mineral Resources Engineering at Technical University of Crete

Chania, September 2021.

The MSc Program in Petroleum Engineering of the Technical University of Crete, was attended and completed by Mr. Predrag Mirković, due to the EKO Serbia A. D. Member of Hellenic Petroleum Group Scholarship award

Abstract

Wax deposition is one of the problems flow assurance engineers deal with during oil production and transportation. Wax deposition usually occurs during the cooling of the reservoir fluid when heavy paraffinic compounds precipitate into a solid-state deposit. If the wax formed is not removed mechanically on time or the appearance of the wax is not avoided using certain chemicals (inhibitors), the precipitated wax within transporting pipeline or producing well might cause blockage and result in huge operational costs. Therefore, predicting the wax appearance conditions is of very high importance in flow assurance engineering. Once the phase behavior of the fluid is predicted, we can avoid wax deposition by keeping the fluid apart from wax stability conditions.

The purpose of this work is to critically evaluate wax appearance temperature (temperature where wax starts to form under certain pressure), wax disappearance temperature (temperature where wax starts to dissolve back to the oil) and wax content. For this purpose, three PVT simulation software packages were used: Calsep`s PVTsim, KBC's Multiflash and Hydrafact's HydraFLASH. The results obtained from the models were compared to the experimental data gathered from the literature.

Contents

Abstract 3
1. Introduction 8
2. Wax precipitation and deposition 9
   2.1. Wax forming molecules 9
   2.2. Wax deposition and precipitation 11
3. Wax Concepts 12
   3.1. Wax appearance temperature 12
   3.2 . Wax disappearance temperature 13
   3.3 Wax content 13
4. Wax Models 13
5. Experimental data and analysis of live oils 15
6. Experimental data and analysis of dead oils 33
7. Experimental data and analysis of wax content 46
8. Conclusions 62
References 63
9. APPENDIX 64

List of Figures

Figure 1 Deep sea oil exploitation (Figure obtained from strukts.com) 8
Figure 2 Wax deposition in pipeline (Singh, et al. 2000) 9
Figure 3 Wax forming molecules (Pederson, et al. 2003) 10
Figure 4 Paraffins branching (Pederson, et al. 2003) 11
Figure 5 Wax phase boundary for Fluid 1 calculated by HydraFLASH 17
Figure 6 Wax phase boundary for Fluid 1 calculated in Multiflash 17
Figure 7 Wax phase boundary for Fluid 1 calculated by PVTsim 18
Figure 8 Wax phase boundary for Fluid 2 calculated by Multiflash 19
Figure 9 Wax phase boundary for Fluid 2 calculated by HydraFLASH 20
Figure 10 Wax phase boundary for Fluid 2 calculated by Multiflash 20
Figure 11 Wax phase boundary for Fluid 2 calculated by PVTsim 21
Figure 12 Wax phase boundary for Fluid 3 calculated by HydraFLASH 23
Figure 13 Wax phase boundary for Fluid 3 calculated by Multiflash 24
Figure 14 Wax phase boundary for Fluid 3 calculated by PVTsim 25
Figure 15 Wax phase boundary for Fluid 4 calculated by HydraFLASH 27
Figure 16 Wax phase boundary for Fluid 4 calculated by Multiflash 28
Figure 17 Wax phase boundary for Fluid 4 calculated by PVTsim 29
Figure 18 Wax phase boundary for Fluid 5 calculated by HydraFLASH 30
Figure 19 Wax phase boundary for Fluid 5 calculated by Multiflash 31
Figure 20 Wax phase boundary for Fluid 5 calculated by PVTSIM 32
Figure 21 Wax phase boundary for Fluid 1 calculated by HydraFLASH 35
Figure 22 Wax phase boundary for Fluid 1 calculated by Multiflash 36
Figure 23 Wax phase boundary for Fluid 1 calculated by PVTsim 37
Figure 24 Wax phase boundary for Fluid 2 calculated by HydraFLASH 38
Figure 25 Wax phase boundary for Fluid 2 calculated by Multiflash 38
Figure 26 Wax phase boundary for Fluid 2 calculated by PVTsim 39
Figure 27 Wax phase boundary for Fluid 10 calculated by HydraFLASH 41
Figure 28 Wax phase boundary for Fluid 10 calculated by Multiflash 41
Figure 29 Wax phase boundary for Fluid 10 calculated by PVTsim 42
Figure 30 Wax phase boundary for Fluid 11 calculated by HydraFLASH 43
Figure 31 Wax phase boundary for Fluid 11 calculated by Multiflash 44
Figure 32 Wax phase boundary for Fluid 11 calculated by PVTsim 45
Figure 33 Wax precipitation curve for Fluid 10 by HydraFLASH 46
Figure 34 Wax precipitation curve for Fluid 10 calculated by Multiflash 47
Figure 35 Wax precipitation curve for Fluid 10 calculated by PVTsim 48
Figure 36 Wax precipitation curve for Fluid 11 calculated by HydraFLASH 49
Figure 37 Wax precipitation curve for Fluid 11 calculated by Multiflash 49
Figure 38 Wax precipitation curve for Fluid 11 calculated by PVTsim 50
Figure 39 Wax precipitation curve for Fluid 12 calculated by HydraFLASH 51
Figure 40 Wax precipitation curve for Fluid 12 calculated by Multiflash 52
Figure 41 Wax precipitation curve for Fluid 12 calculated by PVTsim 52
Figure 42 Wax precipitation curve for Fluid 13 calculated by HydraFLASH 53
Figure 43 Wax precipitation curve for Fluid 13 calculated in Multiflash 54
Figure 44 Wax precipitation curve for Fluid 13 calculated by PVTsim 55
Figure 45 Wax precipitation curve for Fluid 14 calculated by HydraFLASH 56

Figure 46 Wax precipitation curve for Fluid 14 calculated by PVTsim..... 56
Figure 47 Wax precipitation curve for Fluid 14 calculated by PVTsim..... 57
Figure 48 Wax precipitation curve for Fluid 15 calculated by HydraFLASH 58
Figure 49 Wax precipitation curve for Fluid 15 calculated by Multiflash 58
Figure 50 Wax precipitation curve for Fluid 15 calculated by PVTsim..... 59
Figure 51 Wax precipitation curve for Fluid 16 calculated by HydraFLASH 60
Figure 52 Wax precipitation curve for Fluid 16 calculated by Multiflash 60
Figure 53 Wax precipitation curve for Fluid 16 calculated by PVTsim..... 61

Figure A 1 Wax phase boundary for Fluid 3 calculated by HydraFLASH 64
Figure A 2 Wax phase boundary for Fluid 3 calculated by Multiflash 64
Figure A 3 Wax phase boundary for Fluid 3 calculated by PVTsim..... 65
Figure A 4 Wax phase boundary for Fluid 4 calculated by HydraFLASH 65
Figure A 5 Wax phase boundary for Fluid 4 calculated by Multiflash 66
Figure A 6 Wax phase boundary for Fluid 4 calculated by PVTsim..... 66
Figure A 7 Wax phase boundary for Fluid 5 calculated by HydraFLASH 67
Figure A 8 Wax phase boundary for Fluid 5 calculated by Multiflash 67
Figure A 9 Wax phase boundary for Fluid 5 calculated by PVTsim..... 68
Figure A 10 Wax phase boundary for Fluid 6 calculated by HydraFLASH 68
Figure A 11 Wax phase boundary for Fluid 6 calculated by Multiflash 69
Figure A 12 Wax phase boundary for Fluid 6 calculated by PVTsim..... 69
Figure A 13 Wax phase boundary for Fluid 7 calculated by HydraFLASH 70
Figure A 14 Wax phase boundary for Fluid 7 calculated by Multiflash 70
Figure A 15 Wax phase boundary for Fluid 7 calculated by PVTsim..... 71
Figure A 16 Wax phase boundary for Fluid 12 calculated by HydraFLASH 71
Figure A 17 Wax phase boundary for Fluid 12 calculated by Multiflash 72
Figure A 18 Wax phase boundary for Fluid 12 calculated by PVTsim..... 72
Figure A 19 Wax phase boundary for Fluid 13 calculated by HydraFLASH 73
Figure A 20 Wax phase boundary for Fluid 13 calculated by Multiflash 73
Figure A 21 Wax phase boundary for Fluid 13 calculated by PVTsim..... 74
Figure A 22 Wax phase boundary for Fluid 14 calculated by HydraFLASH 74
Figure A 23 Wax phase boundary for Fluid 14 calculated by Multiflash 75
Figure A 24 Wax phase boundary for Fluid 14 calculated by PVTsim..... 75
Figure A 25 Wax phase boundary for Fluid 15 calculated by HydraFLASH 76
Figure A 26 Wax phase boundary for Fluid 15 calculated by Multiflash 76
Figure A 27 Wax phase boundary for Fluid 15 calculated by PVTsim..... 77
Figure A 28 Wax phase boundary for Fluid 16 calculated by HydraFLASH 77
Figure A 29 Wax phase boundary for Fluid 16 calculated by Multiflash 78
Figure A 30 Wax phase boundary for Fluid 16 calculated by PVTsim..... 78

List of Tables

Table 1 Composition of Fluids 1 and 2 15
Table 2 Wax content and saturation properties for Fluids 1 and 2 16
Table 3 Experimental wax disappearance temperature for Fluid 1 16
Table 4 Experimental wax disappearance temperature for Fluid 2 18
Table 5 Composition of Fluid 3 21
Table 6 Wax content and saturation properties for Fluid 3 22
Table 7 Experimental wax disappearance temperature for Fluid 3 22
Table 8 Compositions of Fluids 4 and 5 25
Table 9 Assumed wax content for Fluids 4 & 5 and heavy end properties. 26
Table 10 Experimental WDT and saturation properties for Fluid 4 27
Table 11 Experimental WDT and saturation properties for Fluid 5 29
Table 12 Compositions of 9 dead oils and the experimental WDT 33
Table 13 Natural gas composition 34
Table 14 Compositions of the 7 dead oils and the experimental WDT 40
Table 15 Experimental wax content and WDT for Fluid 10 46
Table 16 Experimental wax content and WDT for Fluid 11 48
Table 17 Experimental wax content and WDT for Fluid 12 50
Table 18 Experimental wax content and WDT for Fluid 13 53
Table 19 Experimental wax content and WDT for Fluid 14 55
Table 20 Experimental wax content and WDT for Fluid 15 57
Table 21 Experimental wax content and WDT for Fluid 16 59

1. Introduction

The waxy components of crude oils, also known as paraffins, represent a group of n-alkanes with carbon numbers that are usually greater than 20 (Lee, H. S. 2008). At the reservoir conditions temperatures are relatively high and the waxy compounds are usually dissolved in the oil. As the oil is produced it leaves the reservoir and on the path towards processing facilities its temperature decreases, if the temperature decrease is large enough it can fall below the wax appearance temperature. If the conditions are favourable, the waxy components might precipitate and form solids.

Wax compounds can form solid deposits on the tubing, pipeline, or any processing equipment. Until the 20th century the wax problems usually occurred in the onshore oil production. (Lee, H. S. 2008) As the oil production took place on the land, accessing the problem of wax deposition was quite easy by heating the pipeline or using mechanical assistance to remove the wax deposits. However, with the technology advance and due to depletion of the onshore reservoirs, the oil production started shifting towards offshore reservoirs, see Figure 1.

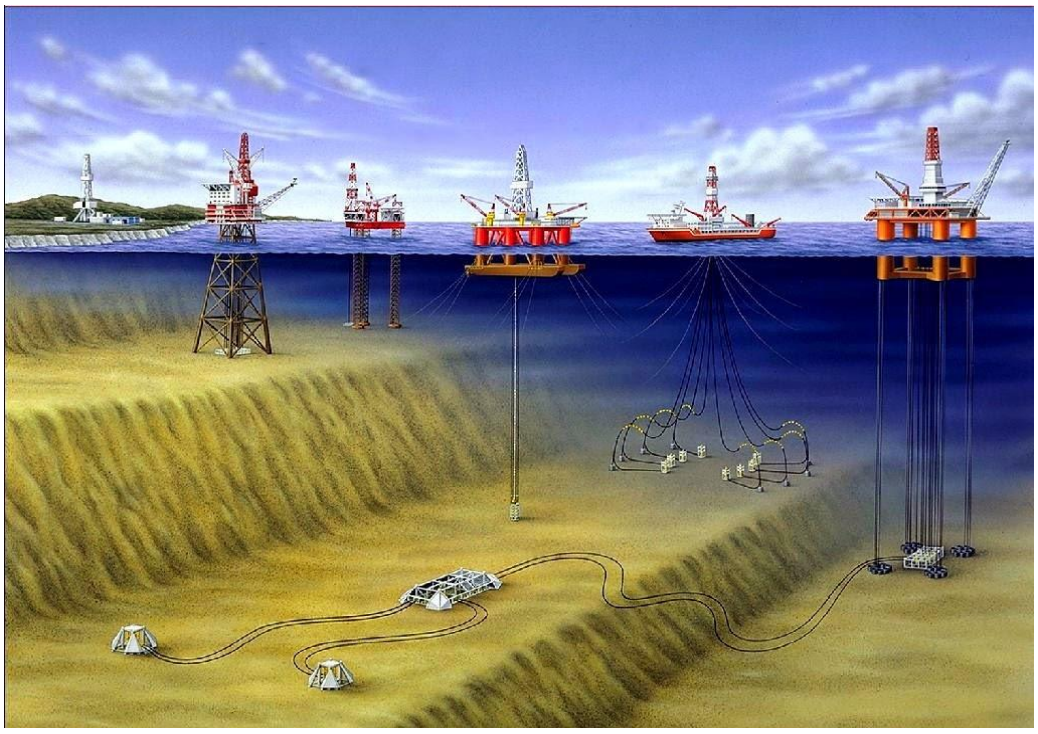

Figure 1 Deep sea oil exploitation (Figure obtained from strukts.com)

Once the production in deep sea reservoirs took place, the problems with wax deposits became more challenging as the transportation of the petroleum fluids took place in pipelines ranging from tens to hundreds of kilometers before reaching surface facilities (Golczynski & Kempton, 2006).

As the produced oil is transported through the pipeline which is located on the ocean floor where the water temperature is around 4 °C, it causes the oil coming out of reservoir which has significantly higher temperature (70 °C +) to cool down. While the oil temperature is decreasing

the wax components might precipitate out of the oil and form significant amount of deposits on the pipe wall as it can be seen on Figure 2.

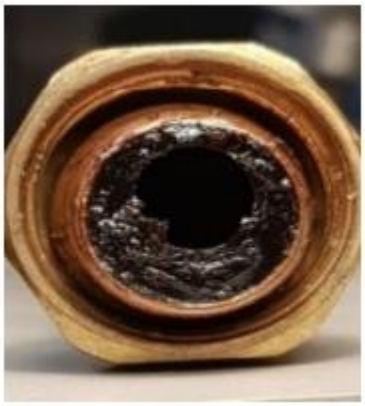

Figure 2 Wax deposition in pipeline (Singh, et al. 2000)

If wax deposition occurs in the pipeline, it could result in reduction of the effective pipe diameter and sometimes complete blockage, all of which require series of technical solutions which slow down the production and increases the overall cost of exploration.

There are numerous methods used to solve the problem of wax deposition. Some methods focus on removing the wax once it has deposited and others are attempting to prevent wax from depositing. In some cases, removing and preventing the deposition is possible using the same method. (Jonathan, 2004).

The most used method to remove the wax deposition is a mechanical method called pigging. Pig is a solid piston with a diameter smaller than the inner diameter of the pipeline. It passes through the pipe by a pressure differential. While the pig is moving through the pipeline it scrapes the wax deposits. In cases however, pig might get stuck inside the pipeline and makes the issue even worse.

Apart from pigging, common methods used are pipeline insulation and pipeline burial where both methods have as a goal to conserve the heat of the oil during transportation through cold surroundings. Also, certain wax inhibitors which contain crystal modifiers can be used to prevent the formation of large wax molecules by deliberately bonding to the wax crystals and making the further growth harder (Jonathan, 2004).

All mentioned methods for resolving wax deposition problem, require additional operating costs, therefore, it is important to have sufficient understanding of the physics and chemistry of wax precipitation/deposition to keep the production running and to minimize the capital and operating costs.

2. Wax precipitation and deposition

In the petroleum industry, wax is a general term used to describe all kinds of solids being either precipitated during cooling or dissolved in the oil while heat applied (Hoopanah, 2017).

2.1. Wax forming molecules

The wax particles are essentially normal paraffins and slightly branched paraffins, but also naphthene's with long paraffinic chains that may take part in wax formation. Typical wax-forming molecules can be seen in Figure 3.

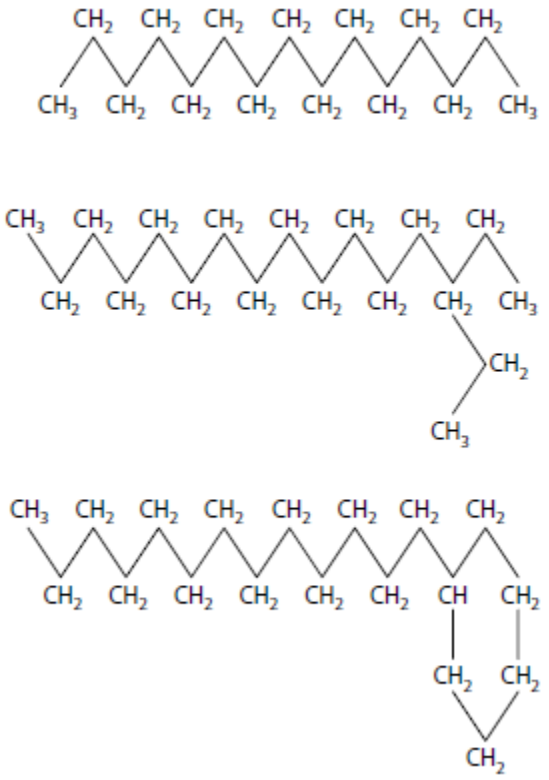

Figure 3 Wax forming molecules (Pederson, et al. 2003)

The saturated hydrocarbons contain only single bonds between carbon atoms. They are called saturated because each carbon atom is bonded to as many hydrogen atoms as possible. In other words, the carbon atoms are saturated with hydrogen. They can be linear or branched and are usually dissolved in oil at reservoir conditions due to high temperature, but they precipitate under certain conditions. The process of precipitation from the oil and forming of solid phase is generally called crystallization.

The solid wax phase typically consists of C_{20}-C_{50} paraffins. (Bishop et al. 1995). The reason why solid wax phase consists of those paraffins is due to paraffin concentration pattern. The higher the molecular weight fractions are, the branching is greater, as it can be seen on Figure 4.

The probability of branched molecules forming solid structure is less, while the paraffins with no or very little branching are found in significant concentrations. However, the amount of lighter components is limited due to their low melting temperatures.

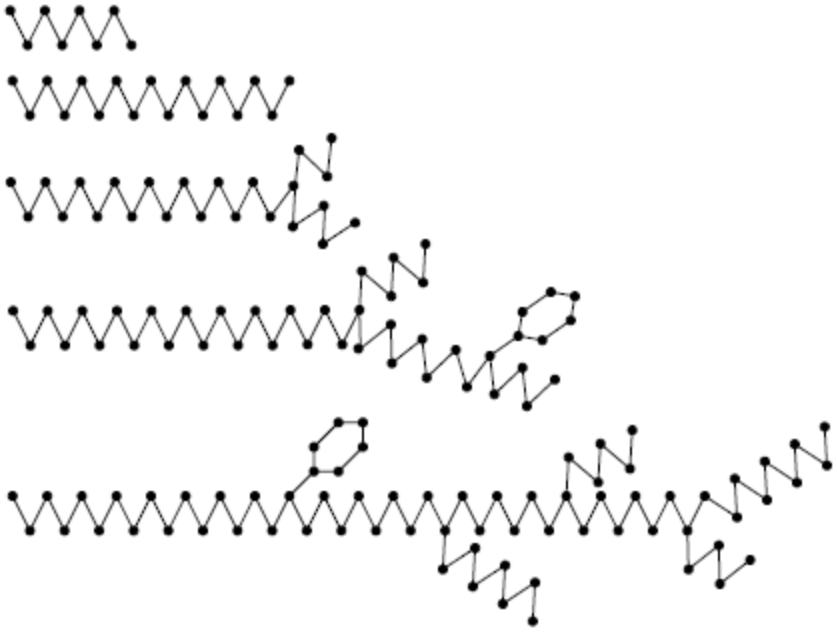

Figure 4 Paraffins branching (Pederson, et al. 2003)

As the temperature decreases the molecules move closer to each other due to van der Waals forces. Consequently, the distance between molecules is reduced and the crystallization process starts. Crystallization is initiated whenever the waxy components solubility limit is approached, which is in accordance with the formation of unstable molecule clusters known as nucleation (Hoopanah, 2017). As these clusters are growing larger, they tend to reach a critical size called nuclei and they become stable.

Nuclei are the smallest stable particles of wax crystal, and they are having a higher magnitude of attractive forces. As they provide suitable sites, they attract other molecules and wax precipitates.

In order for crystals to be formed it is essential for a small solid particle to exist as a nucleation site, whether it is found in oil and forms a homogenous nucleation or as tiny elements from production equipment material or reservoir rock as impurities which leads to forming of heterogenous nucleation.

2.2. Wax deposition and precipitation

Terms wax deposition and wax precipitation are sometimes used for explaining the wax appearance in production or transportation lines, however, those two phenomena are completely different. When a system is at certain conditions, the wax crystalizes and forms a solid structure which is called wax precipitation. Wax precipitation might occur due to oil temperature dropping below the wax appearance temperature, system pressure drop where fluid might encounter wax phase boundary or the evaporation of lighter components.

Wax deposition on the other hand occurs after the wax precipitation. Some of the mechanisms of wax deposition are molecular diffusion, gravity settling, shear dispersion, Brownian diffusion, etc. (Hoopanah, 2017).

The predominant mechanism is the molecular diffusion. While the oil is flowing through the pipe, regardless of flow conditions, a thin laminar sublayer is formed next to the wall of the pipe. The pipe wall temperature has the most impact on that layer and in case the temperature of the pipe wall is lower than the wax appearance temperature the precipitation takes place. In other words, if the conditions are favorable a thin layer of wax deposition is formed. If the oil within center of the pipe is observed, then the concentration of wax particles is much higher in the center of the pipe than on the walls of the pipe. When the thin layer of wax is formed the temperature gradient across the pipe wall enhances the concentration gradient that may cause the diffusion of wax from the fluid in center of the pipe with higher concentration of wax particles towards the wall of the pipe where the concentration of dissolved wax is lower (Hoopanah, 2017).

Oil composition is another factor that influences wax deposition as altering the initial reservoir composition of the oil might encourage wax precipitation and after that wax deposition. Crude oil consists of saturates, aromatics, resins and asphaltenes (SARA). Saturates are distinguishable from other classes, due to their straight chain (n-paraffins) structure. Therefore, they crystalize easier compared to other petroleum fractions.

High molecular weight paraffins tend to be the main reason of wax deposition (Lee, 2008). Some light saturates might serve as solvents for high molecular weight saturates at the desired temperature as they change the solubility which can solve the wax problems sometimes. Other paraffins such as isoparaffins and cycloparaffins are less flexible in comparison to n-paraffins and they form unstable wax depositions.

3. Wax Concepts

Some of wax parameters that are accessed at early stages of flow assurance analysis are Wax Appearance Temperature (WAT), Wax Disappearance Temperature (WDT), and wax content. Values of mentioned parameters are obtained experimentally.

3.1. Wax appearance temperature

As the crude oil is cooled down the fluid reaches the solubility limit for wax, at which point the wax, whereat particles start to crystalize and precipitate. The temperature at which the crystallization happens is referred to as wax appearance temperature. If the system is kept above the wax appearance temperature, then no wax precipitation or deposition will happen, in the other hand if wax appearance temperature is increased due certain factors, then the wax deposition tends to increase as well. (Hoopanah, 2017).

There are numerous methods used to measure the wax appearance temperature. The controlled cooling of the examined fluid is the most common method. They are based on the changes in the physical properties of the oil during the formation of solid wax crystals. The accuracy of WAT measurements depends on the technique and the quality of the analyzed sample, whether it is contaminated or not.

Most of the techniques used for measuring wax appearance temperature have different detection qualities based on various physical properties of the sample. Method often used is differential scanning calorimetry (DSC) (Pederson et al, 2003).

When wax is forming there is certain amount of heat released (exothermic process), in the other hand for wax to be dissolved again, the procedure requires heat (endothermic process). Once the oil sample is cooled down at a constant rate, above the wax appearance temperature the amount of heat that must be removed from the sample is almost constant, while at the wax appearance temperature the amount of heat to continue the constant cooling rate increases noticeably (Pederson et al, 2003). The increase in amount of heat required to be taken from the fluid is the heat released because of the solidification.

Another method is viscometry, when wax precipitates it increases the viscosity of the oil, therefore, wax appearance temperature can be observed from measurements of viscosity versus temperature. There are also microscopic techniques where the measurement is done by observing with the microscope until the first wax particles are seeable. Other techniques such as cross-polarized microscopy (CPM) or Crystal Microbalance (QCM) are also widely used in the industry.

3.2. Wax disappearance temperature

Wax disappearance temperature is the temperature that is closer to thermodynamic equilibrium point and generally it obtains higher values than wax appearance temperature. Wax disappearance temperature is considered as temperature at which all precipitated wax dissolves back in solution when the mixture is heated from the temperature below wax appearance temperature.

3.3 Wax content

Wax content represents the amount of wax that will precipitate in an excess amount of solvents such as dichloromethane, ethanol, diethyl ether, etc. at a very low temperature such as -20 °C to -30 °C, using a combination of distillation and extraction methods (Hoopanah, 2017).

4. Wax Models

In this work three commerciall software packages are compared in predicting the behavior of waxy oils. The software used are Calsep`s PVTsim, KBC's Multiflash and Hydrafact's HydraFLASH.

HydraFLASH is a commercial PVT software which is created by Hydrafact Ltd. group at Heriot-Watt University in Edinburgh, Scotland. It is a gas hydrate and thermodynamic prediction software which is designed for the calculation of the phase equilibrium and physical properties of petroleum reservoir fluids over a big range of pressure and temperature conditions (Hydrafact, 2021). HydraFLASH allows modelling of multicomponent systems, multiphase aqueous and hydrocarbon systems in the existence of hydrates and inhibitors.

For this work modeling in HydraFLASH was completed using Simplified Cubic Plus Association (sCPA) equation of state and the Coutinho wax model.

Multiflash is an advanced PVT simulator software which is developed by KBC, for modelling and simulating the phase behavior of complex mixtures and pure components. For

purposes of this work Multiflash was used for wax modeling. Multiflash use the CPA Infochem (Cubic-Plus-Association) equation of state set by default and the Coutinho wax model.

The Cubic-Plus-Association (CPA) EoS is, as the name suggests, a combination of the classical cubic EoS and Chapman's association term originally developed for PC SAFT equation. In terms of the reduced residual Helmholtz, CPA is given as a physical contribution (cubic EoS) and chemical contribution (association). Unfortunately, the addition of the association term means that CPA is no longer cubic in volume like the classical cubics. Additionally, there are five tuning parameters for CPA, which are adjusted with experimental liquid density and vapor pressure data of pure compounds (like PC-SAFT). Classical cubic equations have three parameters to fit to the critical point. Thus, CPA improves significantly on the liquid-volume predictions produced by the cubics, partly because of a retuning of the model parameters and partly because of the additional association term and more fitting parameters. (Vargas, F., Tavakkoli, M. 2018).

PVTsim is a modular PVT simulation tool which provides flow assurance through EoS modeling, training, and fluid characterization. It is used for models simulation for the oil and gas industry which helps with collection of extensive data material, regression algorithms, and input data for pipeline, reservoir, and process simulators.

PVTsim simulator does not use the sCPA equation of state as a thermodynamic model. The default EoS in PVTsim is the SRK Peneloux and it was used for this work together with wax model Pedersen (1995) extended as proposed by Rønningsen et al. (1997).

SRK stands for Soave‑Redlich‑Kwong Equation. Soave (1972) suggested that the term $\frac{a}{\sqrt{T}}$ in RK equation should be replaced by more general temperature-depended term, a(T), giving the SRK equation the following form

$$P = \frac{RT}{V-b} - \frac{a(T)}{V(V+b)},$$

Where P is system pressure (psia), T is the system temperature (°R), R is the gas constant (psi*ft^3·lbmol^{-1}·°R^{-1}), V is the volume (ft^3), a is the attraction parameter and b is the repulsion parameter.

In this form SRK was limited to phase equilibrium and gas-phase density calculations. Because of poor density predictions SRK was applied with additional liquid density correlations, which caused the problem near critical systems where it is difficult to distinguish between gas and liquid phase. Penelux et al. suggested SRK modification with a volume translation parameter (Pederson et al, 2003). The improved version of SRK equation, SRK-Penelux is in the following form:

$$P = \frac{RT}{V-b} - \frac{a(T)}{(V+c)(V+b)},$$

Where the parameter c is called a volume translation or volume shift parameter. It has no influence on gas-liquid equilibrium calculation results. It is only influencing molar volumes and phase densities and not phase equilibrium.

5. Experimental data and analysis of live oils

In this work 5 different live oils were examined for comparison of 3 commercial software's. In Table 1 compositions of Fluid 1 (Pederson et al, 2003) and Fluid 2 (Mahabadian, 2016) are presented.

Table 1 Composition of Fluids 1 and 2

Component	Fluid 1 (Mole %)	Fluid 2 (Mole %)
Carbon Dioxide	0.3	0.49
Nitrogen	0.39	1.16
Methane	40.71	31.26
Ethane	7.71	2.03
Propane	8.05	0.68
i-Butane	1.21	0.2
n-Butane	4.13	0.68
i-Pentane	1.41	0.86
n-Pentane	2.18	1.47
C_6	0.0	3.94
C_7	2.83	8.55
C_8	4.33	10.59
C_9	4.36	7.1
C_{10}	3.12	5.26
C_{11}	2.5	3.9
C_{12}	1.93	3.05
C_{13}	1.71	2.63
C_{14}	1.61	2.63
C_{15}	1.24	2.18
C_{16}	1.01	1.73
C_{17}	1.0	1.4
C_{18}	0.93	1.35
C_{19}	0.61	1.13
C_{20+}	6.72	5.76

Mw. C_{20+}	453	384
Sp. g. C_{20+}	0.918	0.88

To perform the wax characterization in HydraFLASH and Multiflash the wax content (mass %) must be specified in order for the software to perform the characterization. As wax content was not reported in literature for these two fluids, the wax content has been assumed and the values of assumed wax content are presented in Table 2. For Fluids 1&2 saturation properties were reported in literature and they are presented in the same Table.

Table 2 Wax content and saturation properties for Fluids 1 and 2

Fluid	Wax content (wt. %)	Bubble point (bara)	T (°C)
1	5.5	200	97.5
2	3	94	15

Once the fluid has been characterized, in order for the models to be accountable, they had to be tuned with experimental saturation and wax data. The data used to tune the wax models are the wax disappearance temperatures which represent the equilibrium point.

For Fluid 1 there has been only 1 reported experimental value of wax disappearance temperature and it is presented in the Table 3.

Table 3 Experimental wax disappearance temperature for Fluid 1

WDT	P (bara)
52	1.0135

Once the model has been characterized and tuned, the calculations are performed with all 3 simulators. The wax phase boundary for Fluid 1 has been presented in Figure 5 for HydraFLASH, Figure 6 for Multiflash and Figure 7 for PVTsim.

From the Figures 5-7 it can be seen that all 3 simulators tune the model accordingly and they report the wax disappearance temperature of 52 °C at atmospheric pressure. However, it can be observed that the simulators report differences in the wax phase envelope.

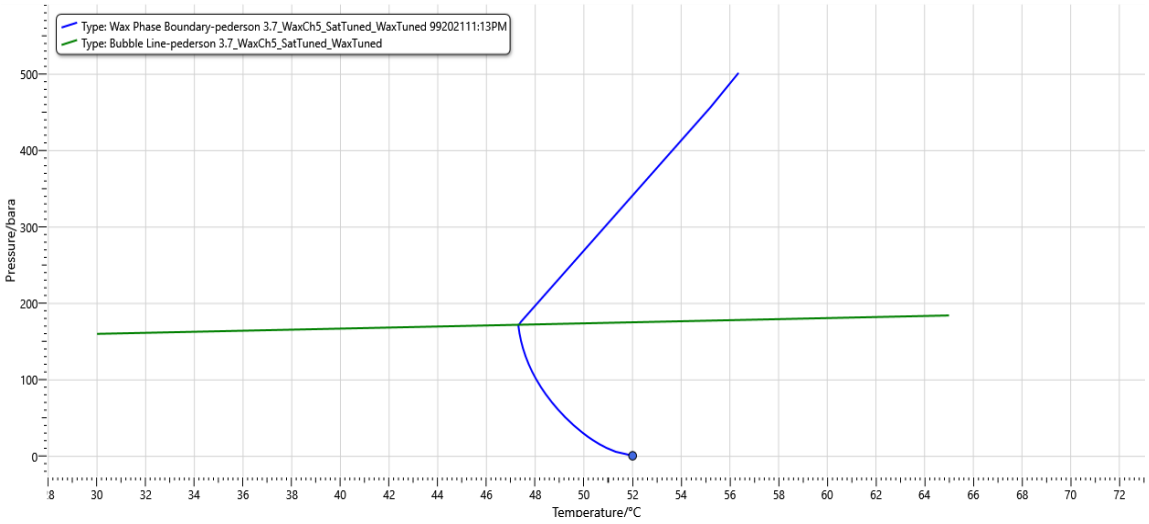

Figure 5 Wax phase boundary for Fluid 1 calculated by HydraFLASH

From the Figure 5, it can be noted that the lowest temperature at which we could operate and not encounter wax phase boundary is 47.5 °C around 160 bara also, as a point of reference at 200 bara we would enter wax phase boundary at temperature of 48 °C.

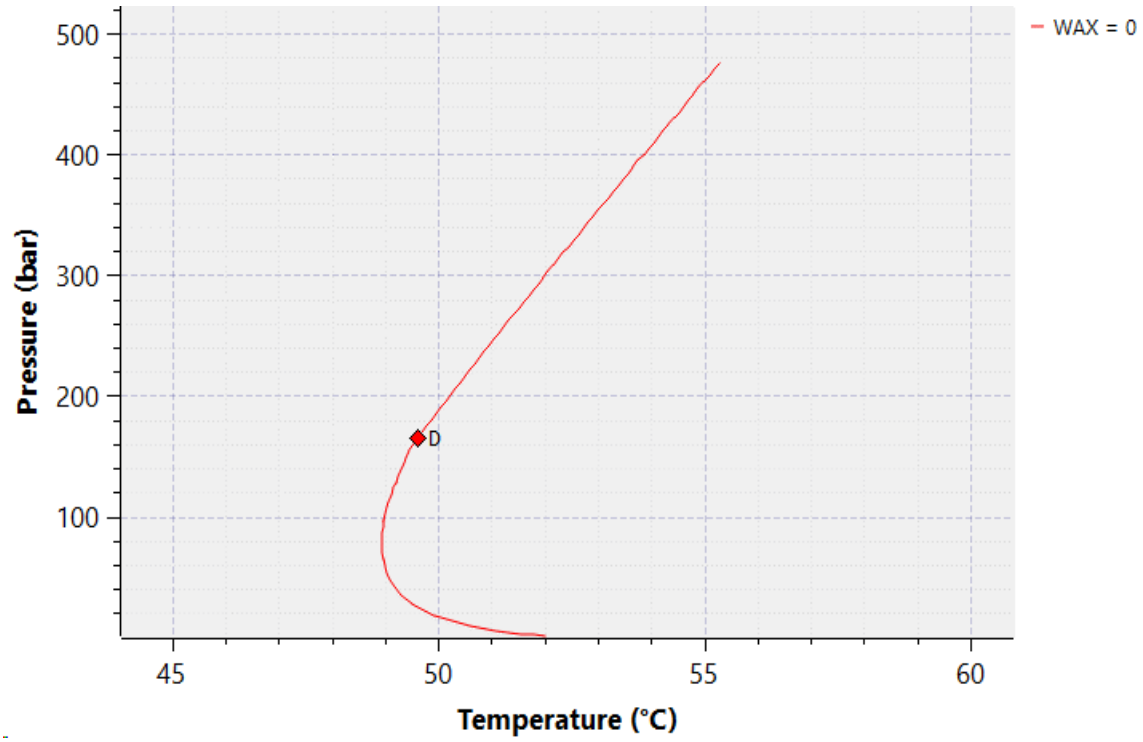

Figure 6 Wax phase boundary for Fluid 1 calculated in Multiflash

From the Multiflash wax phase boundary it can be observed that the lowest operating temperature before entering wax phase boundary is 49 °C at around 70 bara and as a point of reference at 200 bara the temperature at which we enter wax phase boundary is 50.3 °C

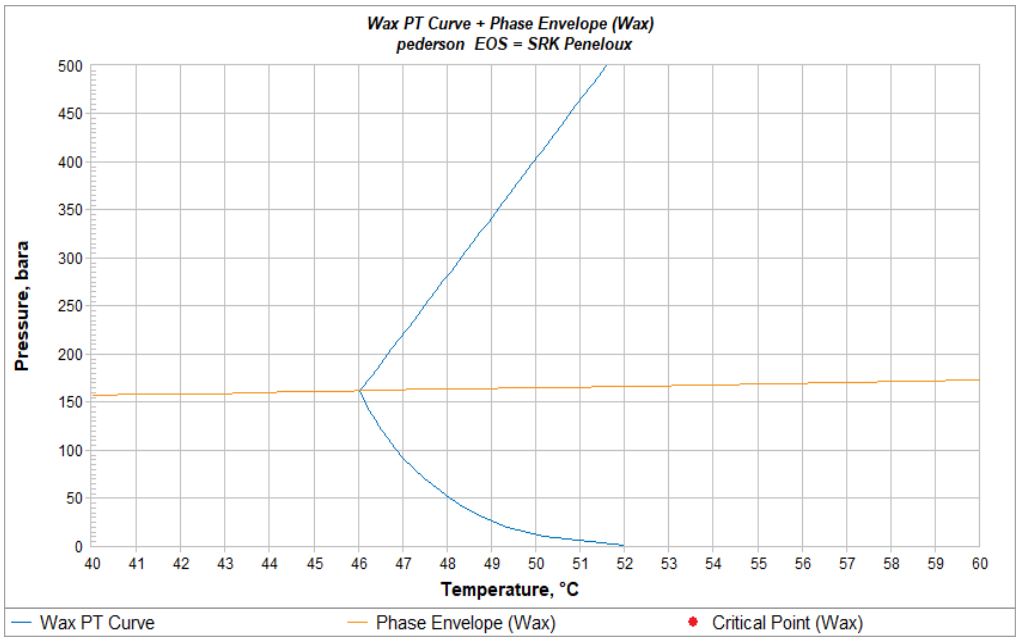

Figure 7 Wax phase boundary for Fluid 1 calculated by PVTsim

From the Figure 7, it is noticed the reference point of 200 bara is around 46.7 °C and the lowest possible operating temperature before entering wax phase boundary is near 46 °C at the pressure of 160 bara so the entire wax phase boundary is shifted to the left compared to previous two models.

For the second fluid that has been examined, 9 WDT experimental data points were reported (Mahabadian, 2016) and the data can be found in Table 4.

Table 4 Experimental wax disappearance temperature for Fluid 2

WDT(°C)	P (bara)
38	2
37	34
37	61
37	79
37	96
38	132
39	193
40	288
41	364

The calculated wax phase boundaries for Fluid 2 is illustrated in Figures 8-11. Unfortunately, in HydraFLASH tuning the model to 9 experimental values has taken significant computational time and yielded high error of 25% in matching the experimental data so the model has been tuned only to first 3 experimental points.

In Multiflash matching has been performed with first 3 and all 9 experimental points.

PVTsim does not provide an option to tune the model to various points so it has been tuned only to the first experimental WDT point.

On the Figure 8 the wax phase boundary of Fluid 2 can be seen, calculated with the model that has been tuned with all 9 experimental values in Multiflash. As it can be seen none of the values lays on the wax phase boundary, so the matching is quite difficult. The lowest temperature at which we could operate before entering wax phase boundary is around 37 °C with pressure being 60 bara.

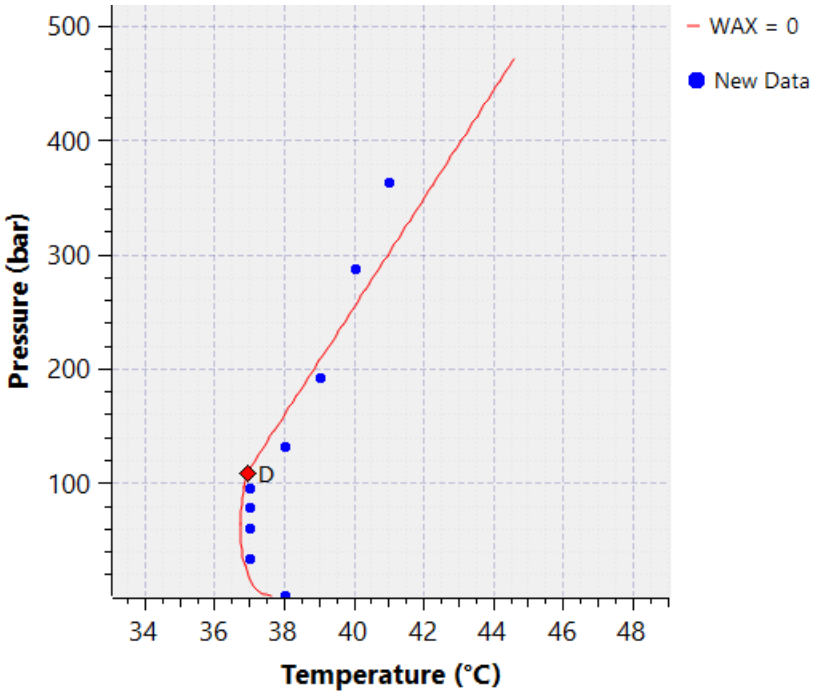

Figure 8 Wax phase boundary for Fluid 2 calculated by Multiflash

In Figure 9 the wax phase boundary calculated by HydraFLASH is presented and it has been tuned only with first 3 experimental WDT values, however, all 9 experimental values have been added on the figure and we can see that the simulator has predicted the behavior quite accurate for 5 out of 9 experimental dots.

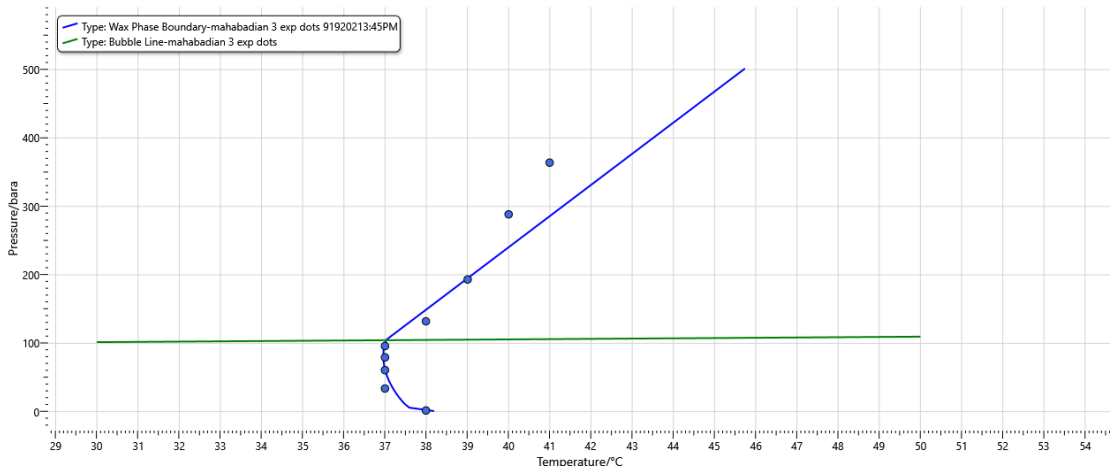

Figure 9 Wax phase boundary for Fluid 2 calculated by HydraFLASH

Multiflash wax phase boundary for the same fluid using the model tuned to first 3 experimental points are shown in Figure 10.

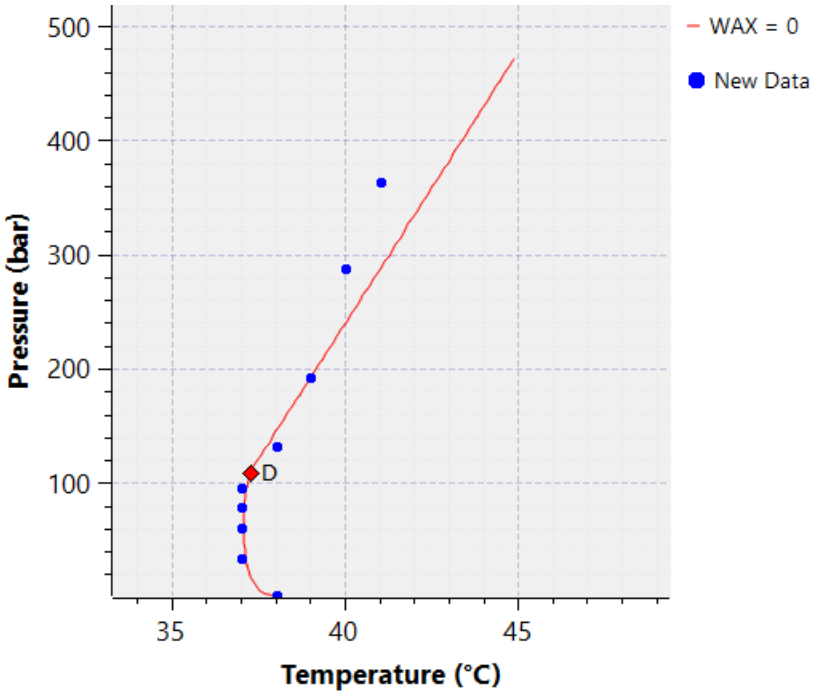

Figure 10 Wax phase boundary for Fluid 2 calculated by Multiflash

It can be noticed that the model has made the satisfactory matching with 6 dots out of 9 and the lowest operating temperature before entering the wax phase boundary is the same as HydraFLASH model and it is around 37 °C and pressure of 60 bara.

PVTsim model has been tuned only with first experimental data and the wax phase boundary is presented in Figure 11 below.

The predicted wax phase boundary using this model, gives 34.9 °C as the lowest temperature before entering wax phase boundary with pressure being 100 bara which is quite different compared to previous two models.

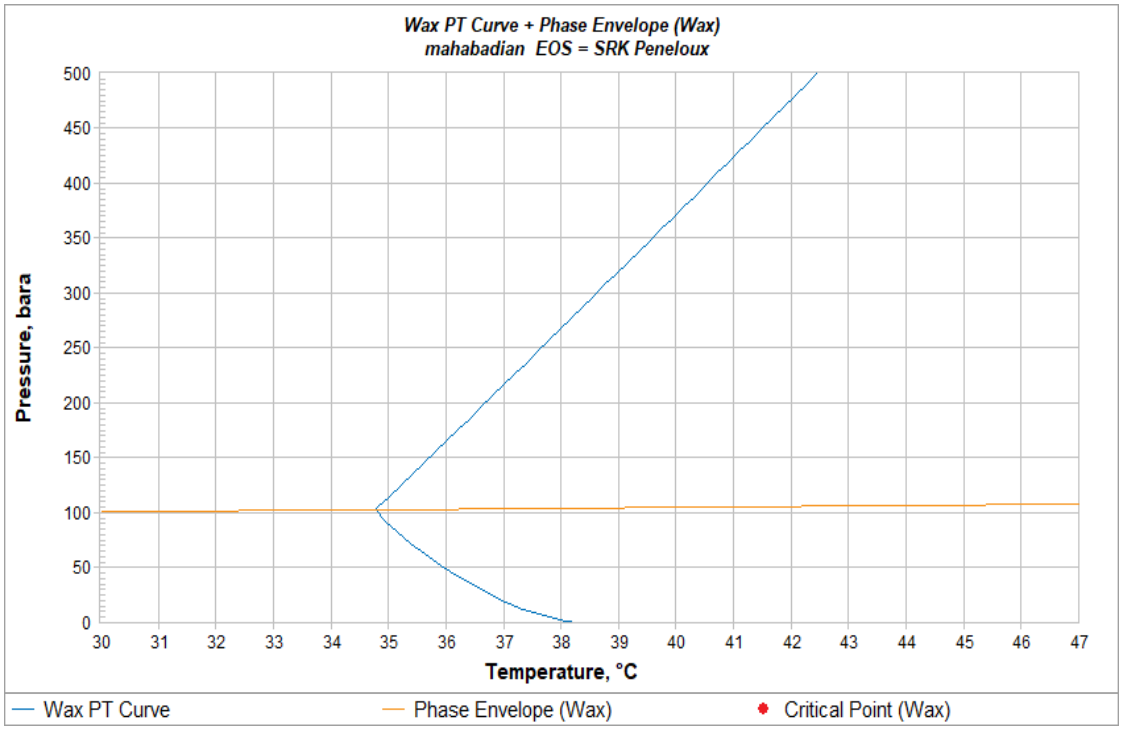

Figure 11 Wax phase boundary for Fluid 2 calculated by PVTsim

The third live fluid analyzed in this work has been taken from Hongyan. J (PhD dissertation). The fluid composition has been reported in the Table 5.

Table 5 Composition of Fluid 3

Component	Mole (%)
Carbon Dioxide	0.64
Nitrogen	1.66
Methane	37.1
Ethane	2.45
Propane	0.7
i-Butane	0.15
n-Butane	0.09
i-Pentane	0.03
n-Pentane	0.03

C_7	28.02
C_{10}	24.91
C_{13}	1.46
C_{16}	1.17
C_{18}	0.19
C_{22}	0.15
C_{24}	0.14
C_{28}	0.94
C_{30}	0.06
C_{36}	0.1
C_{40}	0.01

In order to complete the wax characterization in HydraFLASH and Multiflash for the Fluid 3 the wax content had to be assumed in the same manner as for the first two fluids analyzed. The assumed value of wax content for this fluid and the reported saturation properties are presented in Table 6.

Table 6 Wax content and saturation properties for Fluid 3

Fluid	Wax content (wt. %)	Bubble point (bara)	T (°C)
Fluid 3	3.5	126	25.85

For the third fluid analyzed there has been 6 experimental values of WDT reported (Hongyan. J, 2004) and they are given in Table 7.

Table 7 Experimental wax disappearance temperature for Fluid 3

WDT(°C)	P(bara)
27.85	16
27.85	45
28.85	141
30.85	260
31.85	325
32.85	400

As the experimental data reported are hard to predict, attempt to match the models with all experimental data was unsuccessful and the matching has been done only with first point.

In Figure 12, the HydraFLASH model delivered wax phase boundary for Fluid 3 is presented. The model has been tuned only with the first experimental point, but all the reported WDT points were marked on the Figure for comparison.

It can be noticed that the lowest temperature at which we could operate before entering wax phase boundary is 27 °C and pressure of 100 bara. Apart from the first point laying on the wax phase boundary, points 4 (30.85 °C at 260 bara) and 5 (31.85 °C at 325 bara) have been predicted close enough and they are touching the wax phase boundary.

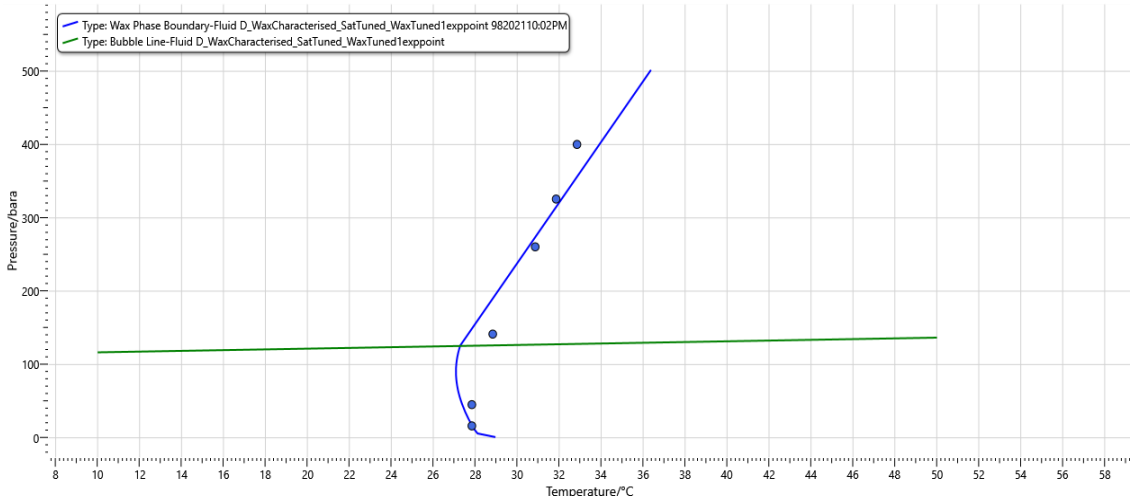

Figure 12 Wax phase boundary for Fluid 3 calculated by HydraFLASH

Also, it can be noticed that at atmospheric pressure the wax disappearance temperature is 29 °C.

On the Figure 13 below, the wax phase boundary modeled in Multiflash for Fluid 3 has been presented. The model in Multiflash has also been tuned only with first experimental point, but all 6 experimental points have been added to the figure for comparing predictions. The only point laying on wax phase boundary is the one the model has been tuned with.

The lowest temperature we could operate before entering the wax phase boundary is 27.5 °C with pressure around 60 bara and it is seen to be different than that predicted by HydraFLASH model which gave 27 °C with pressure being close to 100 bara.

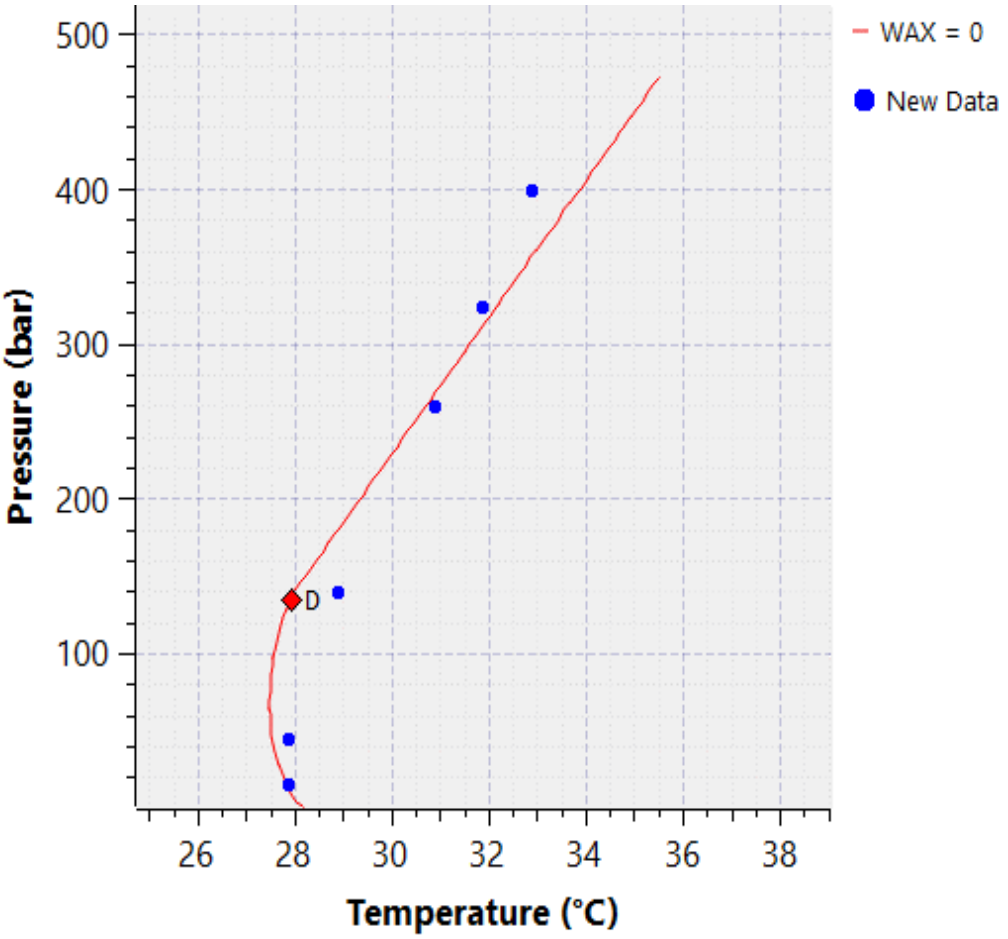

Figure 13 Wax phase boundary for Fluid 3 calculated by Multiflash

Another difference noticed when comparing these two models is the wax disappearance temperature at atmospheric pressure. For HydraFLASH model it is 29 °C while for Multiflash model it is 28.1 °C which gives a difference of almost 1 °C.

The third model for Fluid 3 was created in PVTsim and the model has also been tuned only with first experimental point. The calculated wax phase boundary is presented in Figure 14.

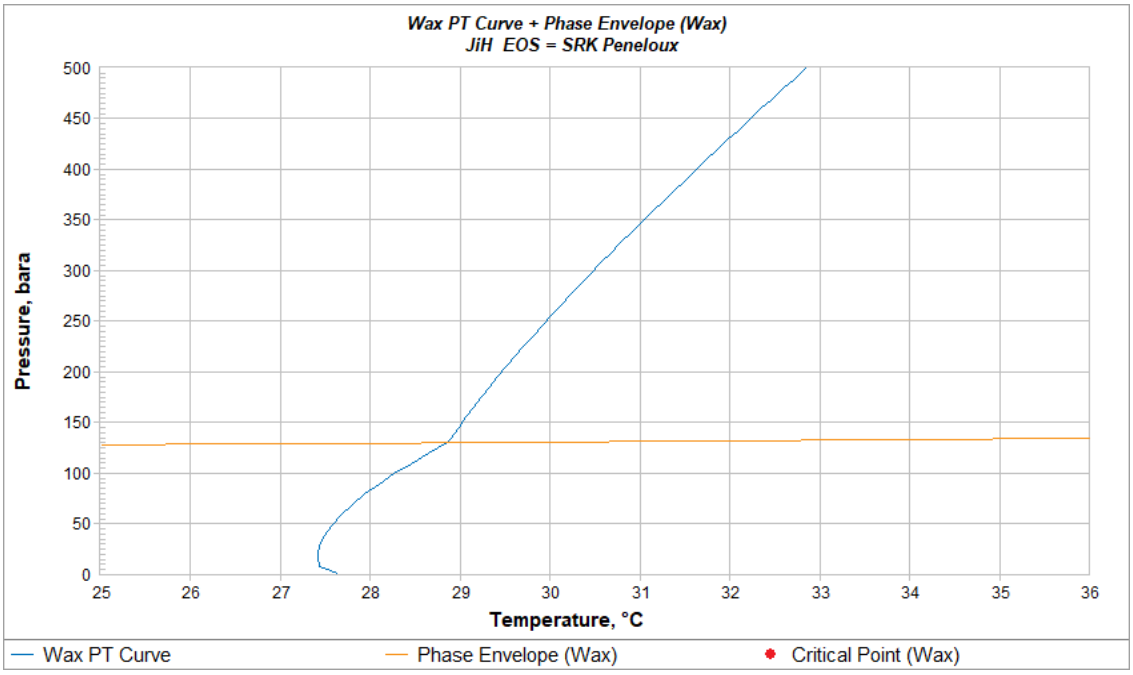

Figure 14 Wax phase boundary for Fluid 3 calculated by PVTsim

On the first look at the model, the irregular shape of the wax phase boundary can be noticed, and it can be prescribed to the fluid composition as this is synthetic oil.

From the Figure 14 it can be noticed that the model did not predict the behavior of the fluid as accurate as the previous two models since the wax phase boundary is shifted to the left from the experimental points.

When compared to previous two models, another difference noticed is the wax disappearance temperature at atmospheric pressure where for PVTsim model it is 27.6 °C which gives a difference of 0.6 °C from Multiflash and 1.5 °C from HydraFLASH model prediction.

The compositions of fourth and fifth live Fluid (Hammami et al.1999**)** analyzed in this work are presented in the Table 8.

Table 8 Compositions of Fluids 4 and 5

Component	Fluid 4 Mole (%)	Fluid 5 Mole (%)	Component	Fluid 4 Mole (%)	Fluid 5 Mole (%)
Carbon Dioxide	0.142	0.115	C_{13}	2.326	2.53
Nitrogen	0.313	0	C_{14}	2.278	2.553
Methane	43.899	29.376	C_{15}	2.285	2.729
Ethane	5.622	5.342	C_{16}	1.97	2.525

Propane	2.456	2.666	C_{17}	1.854	2.551
i-Butane	0.79	0.929	C_{18}	1.821	2.567
n-Butane	1.162	1.343	C_{19}	1.693	2.678
i-Pentane	0.763	0.96	C_{20}	1.508	2.195
n-Pentane	0.56	0.7	C_{21}	1.302	2.151
SCN6	1.085	1.416	C_{22}	1.165	1.976
Methylcyclopentane	0.287	0.33	C_{23}	1.045	1.814
Benzene	0.586	1.027	C_{24}	0.915	1.623
Cyclohexane	0.306	0.343	C_{25}	0.821	1.468
C_7	1.162	1.431	C_{26}	0.708	1.308
Methylcyclohexane	0.762	0.838	C_{27}	0.646	1.192
Toluene	0.991	1.387	C_{28}	0.613	1.114
C_8	1.554	1.785	C_{29}	0.499	0.927
Ethylbenzene	0.097	0.118	C_{30}	0.431	0.735
m-Xylene	0.906	1.153	C_{31}	0.397	0.767
o-Xylene	0.429	0.527	C_{32}	0.336	0.545
C_9	1.394	1.499	C_{33}	0.316	0.5
C_{10}	2.45	2.506	C_{34}	0.25	0.458
C_{11}	2.068	2.071	C_{35+}	3.062	3.162
C_{12}	1.977	2.069			

Since no wax content data was reported for Fluids 4 & 5 the wax content has been assumed as for previous three fluids. The values of assumed wax content, specific gravity and calculated heavy end molecular weight for Fluids 4 and 5 are reported in Table 9.

Table 9 Assumed wax content for Fluids 4 & 5 and heavy end properties.

Fluid	Wax content (wt. %)	Mw. C_{35+}	Sp. g. C_{35+}
4	3.5	786	0.85
5	5	800	0.85

For the fluid 4 there has been reported only one WDT experimental point which will be used for tuning the model and it is presented in Table 10, together with saturation properties.

Table 10 Experimental WDT and saturation properties for Fluid 4

WDT(°C)	P (bara)	Bubble point (bara)	T (°C)
49	118	155	15

HydraFLASH wax model for Fluid 4 has been tuned with experimental WDT point and the wax phase boundary calculated can be seen in Figure 15.

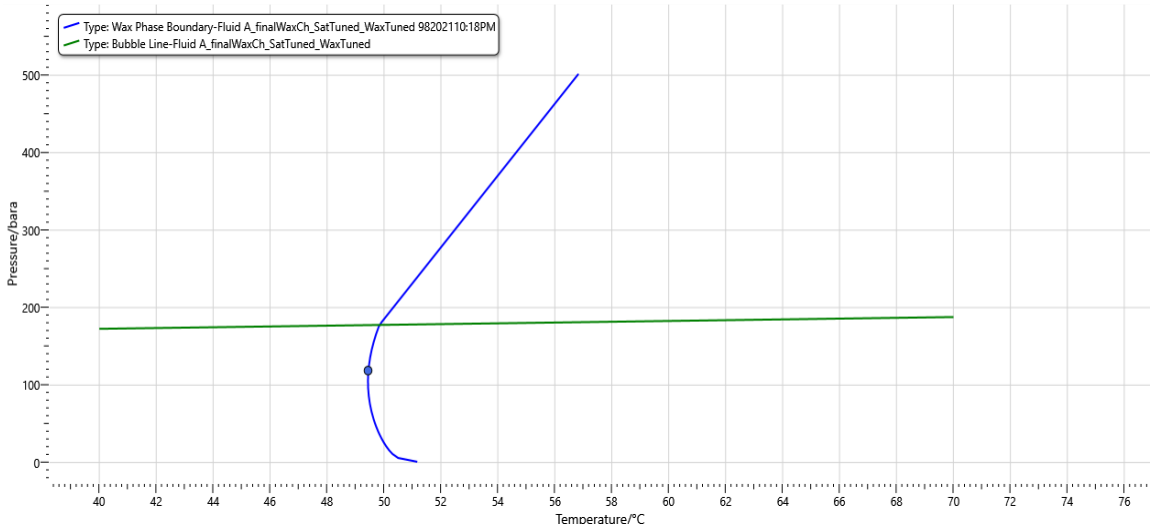

Figure 15 Wax phase boundary for Fluid 4 calculated by HydraFLASH

From Figure 15 it can be observed that the matching was performed successfully as the experimental point lays on wax phase boundary and the lowest temperature at which we could operate before entering wax phase boundary fits at the experimental WDT point with the pressure range from 90-120 bara. Also, it can be noticed the model predicted wax disappearance temperature at atmospheric pressure is 51 °C.

For the same fluid, creating the model in Multiflash has been done and tuning the model with the experimental WDT point has been successful. The calculated wax phase boundary has been presented in Figure 16.

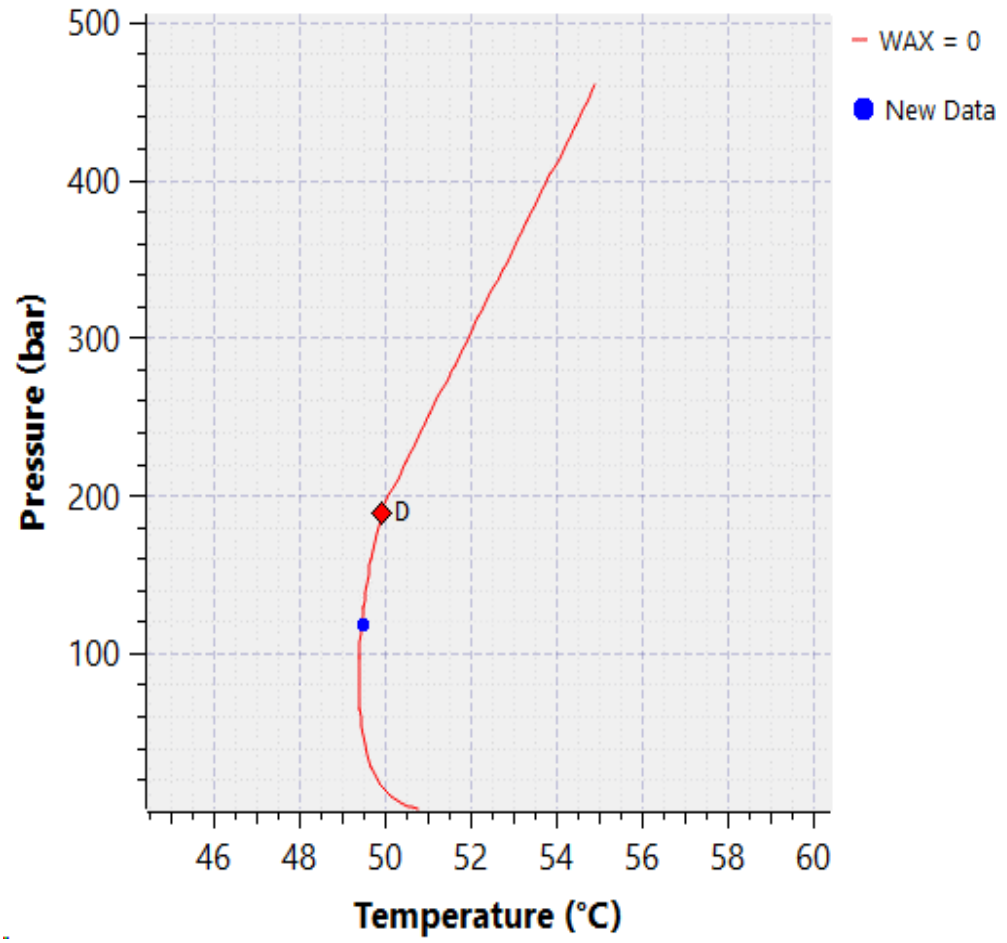

Figure 16 Wax phase boundary for Fluid 4 calculated by Multiflash

From Figure 16 it can be concluded that the model gives similar results as the HydraFLASH model. As seen in the graph, the experimental data and predicted wax phase boundary are in very good agreement. The lowest temperature before entering the wax phase boundary fits the WDT and the pressure range as for the previous model. The wax disappearance temperature at atmospheric pressure for Multiflash model is 50.7 °C.

In Figure 17 the wax phase boundary calculated by model generated in PVTsim has been presented.

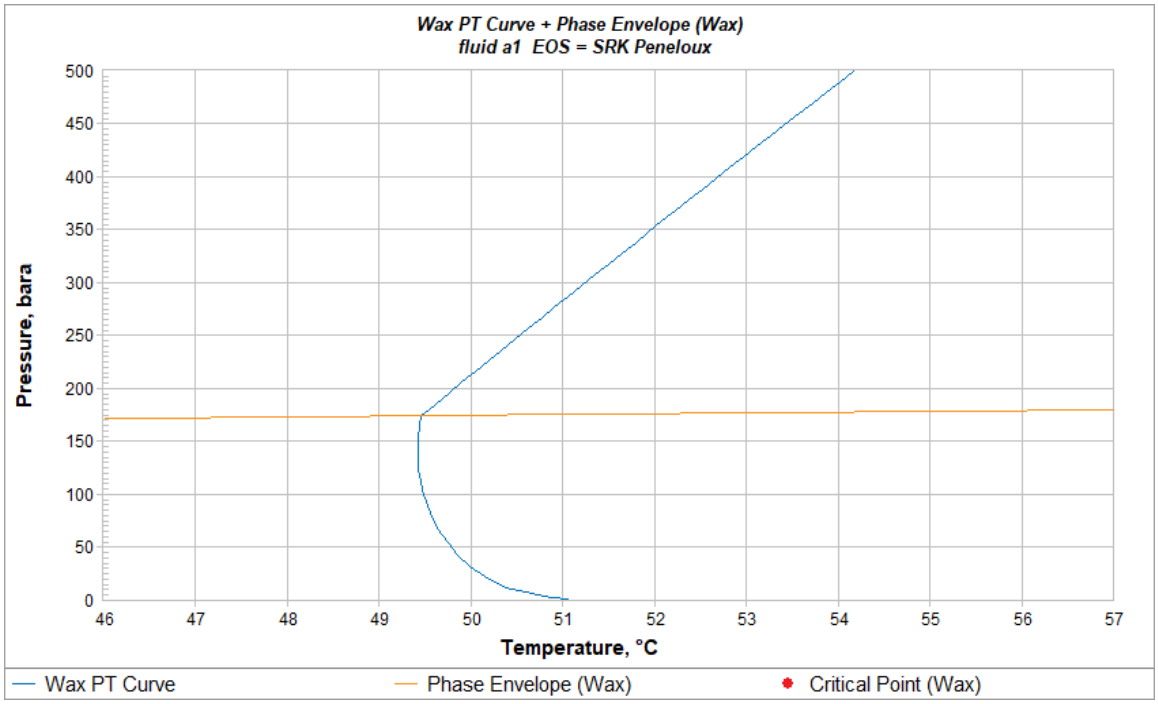

Figure 17 Wax phase boundary for Fluid 4 calculated by PVTsim

From the wax phase boundary in Figure 17, it is observed that the model has matched the experimental data successfully. Also, the lowest temperature before entering the wax phase boundary does correspond to the WDT just like in previous two models, but the pressure range is different with this model, it suits the pressure range from 120-145 bara.

The model has calculated the wax disappearance temperature at atmospheric pressure to be 51.05 °C which is closer to the HydraFLASH model than to Multiflash one. However, the previous two models exhibited more similar wax phase boundary above the bubble point.

As a point of reference, at pressure of 200 bara WDT for the first two models were 50.4 °C, 50.1 °C, and for pressure of 400 bara 54.8 °C and 53.8 °C respectively, while for the PVTsim model WDT at given pressures are 49.7 °C and 52.6 °C respectively.

Same as for the Fluid 4, the number of experimental values of WDT for Fluid 5 is one and it is presented in the Table 11, together with saturation properties.

Table 11 Experimental WDT and saturation properties for Fluid 5

WDT(°C)	P (bara)	Bubble point (bara)	T (°C)
42	77	83	15

The wax phase boundary for Fluid 5, calculated by the three simulators are presented in Figures 18-20.

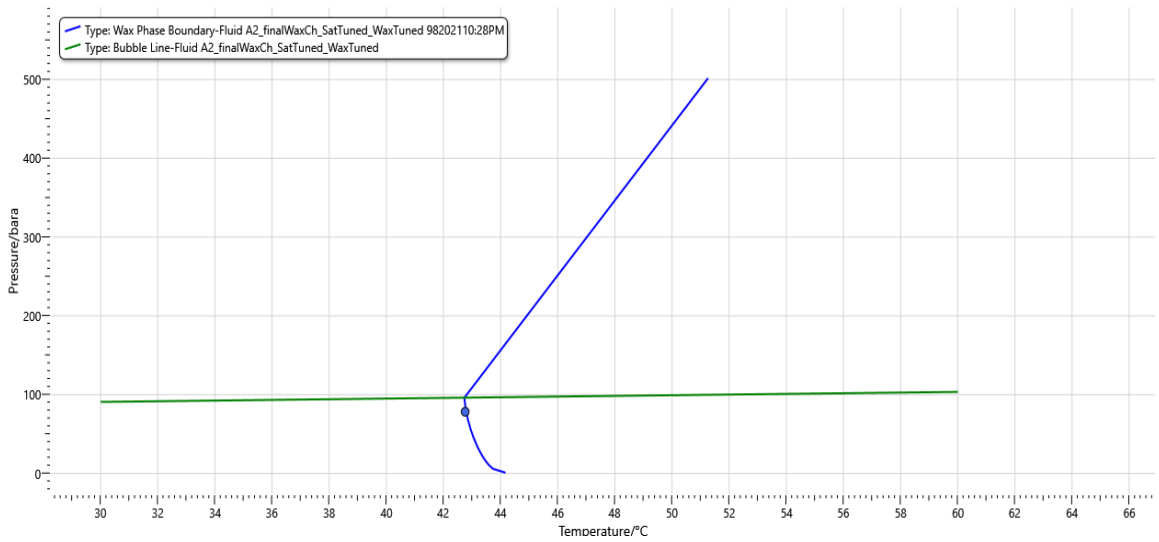

Figure 18 Wax phase boundary for Fluid 5 calculated by HydraFLASH

The wax phase boundary of Fluid 5 calculated by the HydraFLASH simulator is shown in Figure 18 it can be noticed that the model has been tuned successfully as the experimental point lays exactly on the wax phase boundary. From the same figure it can be seen the wax disappearance temperature at atmospheric pressure is 44.2 °C and the lowest temperature before entering the wax phase boundary is 42.8 °C at 100 bara pressure which is near the saturation line.

Wax model for the Fluid 5 which has been generated in Multiflash has also been tuned successfully with the experimental point, as it lays exactly on the wax phase boundary which can be seen in Figure 19.

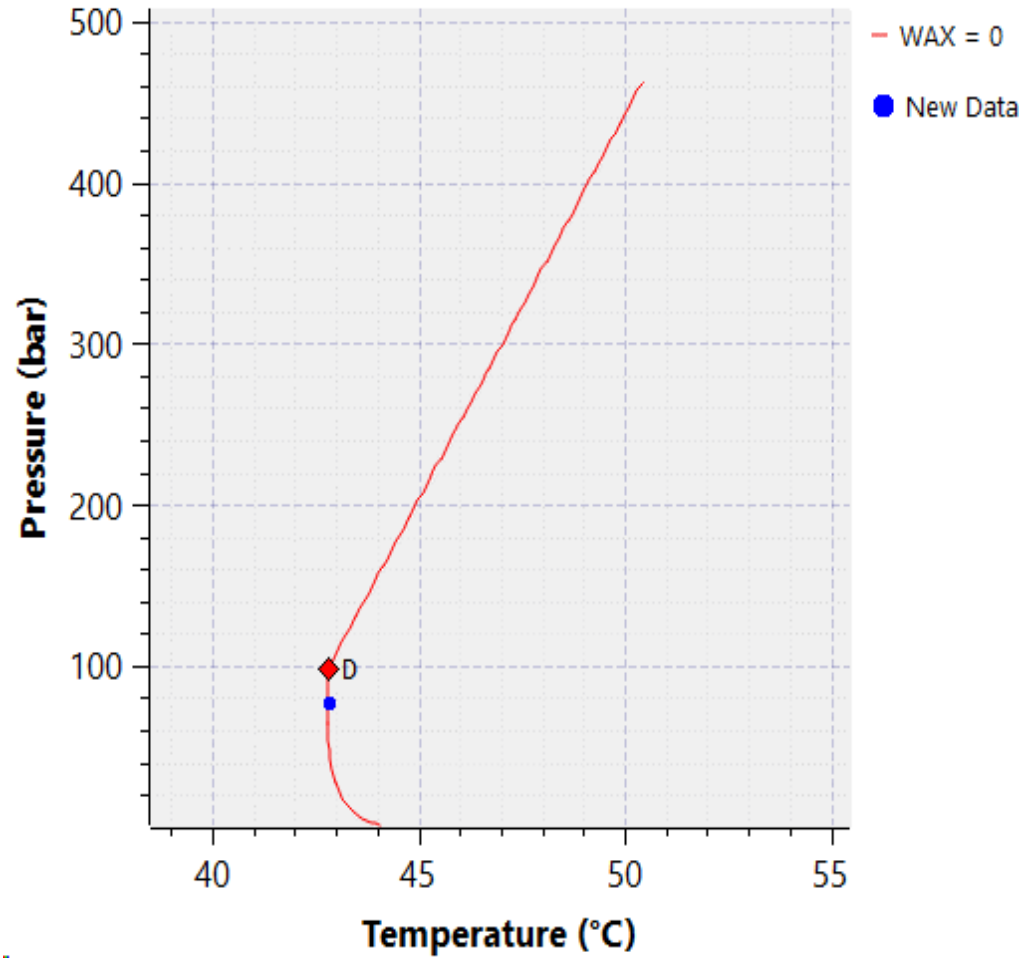

Figure 19 Wax phase boundary for Fluid 5 calculated by Multiflash

Analyzing the Figure 19 it can be noted that the wax disappearance temperature at atmospheric pressure is 44 °C which is very similar to HydraFLASH model, also the slope the wax phase boundary exhibits above the saturation point and the lowest temperature before entering wax phase envelope is matching to the HydraFLASH model predictions.

Finally, the PVTsim model of Fluid 5 has also tunned successfully to the WDT experimental point as it can be seen from Figure 20.

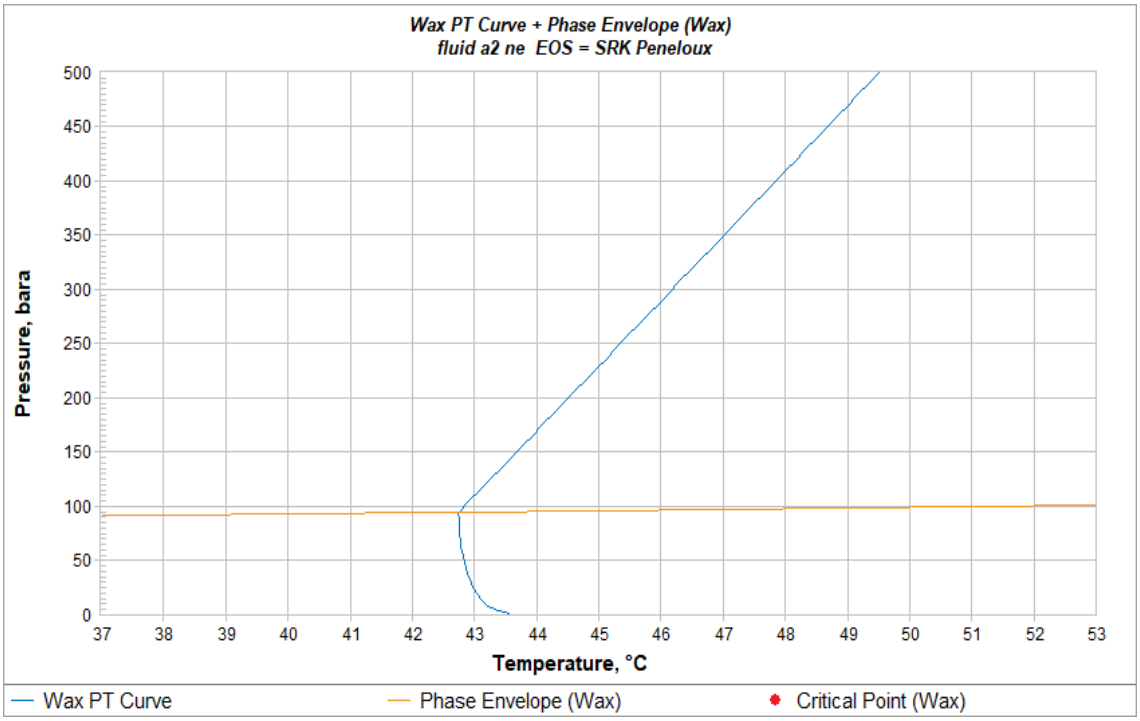

Figure 20 Wax phase boundary for Fluid 5 calculated by PVTSIM

From the figure above, the wax disappearance temperature at atmospheric pressure is 43.5 °C and the lowest temperature before entering the wax phase boundary is near the experimental point of 42.7 °C over pressure range of 75 to 95 bara. By looking at the wax phase boundary above saturation line it can be noticed that the boundary is shifted to the left side in comparison to the previous two models. Where reference points of 200 and 400 bara confirm this as the wax disappearance temperatures at this pressures are 44.5 and 47.8 °C respectively.

Comparing the previous two models with the PVTsim model, the effect of different EoS used is evident, as the wax phase boundary is shifted towards the left side once again while still providing the accurate match to the experimental data.

6. Experimental data and analysis of dead oils

As the wax usually appears within dead oils (oils with very little presence of methane or none), the number of compositions of dead oils containing waxy components in the literature is far greater than for the live oils.

To achieve better understanding of the software`s differences, in this chapter the three simulators wax models will be compared by analyzing 16 dead oils.

The composition of the first 9 fluids as well as experimental values of wax disappearance temperatures are presented in the Table 12.

As there were no saturation properties reported for these fluids, the models were tuned only with WDT data.

Table 12 Compositions of 9 dead oils and the experimental WDT

Component	Fluid 1 (Mole %)	Fluid 2 (Mole %)	Fluid 3 (Mole %)	Fluid 4 (Mole %)	Fluid 5 (Mole %)	Fluid 6 (Mole %)	Fluid 7 (Mole %)	Fluid 8 (Mole %)	Fluid 9 (Mole %)
Methane	0.00	0.00	0.00	0.00	0.00	0.00	0.00	0.00	0.00
Ethane	0.00	0.00	0.00	0.00	0.00	0.00	0.00	0.00	0.00
Propane	0.00	0.00	0.00	0.00	0.00	0.00	0.00	0.00	0.00
i-Butane	0.00	0.00	0.00	0.00	0.00	0.00	0.00	0.00	0.00
n-Butane	0.00	0.00	0.00	0.00	0.00	0.00	0.00	0.00	0.00
i-Pentane	0.00	0.00	0.00	0.00	0.00	2.98	0.00	0.00	2.53
n-Pentane	0.00	0.00	0.00	0.00	0.00	2.98	0.98	0.00	0.00
C_6	2.47	0.00	2.92	2.69	1.47	4.98	1.91	2.84	4.24
C_7	9.46	4.78	5.03	6.94	3.79	8.57	7.52	4.88	12.75
C_8	6.22	6.61	6.61	6.09	6.64	7.52	5.78	6.42	11.19
C_9	9.24	7.85	9.82	9.03	9.86	8.37	9.19	9.53	12.81
C_{10}	6.66	8.85	7.08	6.52	7.11	7.55	8.28	6.87	8.98
C_{11}	6.06	4.83	4.83	5.93	6.47	5.5	6.03	6.26	5.84
C_{12}	5.56	5.91	5.91	9.66	5.94	3.78	5.53	5.74	5.36
C_{13}	5.14	5.46	4.1	4.9	4.12	4.66	5.11	5.3	4.95
C_{14}	3.58	5.08	5.08	4.67	5.1	4.33	4.75	3.7	3.68
C_{15}	4.46	4.74	3.56	3.27	3.57	3.03	4.44	4.6	3.44
C_{16}	4.19	3.34	4.45	4.09	4.47	3.79	3.12	4.32	3.22
C_{17}	2.96	4.19	3.14	2.89	3.16	2.68	2.94	3.05	2.28
C_{18}	1.86	1.98	1.98	1.82	2.98	1.69	2.78	1.92	1.43
C_{19}	1.77	2.81	1.88	1.73	1.88	2.4	1.75	2.73	1.36
C_{20+}	30.36	33.56	33.62	29.77	33.45	25.18	29.88	31.83	15.94
Mw C_{20+}	413.77	420.28	426.9	420.43	423.39	409.64	410.02	414.84	377.94
Sp. g. C_{20+}	0.9	0.9	0.9	0.9	0.9	0.9	0.9	0.9	0.89

WDT (°C)	27.15	28.05	26.07	24.47	25.62	25.98	24.65	23.5	15.01

As it can be seen from Table 12, none of the oils contains methane, or other lighter components such as ethane and propane, etc.

To do wax characterization in HydraFLASH the fluid must contain some lighter components so it can be flashed at standard conditions and still contain gas components as the software requires from user to insert flashed gas and stabilized oil composition to perform wax characterization.

As these dead oils do not contain any of the lighter components flashing them at standard conditions would yield no gas components. Since HydraFLASH software requires flashed gas in order to perform wax characterization the natural gas with composition given in Table 13 has been added to these fluids so the wax characterization can be performed.

Table 13 Natural gas composition

Component	Mole %
Methane	50
Ethane	10
Propane	5
i-Butane	2
n-Butane	1
i-Pentane	0.1
n-Pentane	0.05

There has been no experimental wax content reported for these 9 Fluids, so the value of wax content had to be assumed as another step to do the wax characterization. As all 9 Fluids exhibit similar composition a value of 5 (wt.%) wax content has been assumed for all 9 Fluids.

In Figure 21 the wax phase boundary for Fluid 1 has been calculated by the model generated in HydraFLASH software.

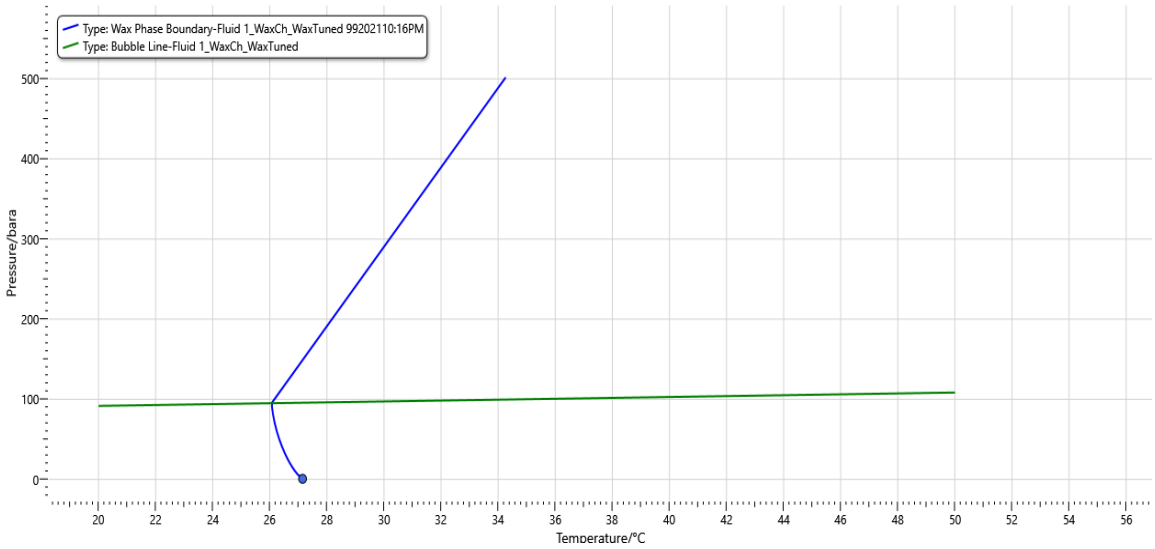

Figure 21 Wax phase boundary for Fluid 1 calculated by HydraFLASH

From the Figure 21, it can be seen that the model has been tuned successfully with the experimental data as the wax disappearance temperature at atmospheric pressure is 27.15 °C. Also, it is clear that the lowest possible temperature before entering the wax phase boundary is 26 °C at saturation point which is close to 100 bara.

In Figure 22, the wax phase boundary of Fluid 1, calculated by Multiflash has been presented.

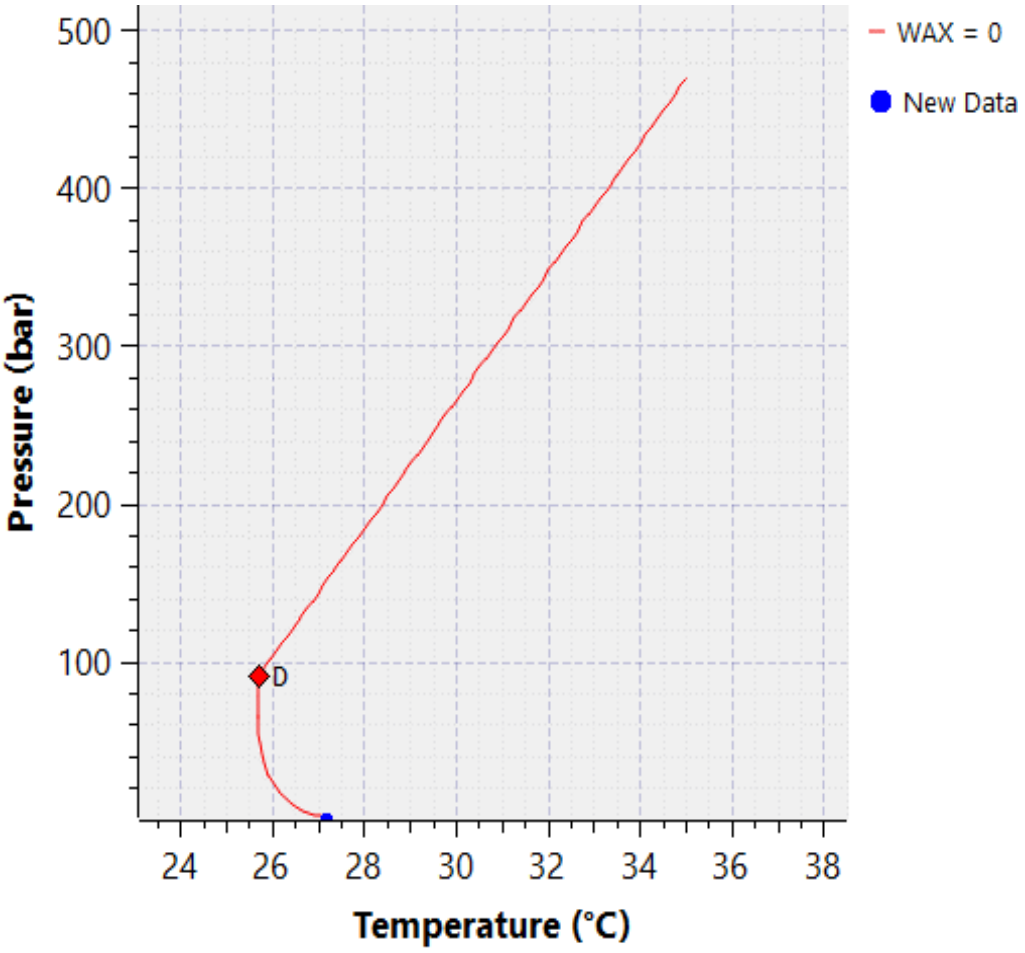

Figure 22 Wax phase boundary for Fluid 1 calculated by Multiflash

The wax phase boundary calculated by Multiflash also fits the experimental data point which is 27.15 °C, however, there is a slight difference in the phase boundary as it can be clearly seen that the lowest temperature before entering wax phase boundary is less than 26 °C which was the case for HydraFLASH model prediction.

The Figure 23 presented contains the wax phase boundary for Fluid 1 that is generated with PVTsim simulator.

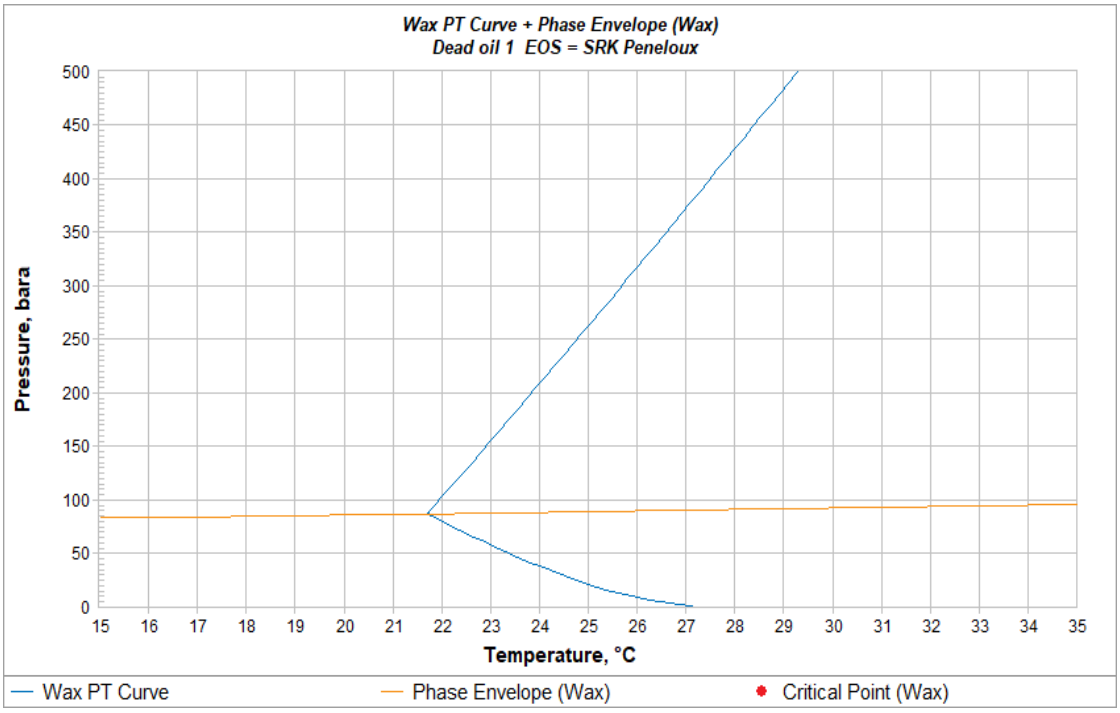

Figure 23 Wax phase boundary for Fluid 1 calculated by PVTsim

In the Figure 23, it can be seen that the PVTsim model has successfully matched the experimental WDT point just like the previous two simulators. By analyzing the wax phase boundary, it can be noticed that it has been shifted towards left side as the lowest temperature before entering wax phase boundary is 21.7 °C which is significantly less than for previous two models.

The Figure 24 shows the wax phase boundary for Fluid 2 calculated by HydraFLASH model. From the figure it can be noticed the model matched the experimental point perfectly just like it did for the previous fluid.

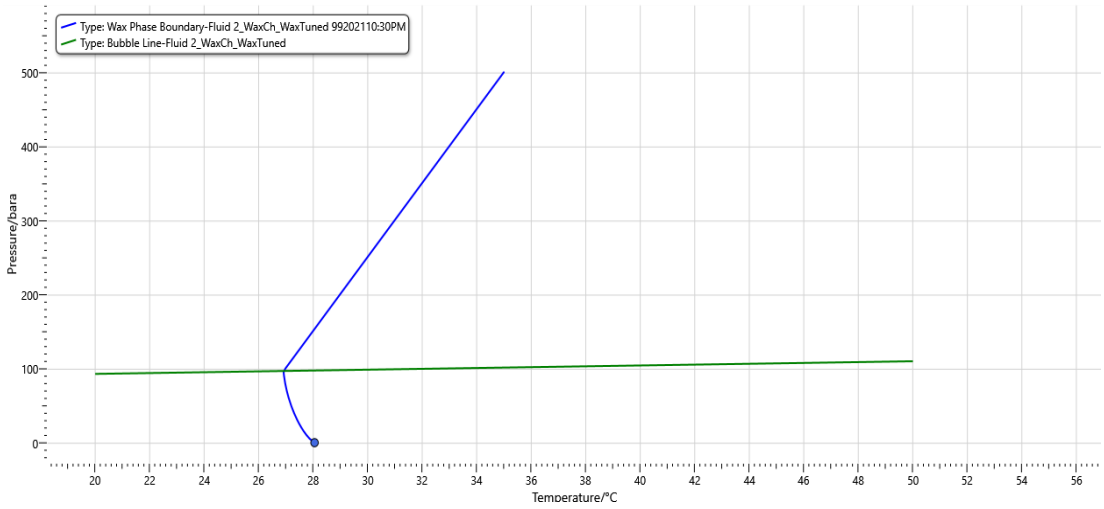

Figure 24 Wax phase boundary for Fluid 2 calculated by HydraFLASH

In the Figure 25 the wax phase boundary for Fluid 2 calculated by Multiflash is presented and it can be noticed the model matched the experimental point just like the HydraFLASH one, however, the difference in the slope above saturation point is observed again.

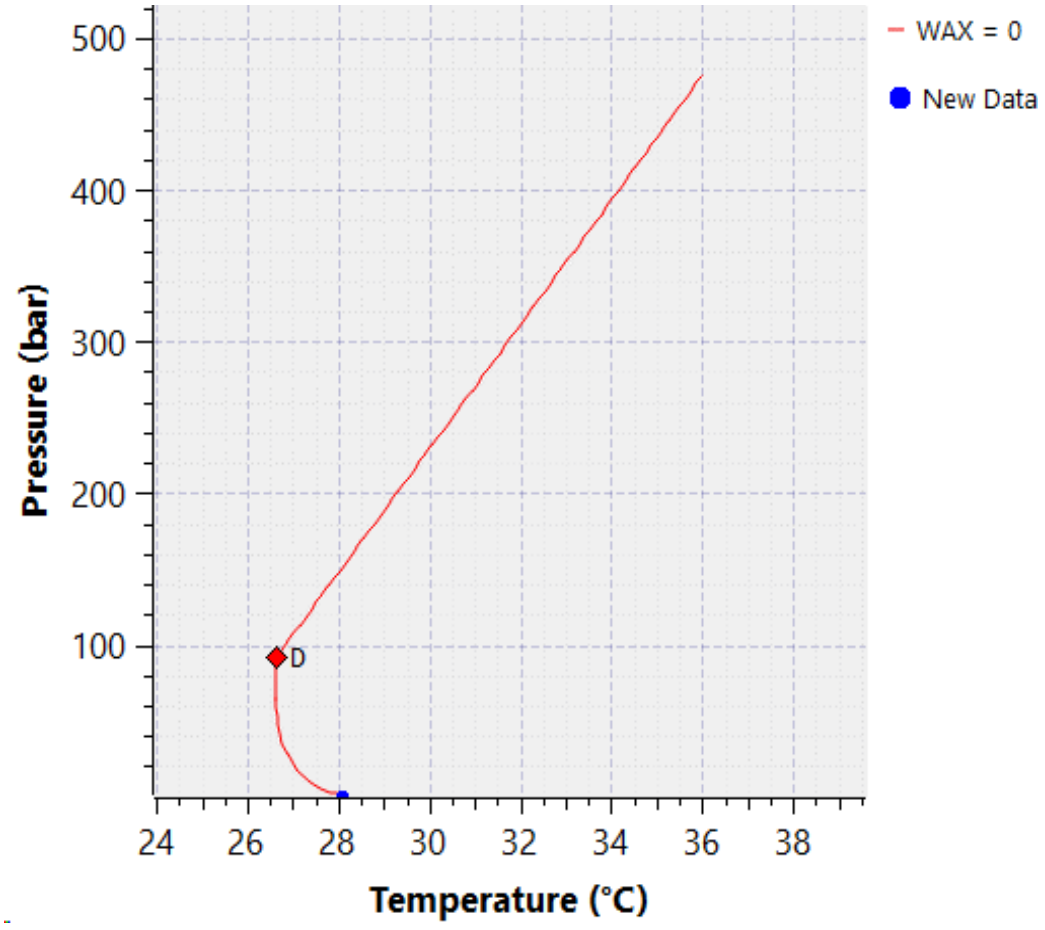

Figure 25 Wax phase boundary for Fluid 2 calculated by Multiflash

PVTsim model has matched the experimental point accordingly and it can be seen in Figure 25 that the wax phase boundary is shifted to the left side in comparison to previous two models.

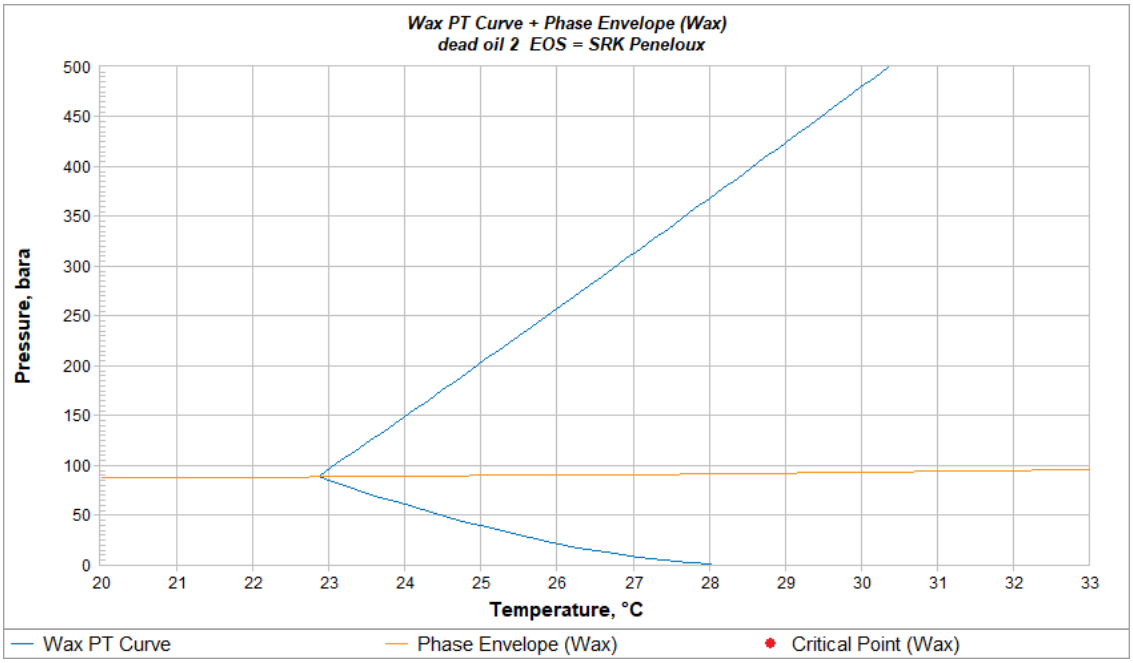

Figure 26 Wax phase boundary for Fluid 2 calculated by PVTsim

As it can be seen from the first two fluids presented, the models have matched the single experimental point quite easy. The calculations for remaining 7 dead oils were completed and all models successfully matched the reported WDT data. However, since there is no significant difference between composition of these 9 dead oils, the differences seen in predictions of wax phase boundaries between three simulators are the same as for first two fluids. The wax phase boundaries of remaining 7 Fluids are presented in Appendix within Figures A1-A15.

All three simulators succeeded at tuning the model with experimental WDT point. From the saturation point HydraFLASH and PVTsim models show similarities in calculating the wax phase boundary as they give much steeper slope with respect to the horizontal axis in comparison to the Multiflash model.

The Multiflash model gives a wax phase boundary with the lowest possible operating temperature before entering the wax phase boundary in matter of 0.3-0.5 °C in comparison to the HydraFLASH model as PVTsim model shifts significantly the wax phase boundary to the left side in comparison to the HydraFLASH and Multiflash models which can be because of the difference in the EoS equation used.

The composition and the experimental wax disappearance temperature of the new 7 dead oils are presented in the Table 14.

As there were no saturation properties reported for these fluids, the models were tuned only with WDT data.

Table 14 Compositions of the 7 dead oils and the experimental WDT

Component	Fluid 10 (Mole %)	Fluid 11 (Mole %)	Fluid 12 (Mole %)	Fluid 13 (Mole %)	Fluid 14 (Mole %)	Fluid 15 (Mole %)	Fluid 16 (Mole %)
Carbon dioxide	0.03	0.05	0.1	0.01	0.06	0.02	0.04
Hydrogen sulphide	0.13	0.19	0.06	0.00	0.00	0.00	0.00
Methane	0.2	0.02	0.00	0.00	1.4	0.02	0.00
Ethane	0.34	0.51	0.73	0.38	0.28	0.46	0.81
Propane	1.62	2.32	2.72	3.11	0.64	1.52	2.17
i-Butane	0.81	1.06	0.72	0.81	0.37	0.61	0.74
n-Butane	3.28	4.09	3.59	4.71	2.33	2.43	2.32
i-Pentane	2.19	2.35	1.85	1.47	2.09	2.09	1.58
n-Pentane	4.1	4.46	3.36	3.87	3.69	3.67	2.95
C_6	7.19	7.37	5.92	7.9	7.02	8.03	8.24
C_7	6.27	4.73	5.65	2.36	4.32	4.67	4.21
C_8	5.78	4.42	5.25	2.3	4.1	4.4	3.99
C_9	5.33	4.15	4.89	2.24	3.88	4.16	3.8
C_{10+}	62.71	64.28	65.16	70.84	69.82	67.92	69.15
Mw C_{10+}	300	300	300	300	300	300	300
Sp. g. C_{10+}	0.8	0.8	0.8	0.8	0.8	0.8	0.8
WDT (°C)	51	60	53	50	56	42	45

From the Table 14 it can be seen that the samples are dead, so the same procedure of adding natural gas has been performed in order to flash the compositions for modeling in HydraFLASH.

In the Figure 27 the wax phase boundary calculated by HydraFLASH model has been presented.

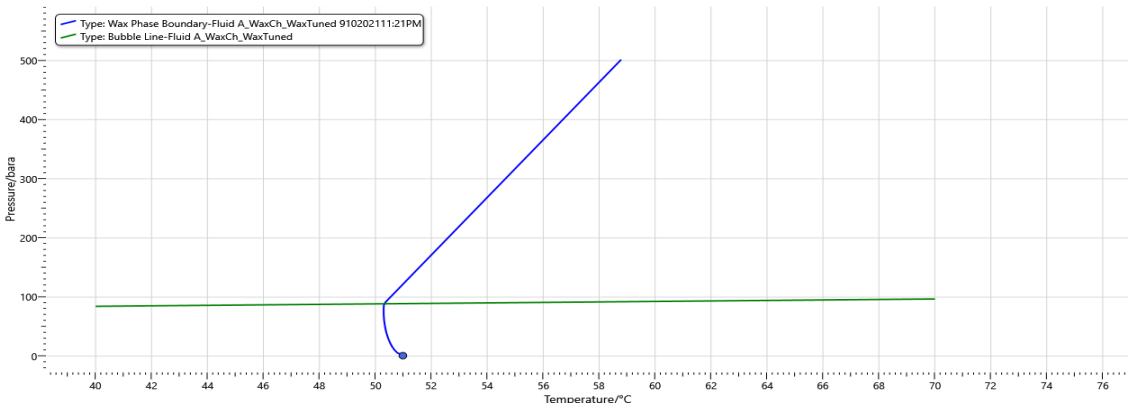

Figure 27 Wax phase boundary for Fluid 10 calculated by HydraFLASH

The model has been tuned successfully and the wax disappearance temperature at atmospheric pressure matches the experimental point which is 51 °C. Figure 27, indicates the lowest temperature before entering the wax phase boundary to be 50.2 °C with the pressure being near saturation point which corresponds to 90-100 bara.

In the Figure 28 the wax phase boundary calculated by Multiflash model has been presented.

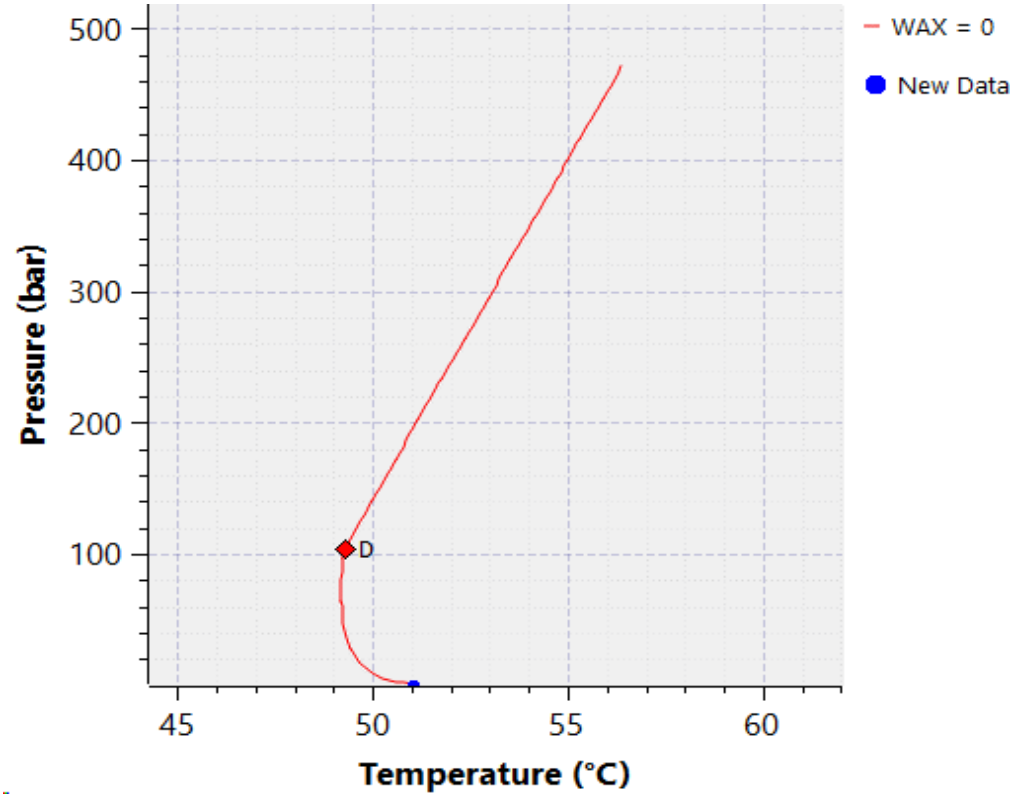

Figure 28 Wax phase boundary for Fluid 10 calculated by Multiflash

The figure shows that the model has been tuned successfully with experimental wax disappearance temperature as it predicts the same value at atmospheric pressure. If the wax phase boundary curve is extrapolated above the saturation point, until 500 bara, it could be noted the temperature corresponding to that pressure would be 57 °C and the lowest temperature before entering the wax phase boundary is 49.5 °C which shows that the wax phase boundary is shifted towards the left in comparison to model presented in Figure 27.

Wax phase boundary calculated by PVTsim for Fluid 10 can be seen on the Figure 29.

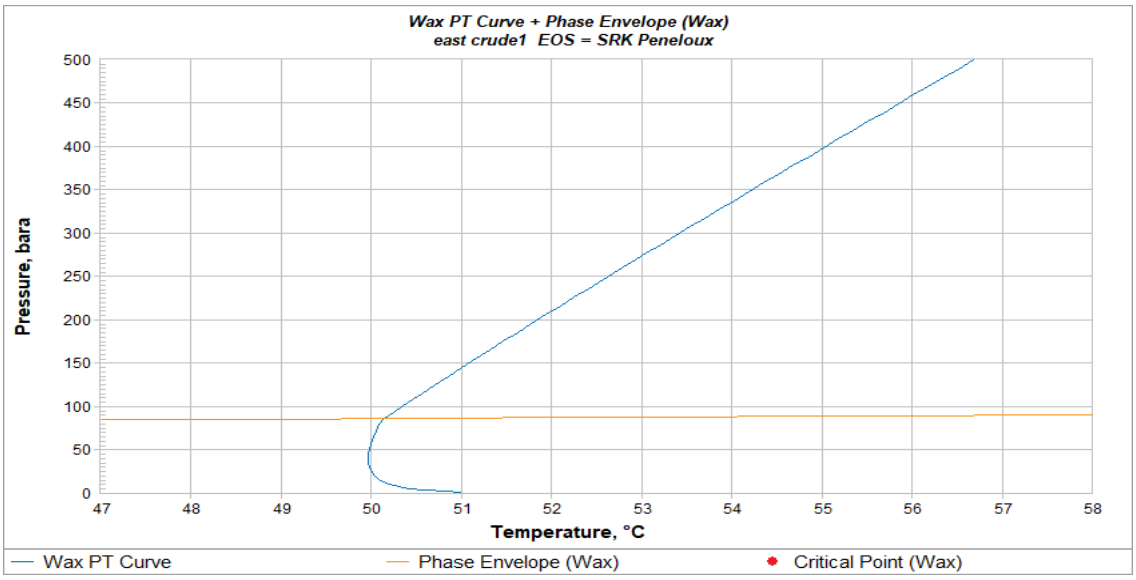

Figure 29 Wax phase boundary for Fluid 10 calculated by PVTsim

In can be noticed from the Figure 29 the PVTsim model has also tunned successfully to the experimental wax disappearance temperature as it shows the value of 51 °C to be at atmospheric pressure. The lowest temperature before entering the wax phase boundary is 50 °C and the temperature of 56.7 °C corresponding to pressure of 500 bara which indicates the slope of the wax phase boundary above the saturation point is like the Multiflash model one.

On the Figure 30, the wax phase boundary can be seen for Fluid 11 calculated with HydraFLASH model.

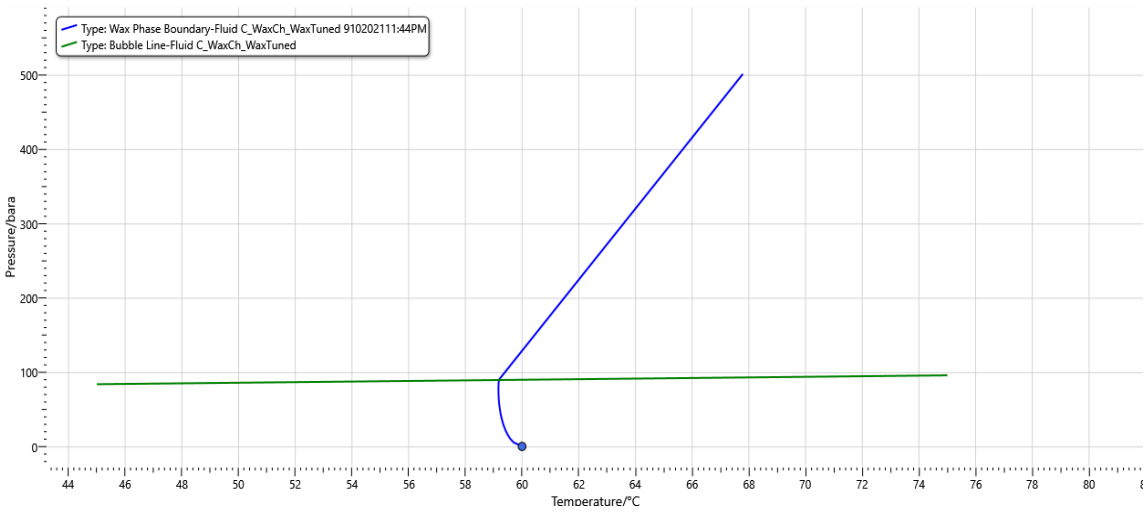

Figure 30 Wax phase boundary for Fluid 11 calculated by HydraFLASH

As it can be seen from the Figure 30, the tuning of the model with experimental data was successful as the model has predicted the wax disappearance temperature at atmospheric pressure to be exactly 60 °C which is the value of experimental point. If two reference points are taken at 200 and 400 bara the values of wax disappearance temperatures are 61.5 and 65.5 °C respectively.

In the Figure 31, the wax phase boundary for Fluid 11 calculated by Multiflash model can be found. The model has matched the experimental wax disappearance temperature successfully as the experimental point of 60 °C lays exactly on the predicted wax phase boundary. Also, it can be seen that the shape of the wax phase boundary is quite similar to that predicted for Fluid 11 as there is very little difference in composition between these two fluids.

It can be noticed from the figure that the lowest temperature before entering the wax phase boundary is 58.5 °C with pressure around 80 bara, also, comparing the two reference points of 200 and 400 bara the values of wax disappearance temperatures are 59.8 and 63.5 °C respectively.

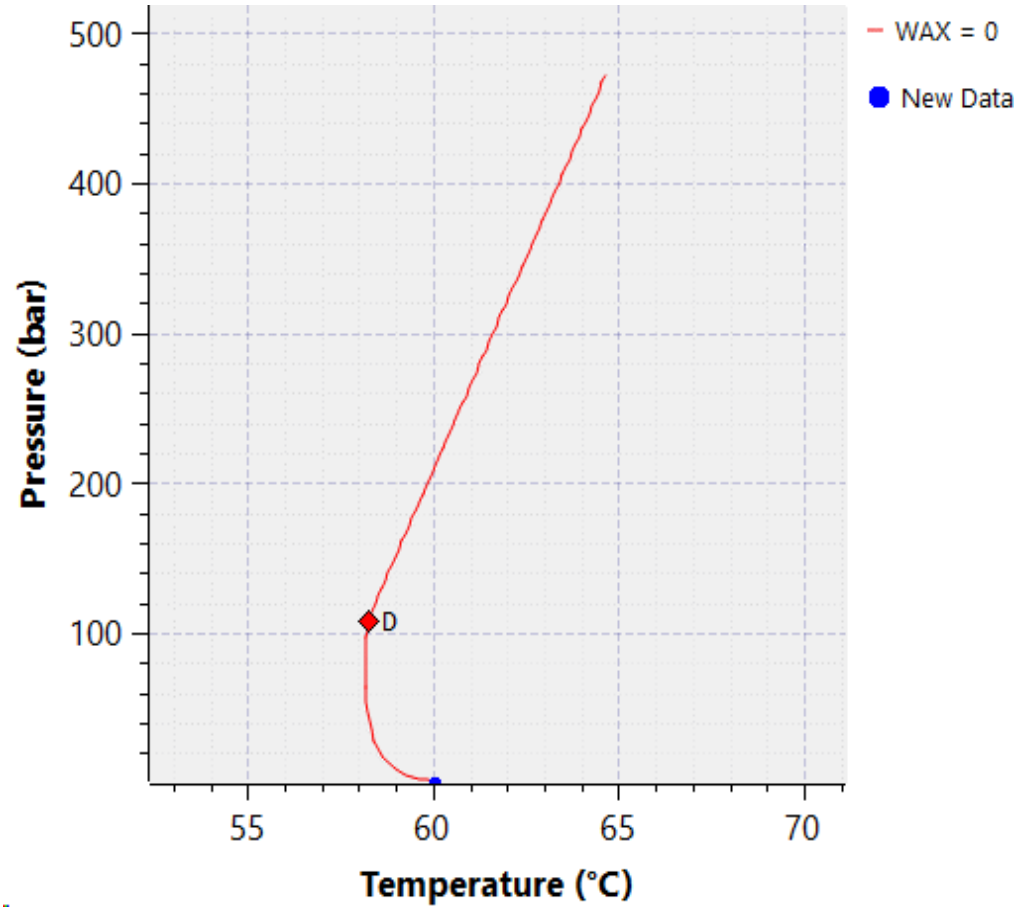

Figure 31 Wax phase boundary for Fluid 11 calculated by Multiflash

The third wax phase boundary calculated for this fluid is performed with PVTsim wax model and it is presented in Figure 32.

The predicted wax disappearance temperature at atmospheric pressure is 60°C which corresponds to the given experimental wax disappearance temperature which confirms the tuning of the model was successful. As for the previous two simulators the results received from PVTsim for fluid 11 are quite similar as for the previous fluid examined. As far as the reference points are concerned, for PVTsim model the wax disappearance temperatures at the reference pressures of 200 and 400 bara are 60.8 and 64 °C respectively and the lowest temperature before entering the wax phase boundary is 58.85 °C. It can be concluded all three models are giving different wax phase boundary predictions.

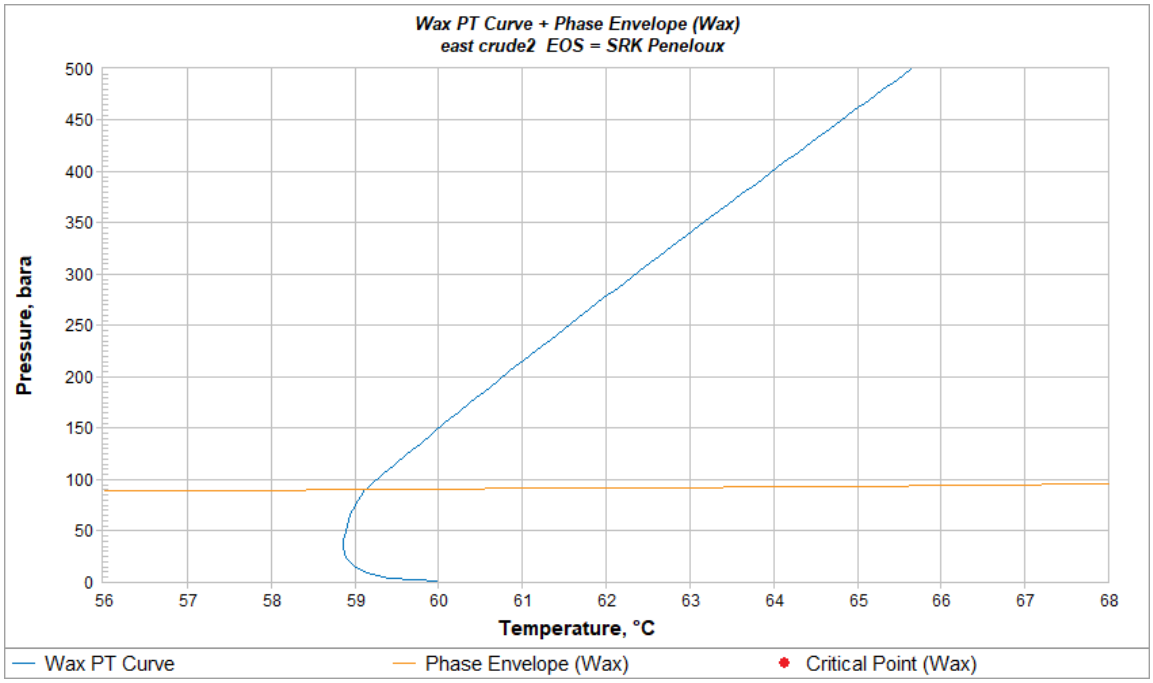

Figure 32 Wax phase boundary for Fluid 11 calculated by PVTsim

The calculations of remaining 5 fluids were completed and all models have managed to tune with experimental data successfully. From analysis performed on Fluids 10 & 11 the differences in performance of the simulators have been noticed and the observed difference continues within the calculations for remaining 5 fluids. As the differences noticed are the same, the remaining 5 Fluids calculations are presented in Appendix within Figures A16-A30.

7. Experimental data and analysis of wax content

In the Table 15 the experimental wax content wt. % can be found for Fluid 10 as well as the experimental wax disappearance temperature and the pressure at which measurement took place.

Table 15 Experimental wax content and WDT for Fluid 10

Fluid	Wax content (wt. %)	WDT (°C)	Pressure at WDT (bara)
Fluid 10	5.5	51	1.0135

From the literature (Elsharkawya, et al. 1999) it is noted the samples from which the wax content wae jbs measured were placed into a deep freeze at -20 to -30 °C, therefore, all the wax precipitation curves regarding these 7 Fluids were calculated from -30 °C to the wax disappearance temperature at atmospheric pressure.

Wax precipitation curve calculated by the HydraFLASH wax model is presented in Figure 33.

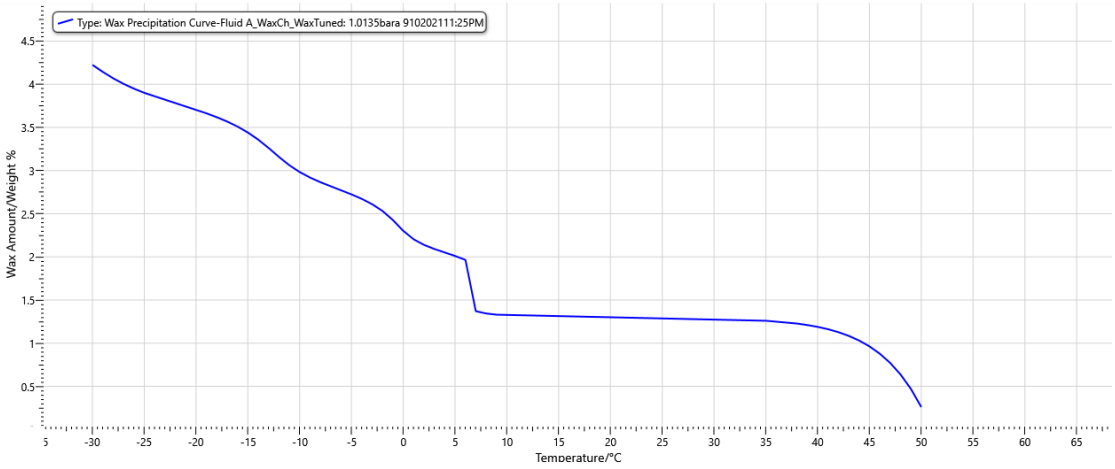

Figure 33 Wax precipitation curve for Fluid 10 by HydraFLASH

From Figure 33 the change in wax content with temperature can clearly be seen.

The model has predicted the wax content to be around 1.25% within temperature range of 10-35 °C. Once the fluid reaches temperature of 7 °C the increase in wax content is significant. The experimental wax content for Fluid 10 is 5.5 wt.%. The maximum value of wax content calculated by this model is 4.2 wt.% at -30 °C. However, it can be seen from Figure 33, the wax amount calculated with HydraFLASH is with respect to whole system.

The reported experimental data is given with respect to liquid as it is measured on dead oil.

Wax precipitation curve has been calculated in Multiflash for Fluid 10 and it can be seen in Figure 34.

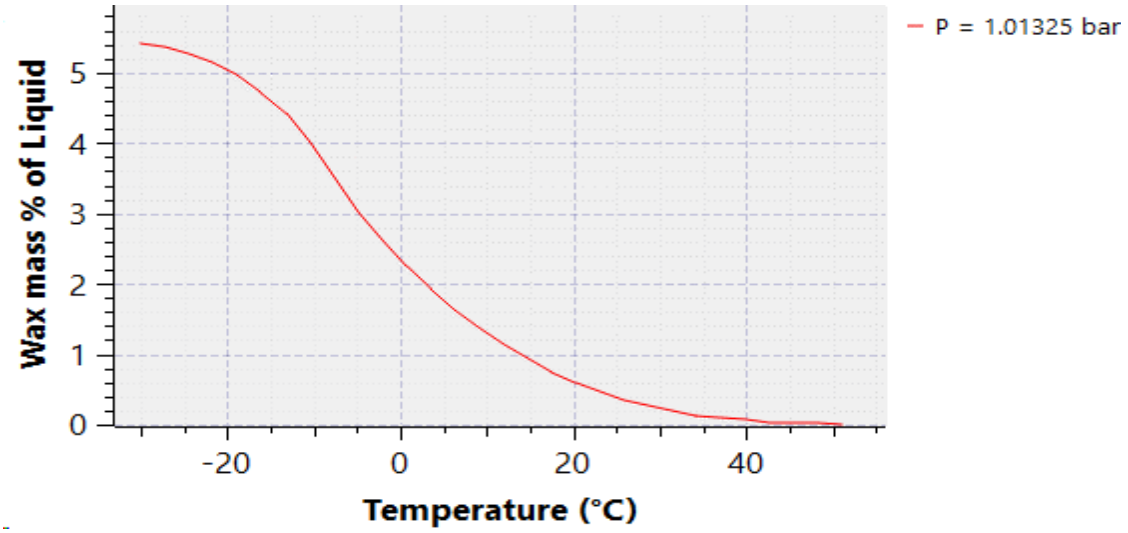

Figure 34 Wax precipitation curve for Fluid 10 calculated by Multiflash

As the first impression when comparing this model with the previous HydraFLASH one, the milder curvature of the wax precipitation curve can be noticed. Just like in the previous model, the wax content increase starts from 45 °C, however, this model does not calculate the wax content of 1.25% to be within the temperature range of 10-35 °C, but it shows more of a linear increase of wax content with decreasing the temperature.

The maximum wax content is calculated to be 5.4% at -30 °C which is more accurate than the previous model as the experimental value is 5.5 wt.% of wax content at -30 °C. However, from the Figure it can be seen the wax content report is with respect to liquid. Therefore, it is reasonable the Multiflash reported higher wax content compared to previous model.

The wax precipitation curve calculated in PVTsim is presented in Figure 35. It can be noticed that the model gives linear relation of wax content with temperature starting from 42 °C

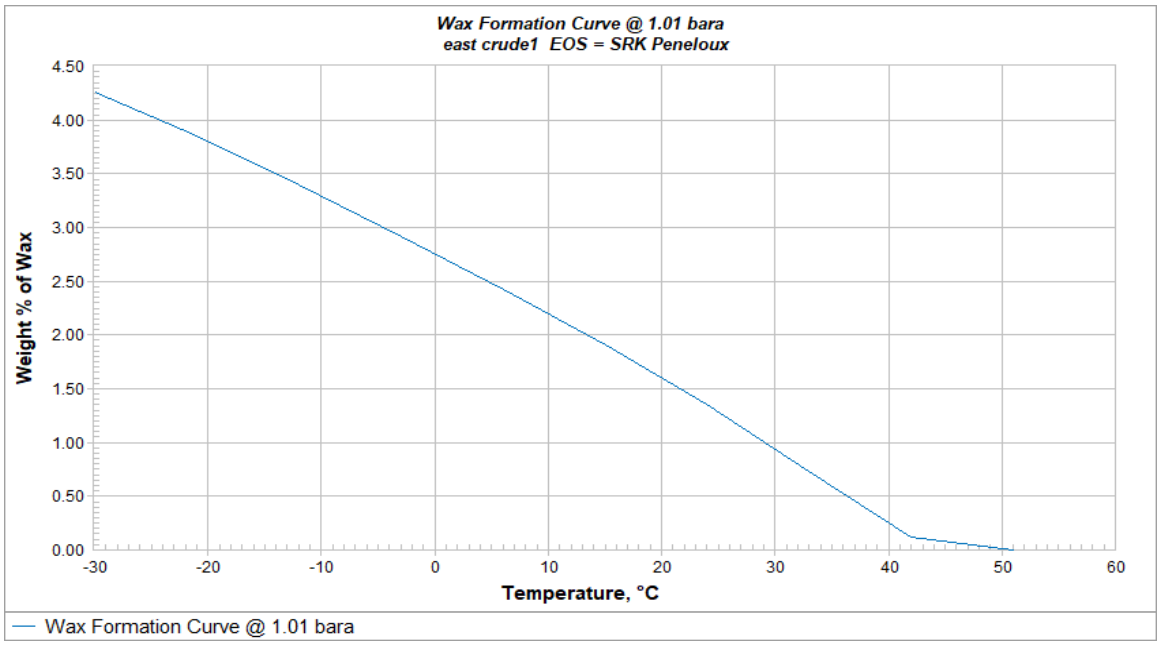

Figure 35 Wax precipitation curve for Fluid 10 calculated by PVTsim

The maximum value of wax content calculated by PVTsim model is 4.25 % wax content at -30 °C which is the very close to the value HydraFLASH model has calculated, however, both simulators report wax content with respect to whole system, which is the reason the maximum wax content predicted is lower than experimental wax content data.

If temperature of 10 °C is taken as a reference point, PVTsim has calculated the wax content to be ~2.2 wt. % while the HydraFLASH and Multiflash models both gave 1.3% of wax content at given temperature.

In Table 16 the experimental wax content and wax disappearance temperature for Fluid 11 has been presented.

Table 16 Experimental wax content and WDT for Fluid 11

Fluid	Wax content (wt. %)	WDT (°C)	Pressure at WDT (bara)
Fluid 11	6.5	60	1.0135

Wax precipitation curve calculated by HydraFLASH model for Fluid 11 has been presented in Figure 36.

From the figure it can be observed that the shape of wax precipitation curve is similar to the wax precipitation curve calculated by the model created for Fluid 10, as it is a reasonable

output considering the minor changes in composition between these two fluids. From Figure 36 it can be seen the wax content calculated by HydraFLASH model at -30 °C is 5.4 wt.%.

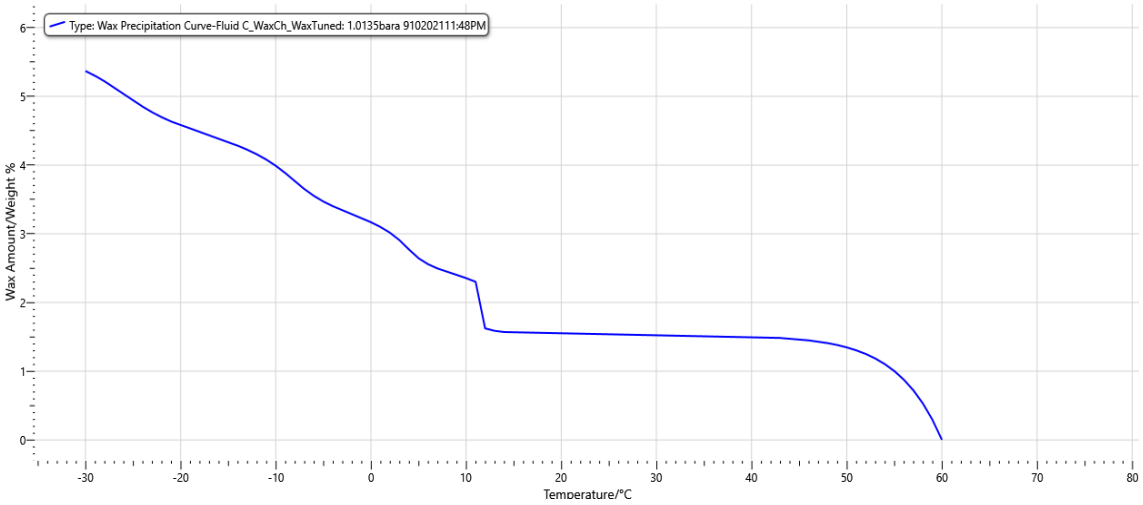

Figure 36 Wax precipitation curve for Fluid 11 calculated by HydraFLASH

In Figure 37, the wax precipitation curve calculated with Multiflash can be seen.

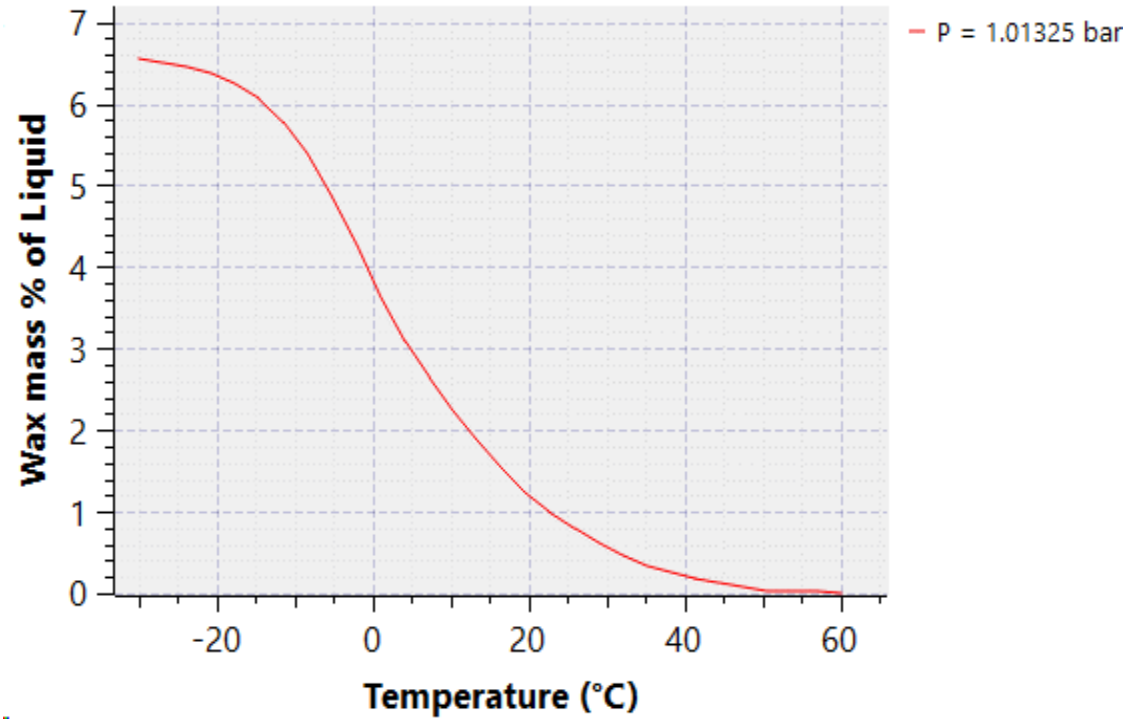

Figure 37 Wax precipitation curve for Fluid 11 calculated by Multiflash

From the Figure 37 it can be seen the wax model has matched the experimental value of wax content successfully as the maximum wax content of 6.5 wt.% is recorded at -30 °C which

corresponds to the experimental value. The wax precipitation curve generated for Fluid 11 in Multiflash has the same shape as for the Fluid 10, which was noted for HydraFLASH model as well.

In Figure 38, the wax precipitation curve for Fluid 11 calculated by PVTsim simulator can be seen.

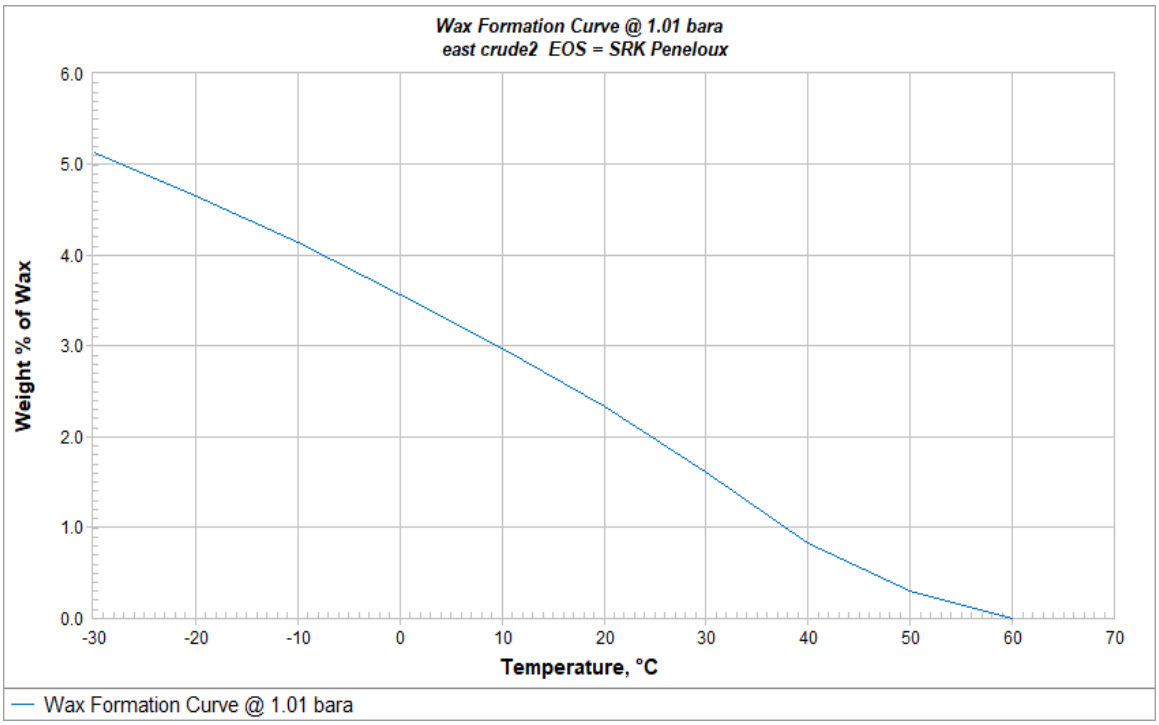

Figure 38 Wax precipitation curve for Fluid 11 calculated by PVTsim

The PVTsim model predicted the maximum wax content to be 5.1 wt.% which is the lowest value of all 3 simulators for this fluid. Apart from the low wax content, a linear increase of wax content with temperature decrease is more noticeable in comparison to PVTsim model for Fluid 10.

Experimental wax content and the wax disappearance temperature of the Fluid 12 have been presented in Table 17.

Table 17 Experimental wax content and WDT for Fluid 12

Fluid	Wax content (wt. %)	WDT (°C)	Pressure at WDT (bara)
Fluid 12	3.6	53	1.0135

The wax precipitation curve for Fluid 12 calculated by HydraFLASH model has been presented in Figure 39.

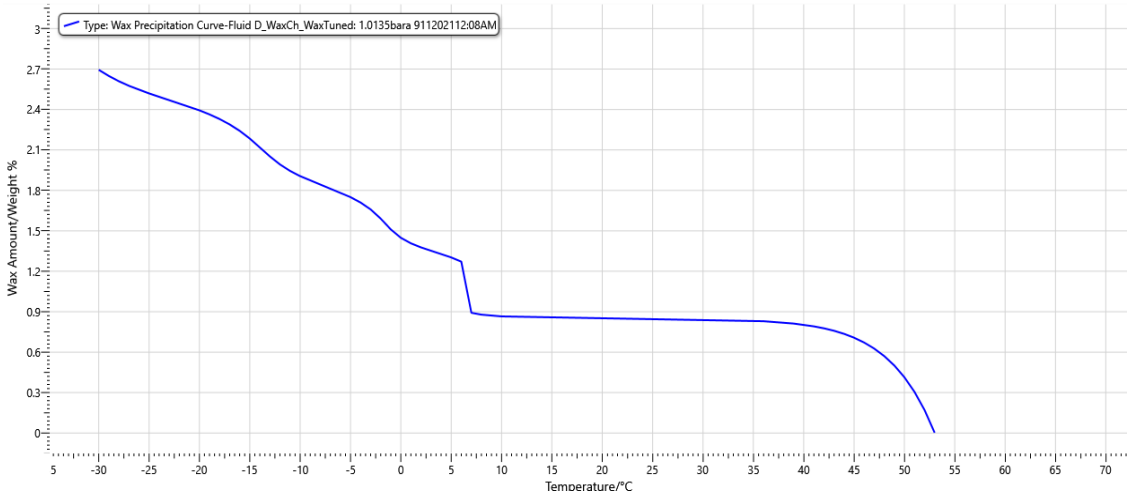

Figure 39 Wax precipitation curve for Fluid 12 calculated by HydraFLASH

The model has calculated the wax content at -30 °C to be 2.7%. From the Figure it can be seen the model tends to linearize one half of the curve and to keep almost constant value of wax content for the other half which is also seen from previous 3 HydraFLASH wax models.

The Multiflash wax model has generated the wax precipitation curve for Fluid 12 which yielded 3.5% of wax content at -30 °C which is the exact match with experimental wax content. The wax precipitation curve has been presented in Figure 40.

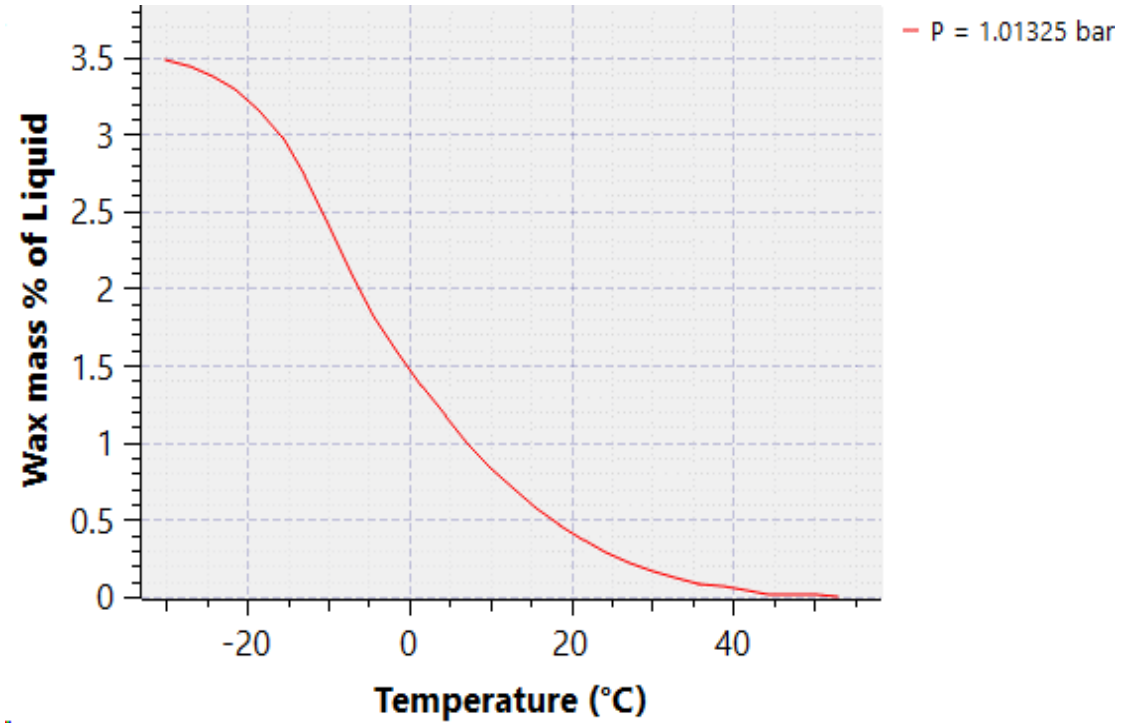

Figure 40 Wax precipitation curve for Fluid 12 calculated by Multiflash

In Figure 41 the wax precipitation curve calculated by PVTsim model for Fluid 12 has been presented.

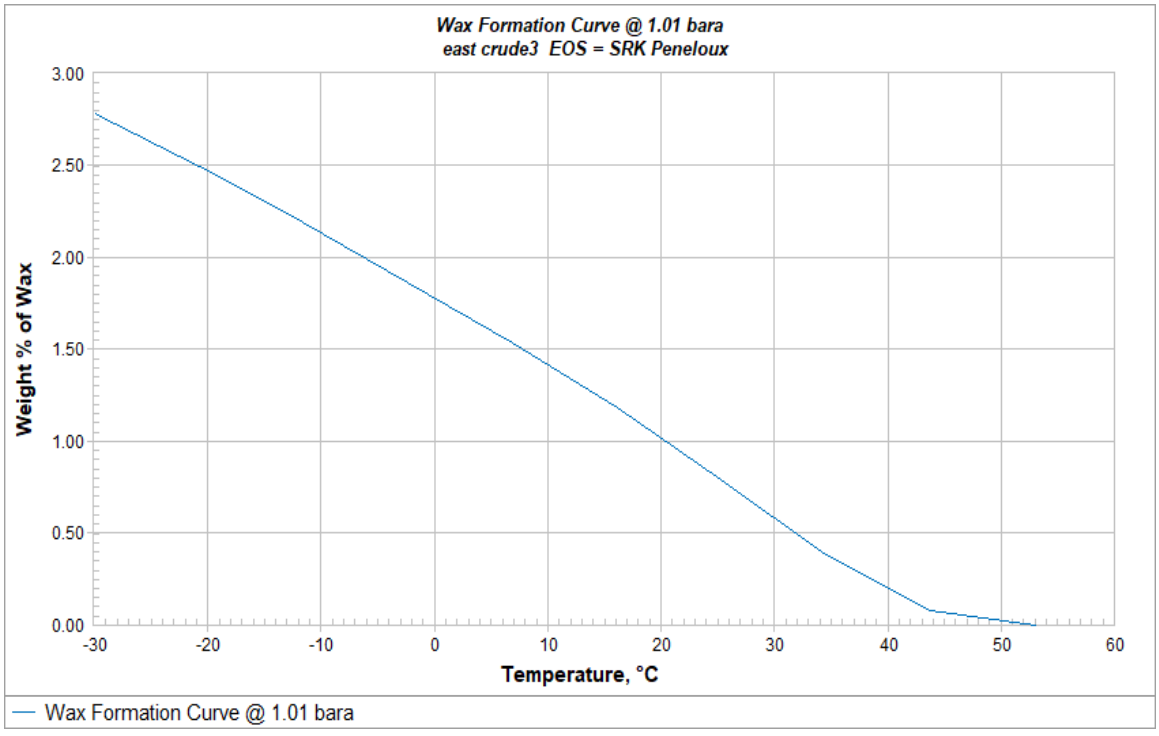

Figure 41 Wax precipitation curve for Fluid 12 calculated by PVTsim

From Figure 41 it can be noticed the model has calculated wax content of 2.8% at the temperature of -30 °C which is quite close to the value calculated with the HydraFLASH model. PVTsim model tends to linearize the wax precipitation curve, which results in giving higher values of wax content for the middle range. As a point of reference 1 wt.% of wax content is achieved at 20 °C for PVTsim while for the HydraFLASH model it reached at 7 °C range, which gives significant difference.

Experimental wax content and the wax disappearance temperature of the Fluid 13 have been presented in Table 18.

Table 18 Experimental wax content and WDT for Fluid 13

Fluid	Wax content (wt. %)	WDT (°C)	Pressure at WDT (bara)
Fluid 13	14.6	50	1.0135

For the Fluid 13, the reported experimental value of wax content is 14.6% which is significantly higher than for the previous 3 fluids, the reason of such a big difference is the nearly 10 mol % more of the heavy end C_{10+} which can be seen in Table 14 where the compositions of these dead oils were presented.

The wax model for Fluid 13 created in HydraFLASH calculated the value of 12.3 wt.% wax content at -30 °C and atmospheric pressure and the wax precipitation curve can be seen in Figure 42.

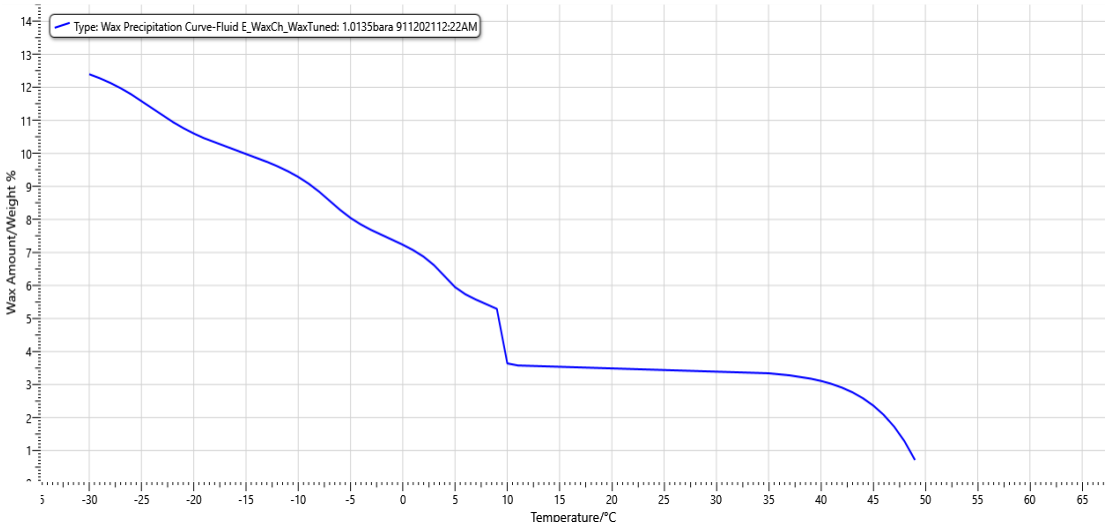

Figure 42 Wax precipitation curve for Fluid 13 calculated by HydraFLASH

The second model for Fluid 13 was created in Multiflash and the wax precipitation curve can be seen in Figure 43. As the models in Multiflash for previous 3 Fluids were giving accurate wax content prediction in comparison to experimental data it is expected the software will give quite accurate wax content for the following fluid as well.

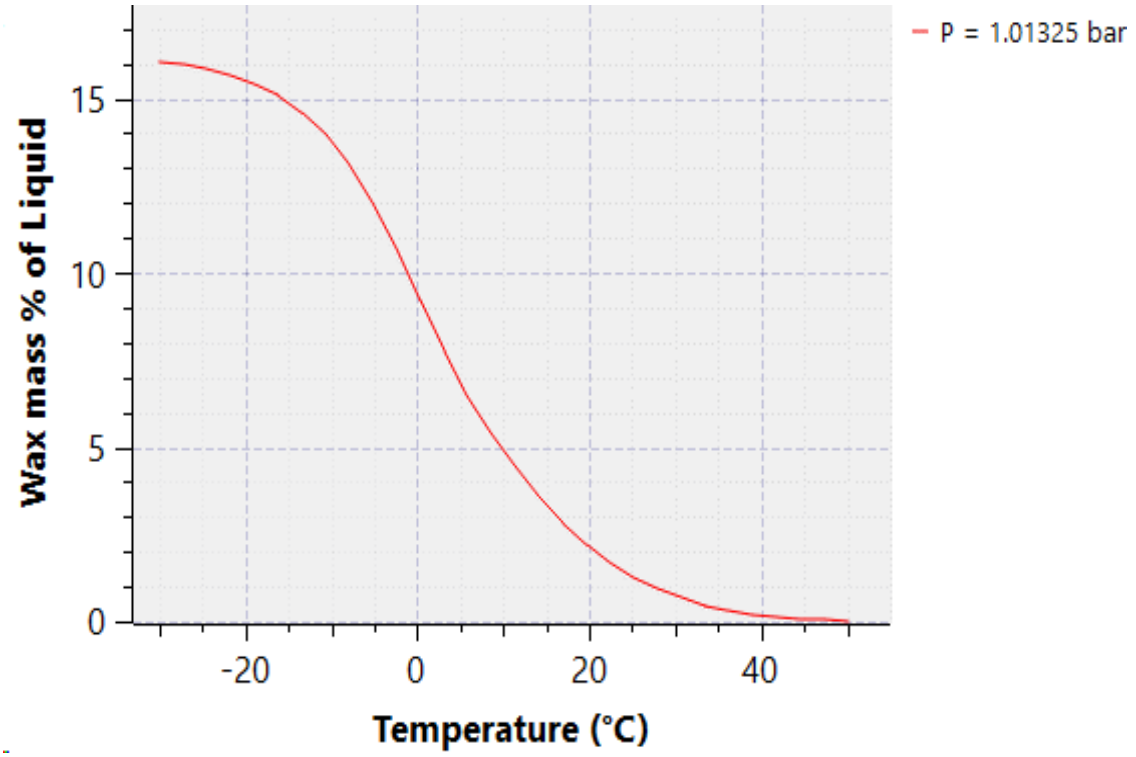

Figure 43 Wax precipitation curve for Fluid 13 calculated in Multiflash

From Figure 43 it can be noticed the Multiflash wax model has calculated wax content of 16 wt.% at -30 °C which is a difference of 1.4 wt.% of wax content in comparison to experimental data. For previous 3 Fluids the Multiflash has given accurate predictions of experimental wax content data. Model predictions for Fluid 13, when compared to previous 3 Fluids a slight composition change has happened where the heavy end of C_{10+} was slightly higher than for previous Fluids. The model has overestimated the wax content by 1.4 wt.%.

The third model has been created in PVTsim and the wax precipitation curve is presented in Figure 44.

At the temperature of -30 °C it predicted wax content of 11.5 wt.%. The difference from experimental point is 3.1% wax content. From the wax precipitation curve it can also be seen that the model has a complete linear dependency between wax content and temperature.

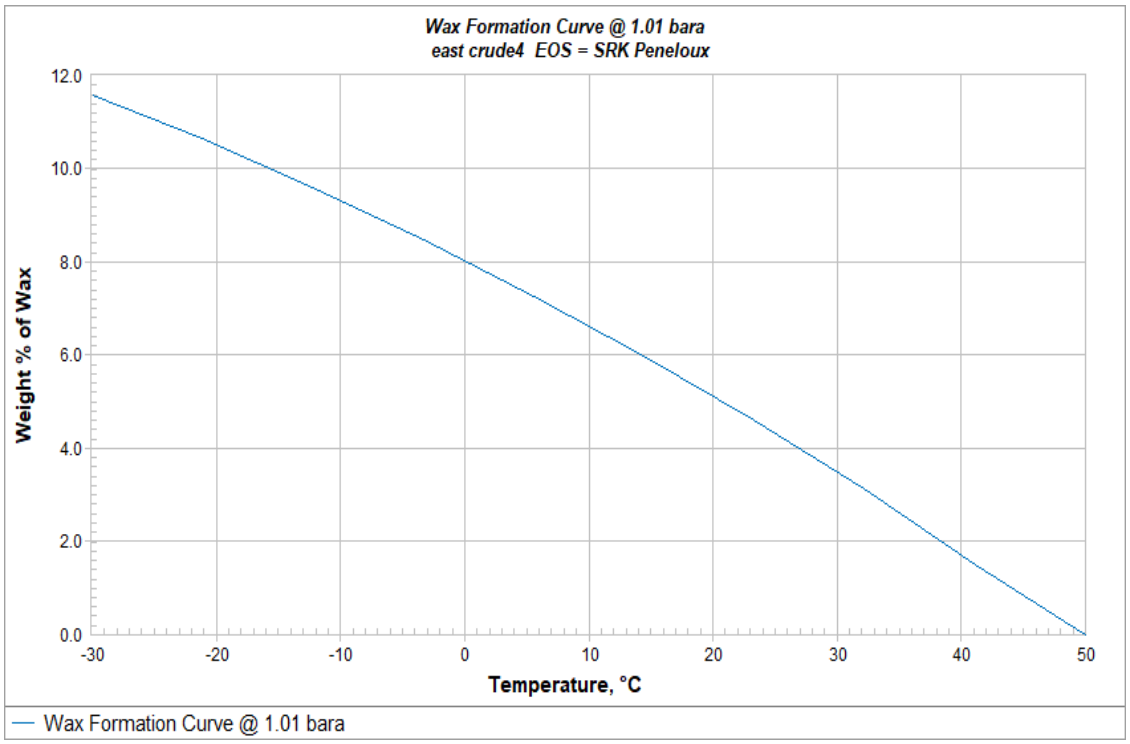

Figure 44 Wax precipitation curve for Fluid 13 calculated by PVTsim

Experimental wax content and the wax disappearance temperature for Fluid 14 have been presented in Table 19.

Table 19 Experimental wax content and WDT for Fluid 14

Fluid	Wax content (wt. %)	WDT (°C)	Pressure at WDT (bara)
Fluid 14	5	56	1.0135

In Figure 45 the wax precipitation curve calculated by HydraFLASH model for Fluid 14 has been presented.

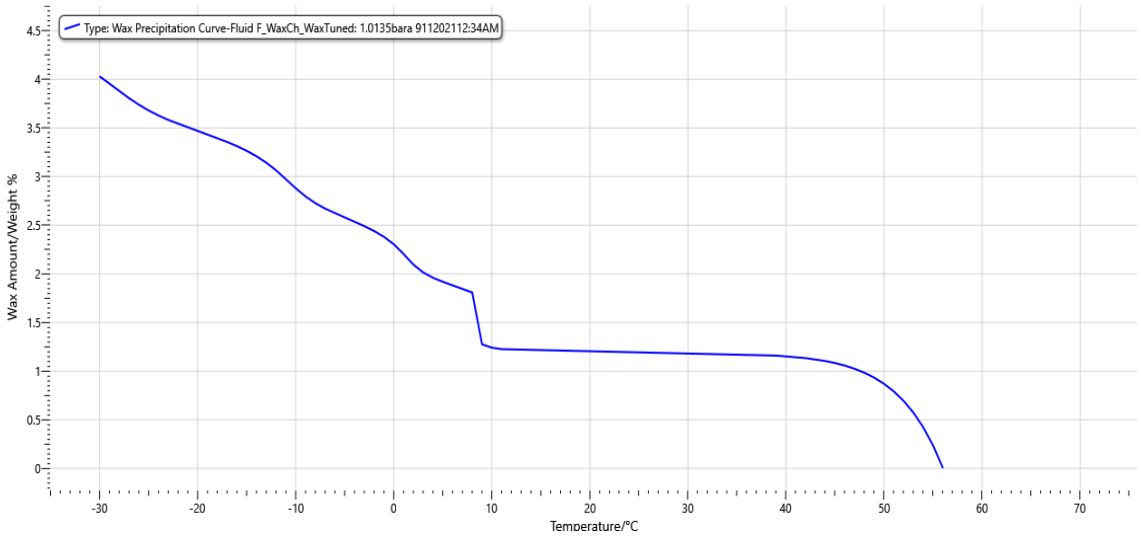

Figure 45 Wax precipitation curve for Fluid 14 calculated by HydraFLASH

According to Figure 45 at the temperature of -30 °C the wax content is 4 wt.%. On the Figure 45 it can also be noticed the model keeps the tendency to linearize the left side of the chart while it keeps almost constant the value of wax content % on the right half side.

Multiflash model has calculated the exact value of 5% wax content at the temperature of -30 °C which corresponds to the experimental value, so the model has been tuned successfully and the predicted value is in agreement with experimental value. The wax precipitation curve for this model is presented in Figure 46.

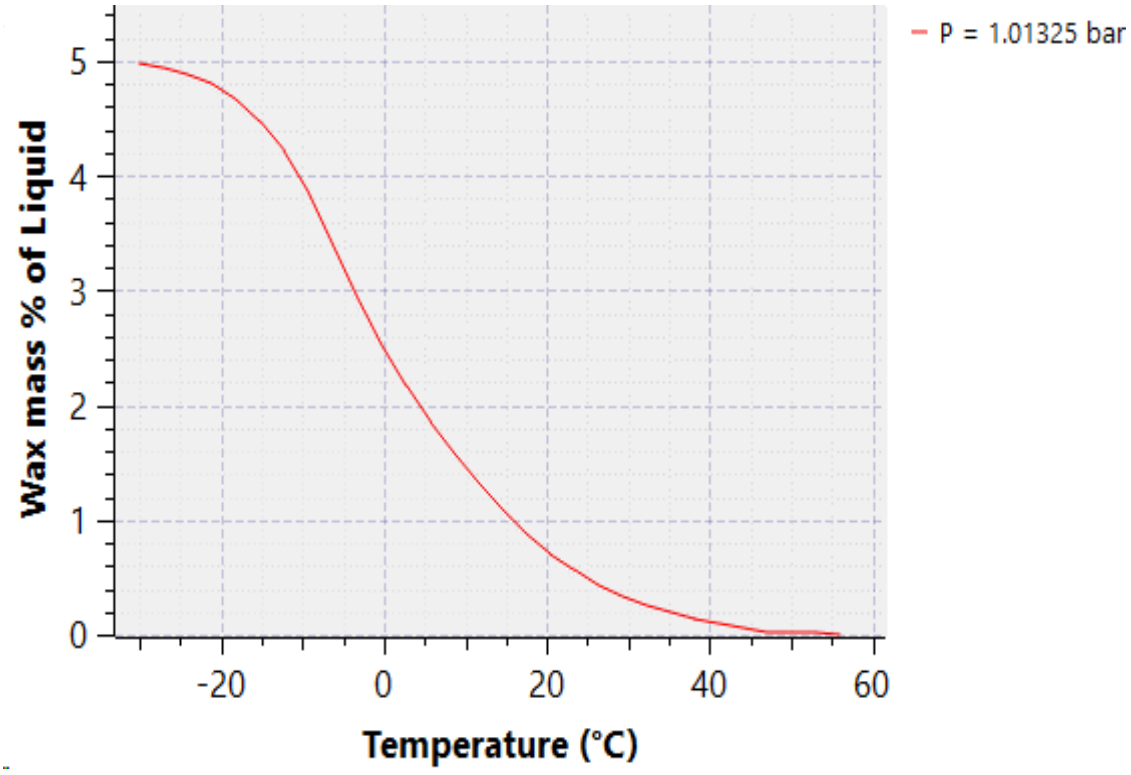

Figure 46 Wax precipitation curve for Fluid 14 calculated by PVTsim

The wax precipitation curve for Fluid 14 has been calculated by the PVTsim model and it is presented in Figure 47. From the figure it can be noticed the model predicted at temperature of -30 °C 3.9 wt.% of wax content which is quite close to HydraFLASH model.

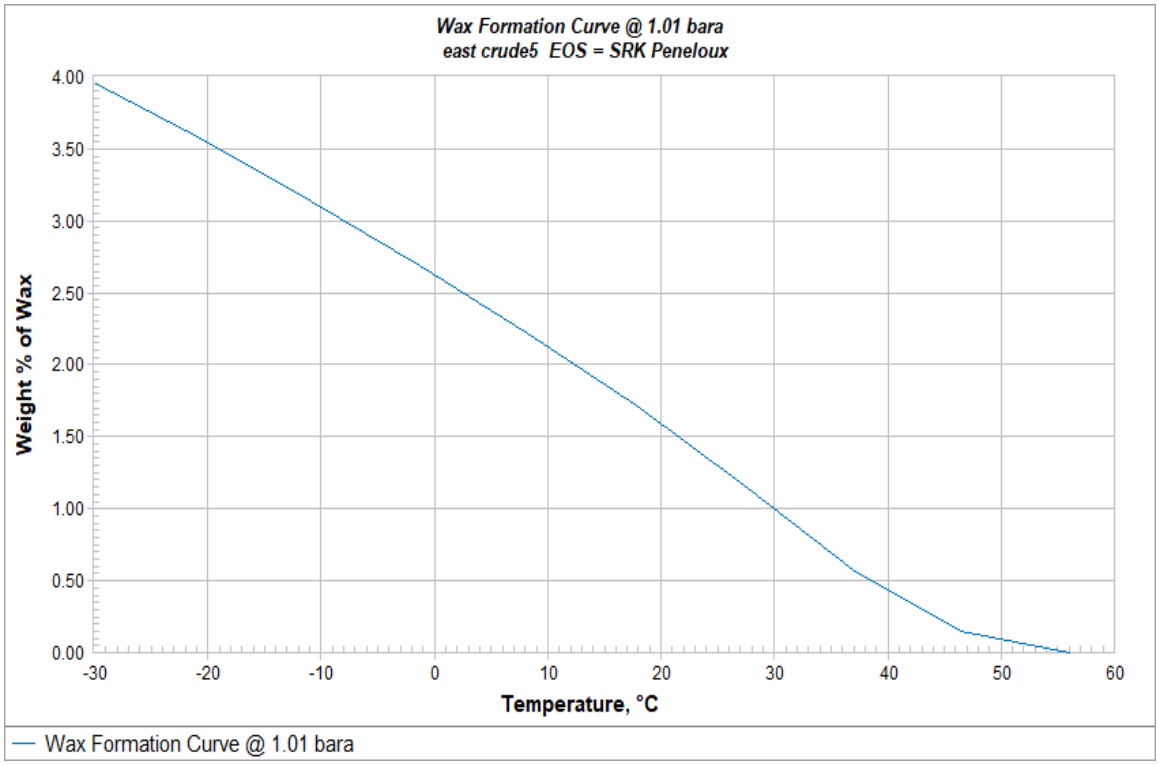

Figure 47 Wax precipitation curve for Fluid 14 calculated by PVTsim

Experimental wax content and the wax disappearance temperature of the Fluid 15 have been presented in Table 20.

Table 20 Experimental wax content and WDT for Fluid 15

Fluid	Wax content (wt. %)	WDT (°C)	Pressure at WDT (bara)
Fluid 15	6.4	42	1.0135

The HydraFLASH wax precipitation curve for Fluid 15 has been presented in Figure 48 and the wax content at -30 °C is calculated to be 4.7 wt.%. HydraFLASH model has predicted wax content of 1.5 wt.% within temperature range from 4 °C to 28 °C.

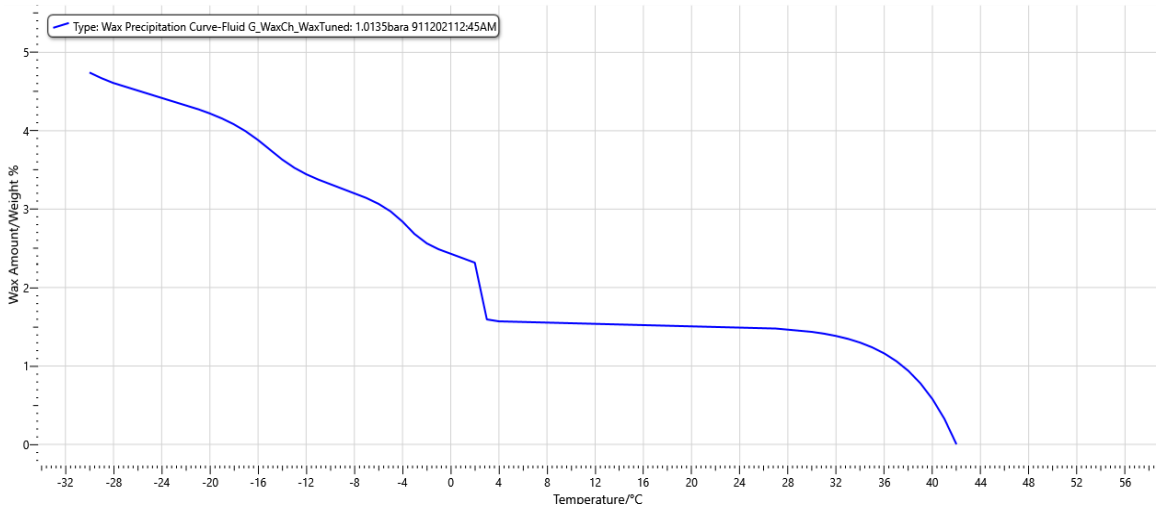

Figure 48 Wax precipitation curve for Fluid 15 calculated by HydraFLASH

Wax precipitation curve for Fluid 15 calculated by Multiflash model has been presented in Figure 49 and it can be noticed the model has matched the reported experimental data quite accurately as the wax content is 6.3 wt.% at the temperature of -30 °C and atmospheric pressure, which gives a difference of only 0.1 wt.% in wax content between experimental data and calculated one.

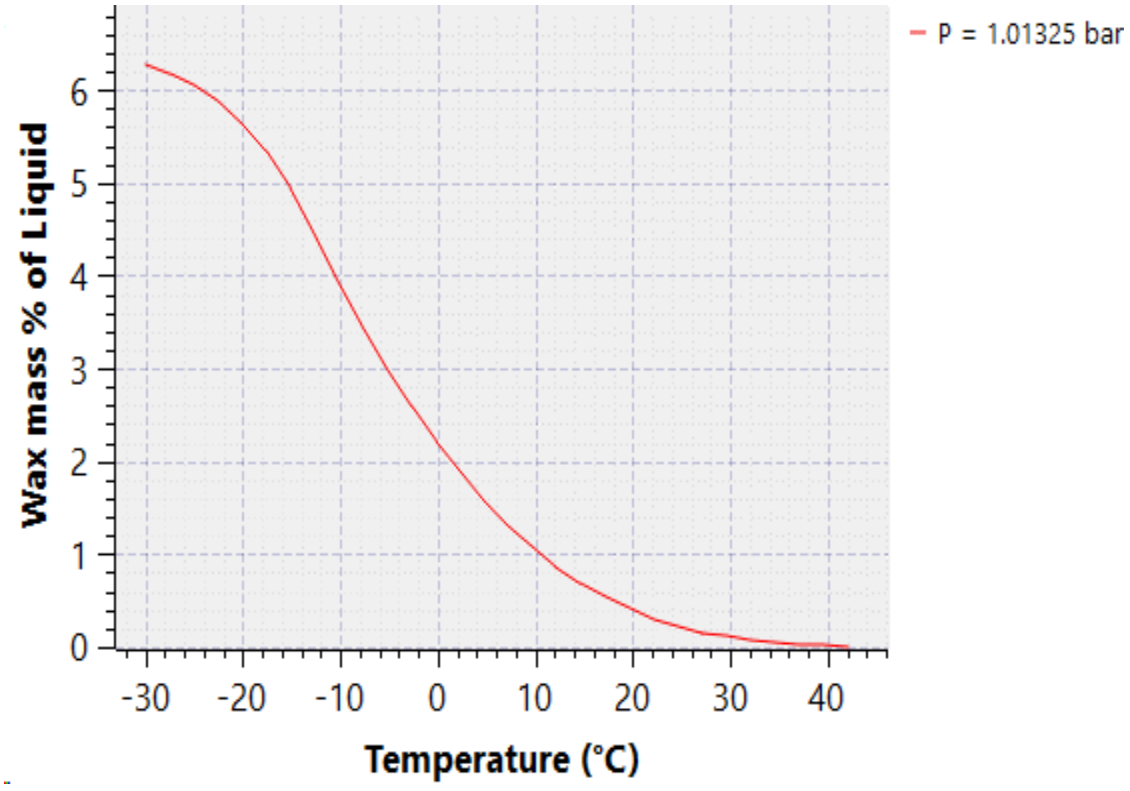

Figure 49 Wax precipitation curve for Fluid 15 calculated by Multiflash

In Figure 50 wax precipitation curve for Fluid 15 calculated by PVTsim model has been presented. Analyzing the figure, linear dependency of the model between temperature and wax

content can be seen and as well the wax content of 5 wt.% at the temperature of -30 °C and atmospheric pressure. The PVTsim model predicted 0.3 wt.% more wax content than the HydraFLASH model that calculated 4.7 wt.% of wax content on same conditions.

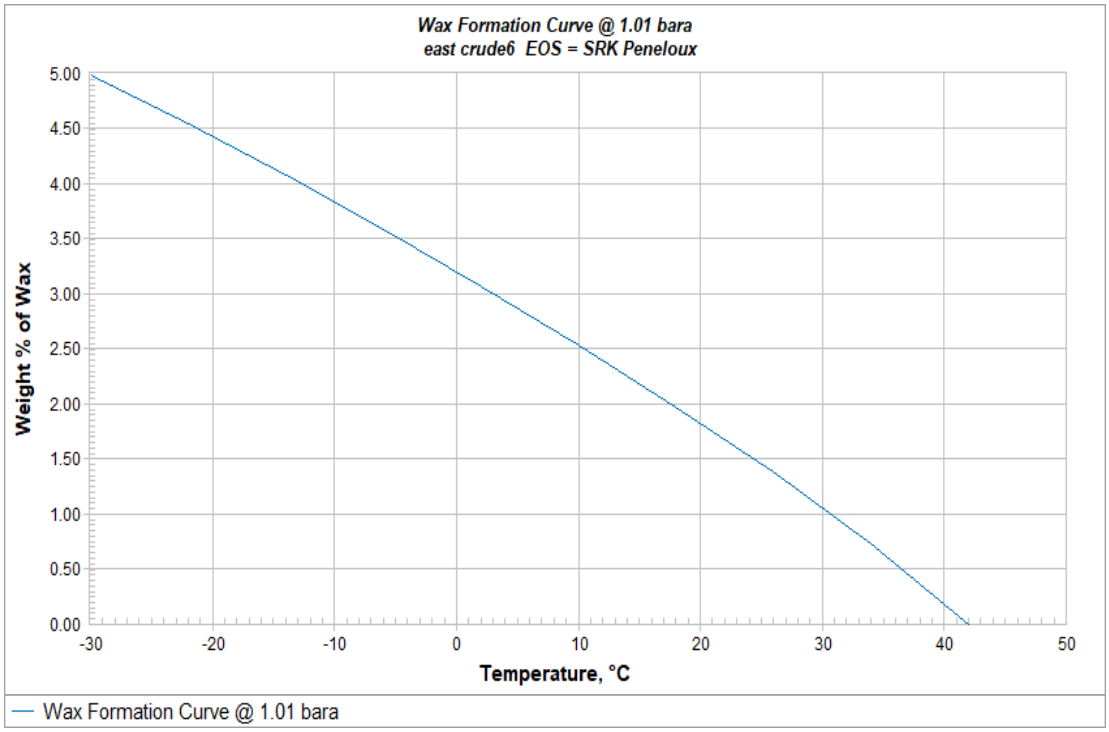

Figure 50 Wax precipitation curve for Fluid 15 calculated by PVTsim

The experimental wax content and the wax disappearance temperature of the Fluid 16 have been presented in Table 21.

Table 21 Experimental wax content and WDT for Fluid 16

Fluid	Wax content (wt. %)	WDT (°C)	Pressure at WDT (bara)
Fluid 16	7.1	45	1.0135

Wax precipitation curve for Fluid 16 calculated by the HydraFLASH model has been presented in Figure 51.

The model has calculated the wax content of 5.5 wt.% at -30 °C.

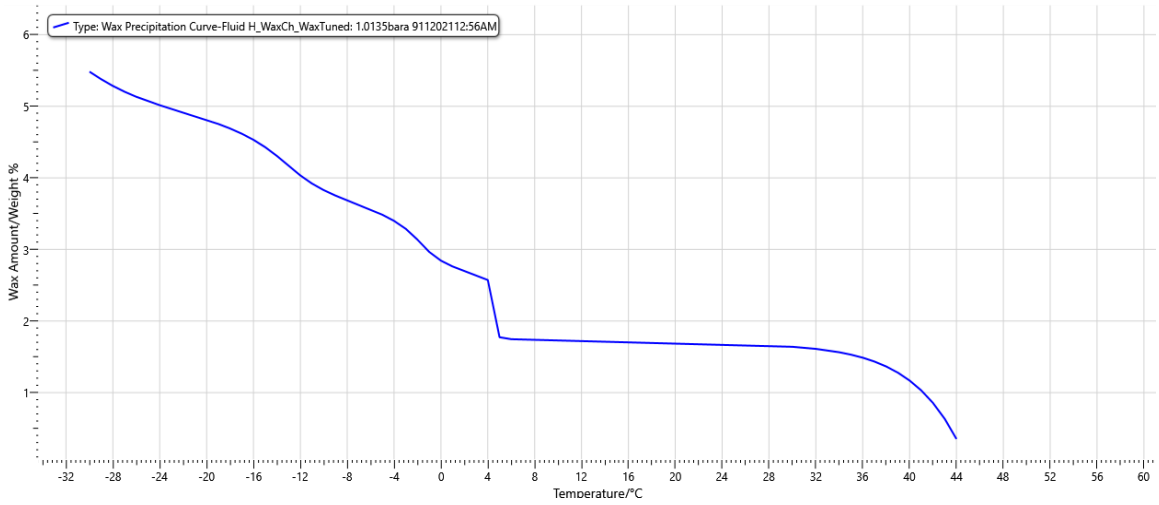

Figure 51 Wax precipitation curve for Fluid 16 calculated by HydraFLASH

In Figure 52 the wax precipitation curve for Multiflash model has been presented. It can be noticed from the Figure that the model has matched the reported experimental data of 7.1 wt. % wax content at -30 °C and atmospheric pressure.

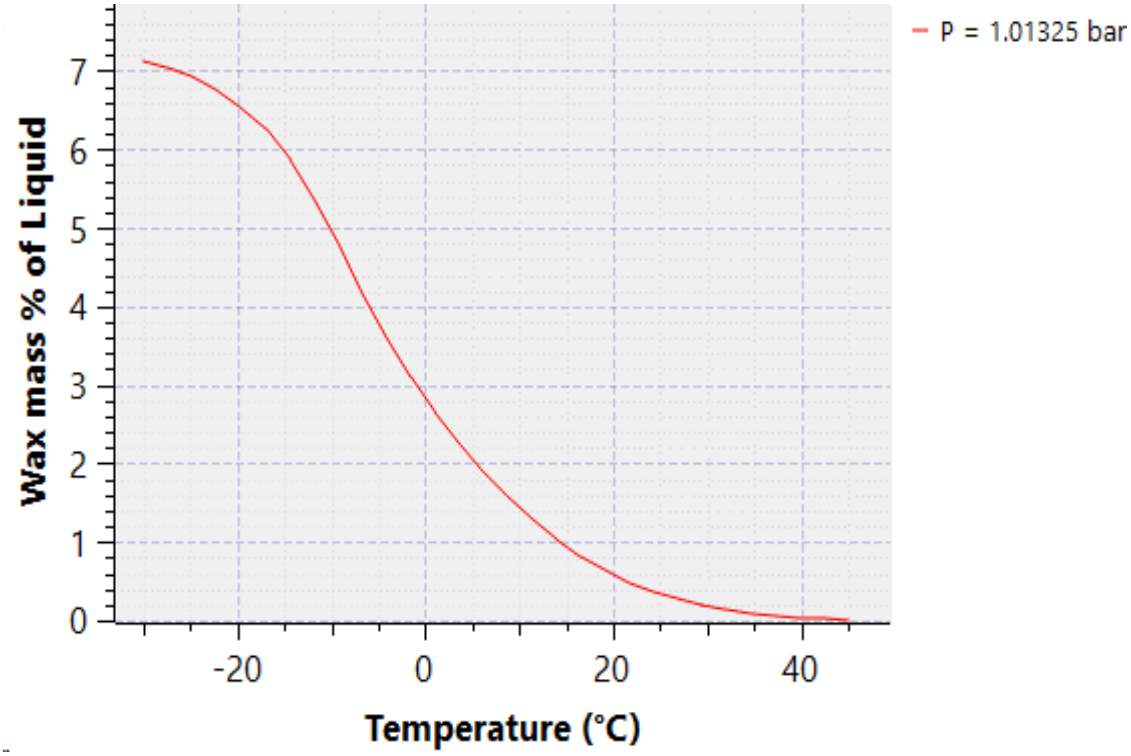

Figure 52 Wax precipitation curve for Fluid 16 calculated by Multiflash

As the model has given once again the satisfactory match, apart from the Fluid 13 where the model overestimated the wax content, it can be concluded the Multiflash simulator is giving quite accurate results for calculating wax content.

Finally, the PVTsim wax precipitation curve for Fluid 16 is presented in Figure 53. From the Figure it can be noticed the model has calculated wax content of 5.85 wt.% at -30 °C and atmospheric pressure.

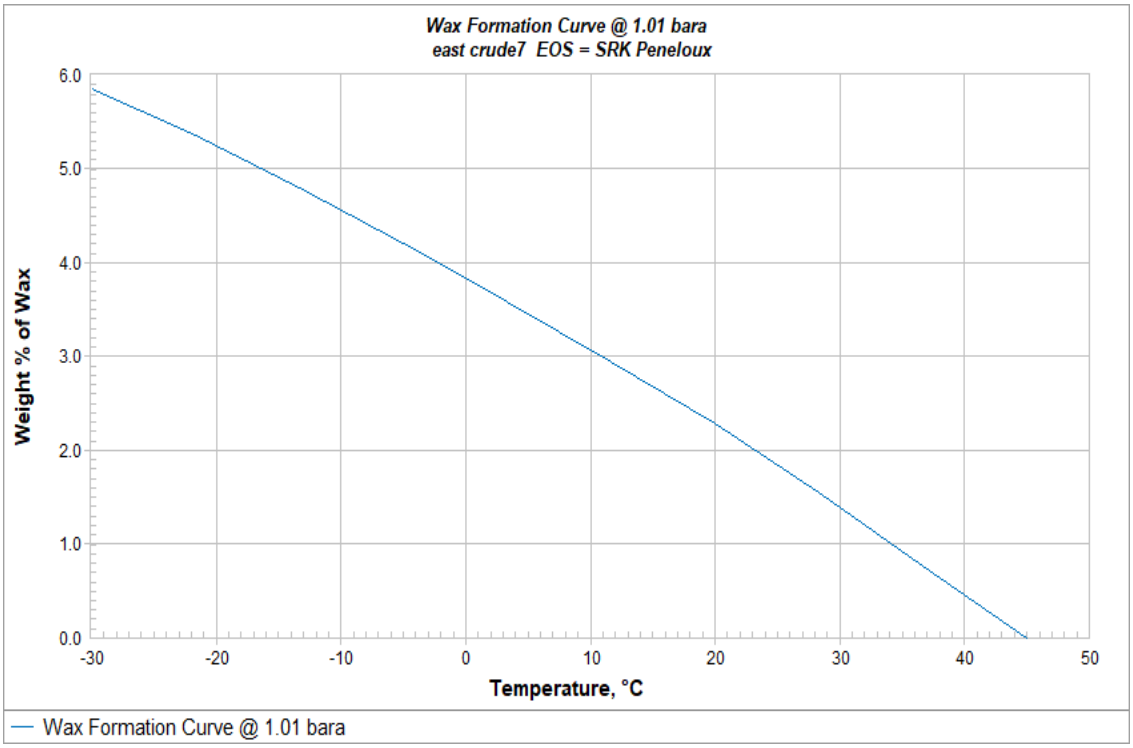

Figure 53 Wax precipitation curve for Fluid 16 calculated by PVTsim

Analyzing the figure, it can be confirmed the model tends to give linear dependency of wax content with temperature for dead oils of such compositions that have wax disappearance temperatures below 50 °C and like HydraFLASH it reports the wax content with respect to entire system, and not liquid only like Multiflash.

8. Conclusions

The scope of the thesis was to evaluate various wax models in order to compare three commercial PVT simulators.

The analysis of live oils has shown that when faced with a great deal of experimental values, Multiflash simulator completes the tuning faster than HydraFLASH or PVTsim. However, the accuracy of Multiflash model tuning with many experimental points is questionable, as it was seen from analysis of live Fluids where the model did not match with experimental data successfully.

When dead oils were compared, all three simulators gave good results with matching to experimental values. It has also been observed that the PVTsim shifts the wax phase boundary to lower temperatures in comparison to HydraFLASH and Multiflash.

In the last section wax content calculations were analyzed. Experimental values of wax content are reported with respect to liquid of the system as the wax content is measured on dead oil. The predictions of wax content in Multiflash are reported with respect to liquid, so the model predictions were compared with experimental data and it was noticed that Multiflash has successfully predicted the wax content values. However, the software does not allow user to choose wax content reported with respect to the whole system. On the other hand, HydraFLASH and PVTsim report wax content with respect to the whole system which is the reason values of predicted wax content were lower than experimental wax content data. Both PVTsim and HydraFLASH do not have option to report wax content with respect to liquid only which could be useful for comparison of simulators.

It was seen that the PVTsim wax model prediction linearizes the wax content with temperature and provides similar matching to experimental values as HydraFLASH. However, HydraFLASH did not linearize the wax precipitation curve, instead the wax content predictions are almost constant for certain range of temperature. Investigating the cause might be one of recommendations for future work.

When wax appearance calculations were compared, Multiflash and HydraFLASH have provided different results than PVTsim possibly due to difference of wax model and EoS used. However, regarding the wax content analysis, HydraFLASH and Multiflash both use same wax models and yet they provided different shapes of wax precipitation curves which is interesting observation, and it requires more investigation as the data available for this work was limited.

Recommendation for future work is finding more data and investigating simulators performance on various conditions which would make it possible to conclude which software performs better under which conditions.

References

Lee, H. S. (2008). Computational and Rheological Study of Wax Deposition and Gelation in Subsea Pipelines. 127.

Golczynski, T.S. and Kempton, E.C. (2006) Understanding Wax Problems Leads to Deepwater Flow Assurance Solutions. World Oil, 227, 7-10.

Singh, P., R. Venkatesan, H.S. Fogler, and N.R. Nagarajan, "Formation and Aging of Incipient Thin Film Wax-Oil Gels," AIChE J. 46, 1059 (2000).

Southgate, J .(2004). Wax removal using pipeline pigs. 296. http://etheses.dur.ac.uk/2995/1/2995_1018.pdf

Pedersen, K. S., & Rønningsen, H. P. (2003). Influence of wax inhibitors on wax appearance temperature, pour point, and viscosity of waxy crude oils. *Energy and Fuels*, *17*(2), 321–328. https://doi.org/10.1021/ef020142+

Bishop, A.N., Philip, R.P., Allen, J., and Ruble, T.E., High molecular weight hydrocarbons and the precipitation of petroleum-derived waxes. In *Organic Geochemistry: Development and Applications to Energy, Climate, Environment and Human History*, Grimalt, J.O. and Dorronsoro, C., Eds., AIGOA, Donoslia-San Sebastian, Spain, 1995.

Nguyen, D. A., Ph.D. Thesis, University of Michigan 2004.

Mahabadian, M. A. (2016). Solid-Fluid Phase Equilibria Modelling in Wax , Hydrate and Combined Wax-Hydrate Forming Systems Petroleum Engineering Institute of Petroleum Engineering. November.

Ji, H. (2004). Thermodynamic modelling of wax and integrated wax-hydrate.

Hammami, A., & Raines, M. A. (1999). Paraffin deposition from crude oils: Comparison of laboratory results with field data. *SPE Journal*, *4*(1), 9–18. https://doi.org/10.2118/54021-PA

Mansourpoor, M., Azin, R., Osfouri, S., & Izadpanah, A. A. (2019). Study of wax disappearance temperature using multi-solid thermodynamic model. *Journal of Petroleum Exploration and Production Technology*, *9*(1), 437–448. https://doi.org/10.1007/s13202-018-0480-1

Elsharkawy, A. M., Al-Sahhaf, T. A., & Fahim, M. A. (2000). Wax deposition from Middle East crudes. *Fuel*, *79*(9), 1047–1055. https://doi.org/10.1016/S0016-2361(99)00235-5

9. APPENDIX

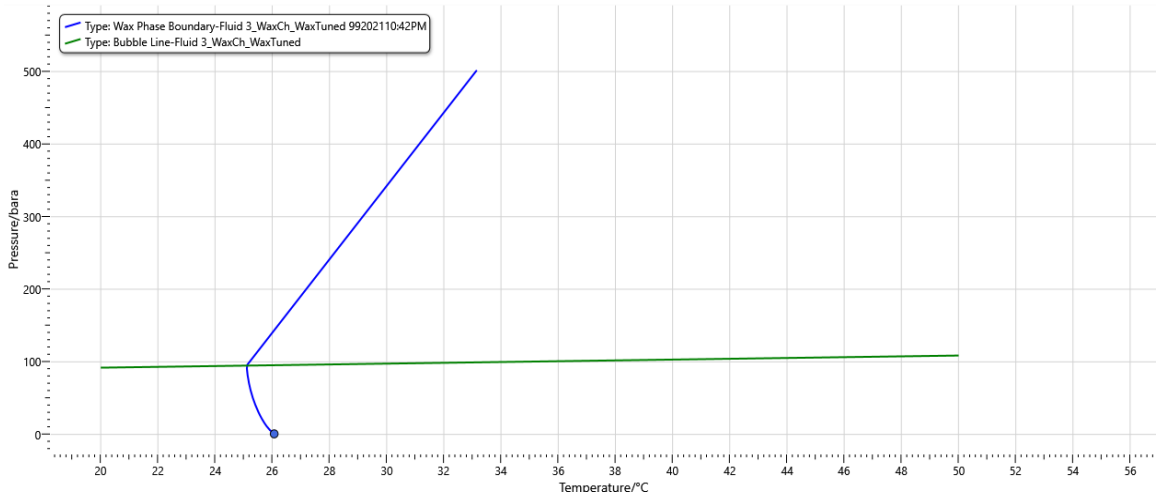

Figure A 1 Wax phase boundary for Fluid 3 calculated by HydraFLASH

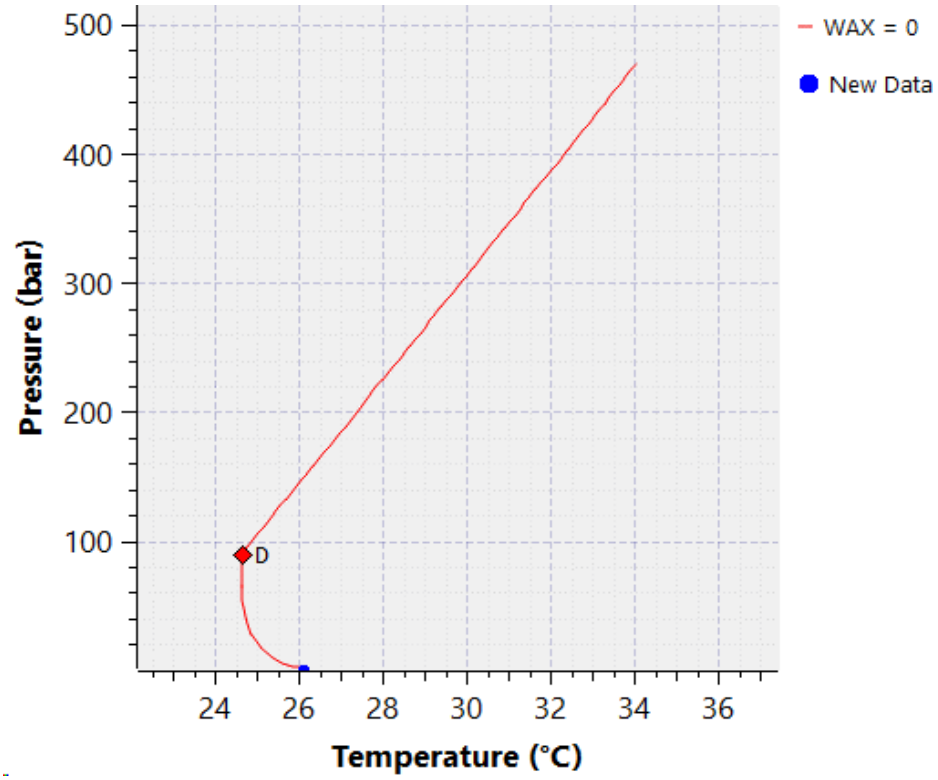

Figure A 2 Wax phase boundary for Fluid 3 calculated by Multiflash

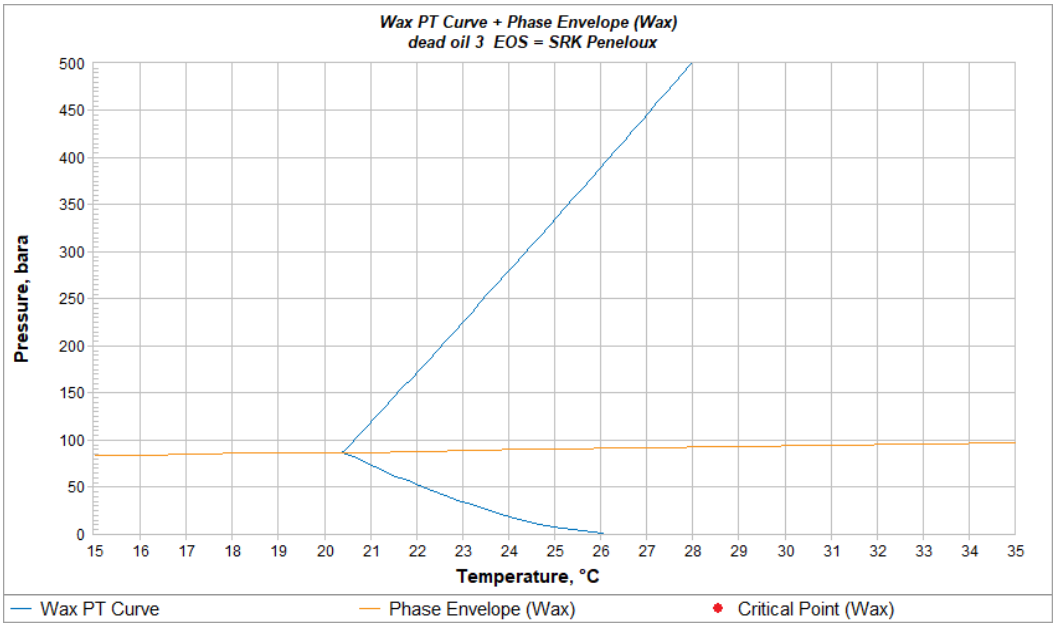

Figure A 3 Wax phase boundary for Fluid 3 calculated by PVTsim

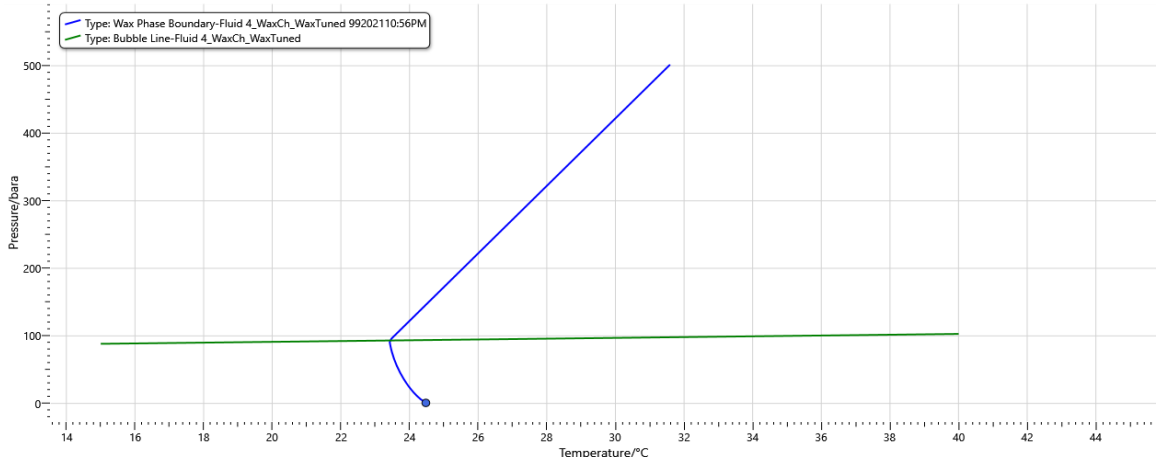

Figure A 4 Wax phase boundary for Fluid 4 calculated by HydraFLASH

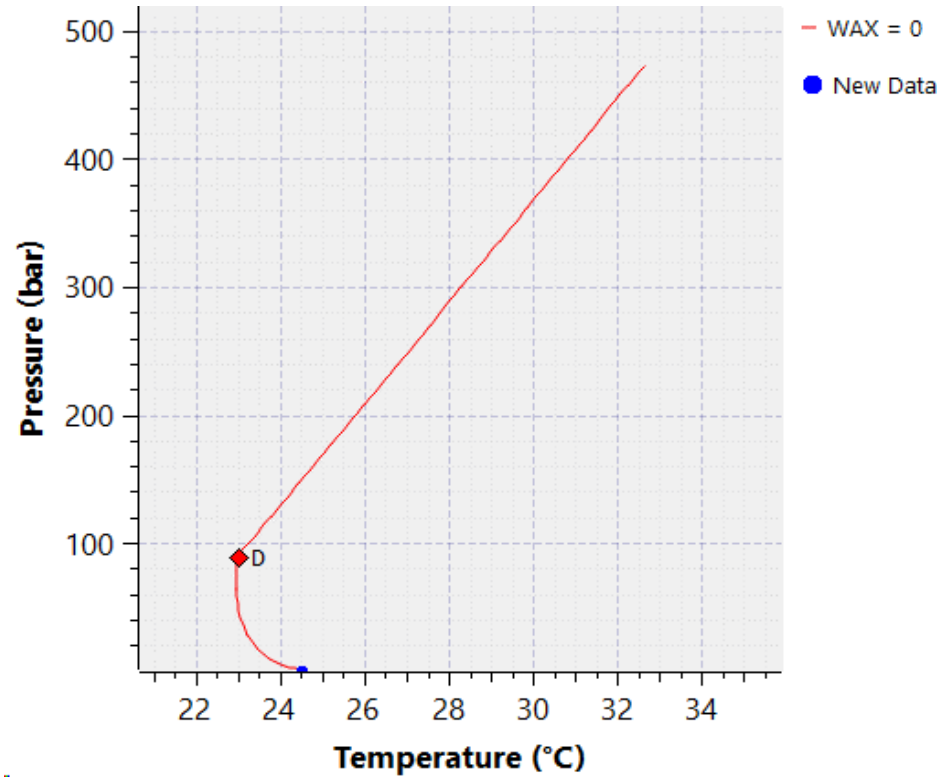

Figure A 5 Wax phase boundary for Fluid 4 calculated by Multiflash

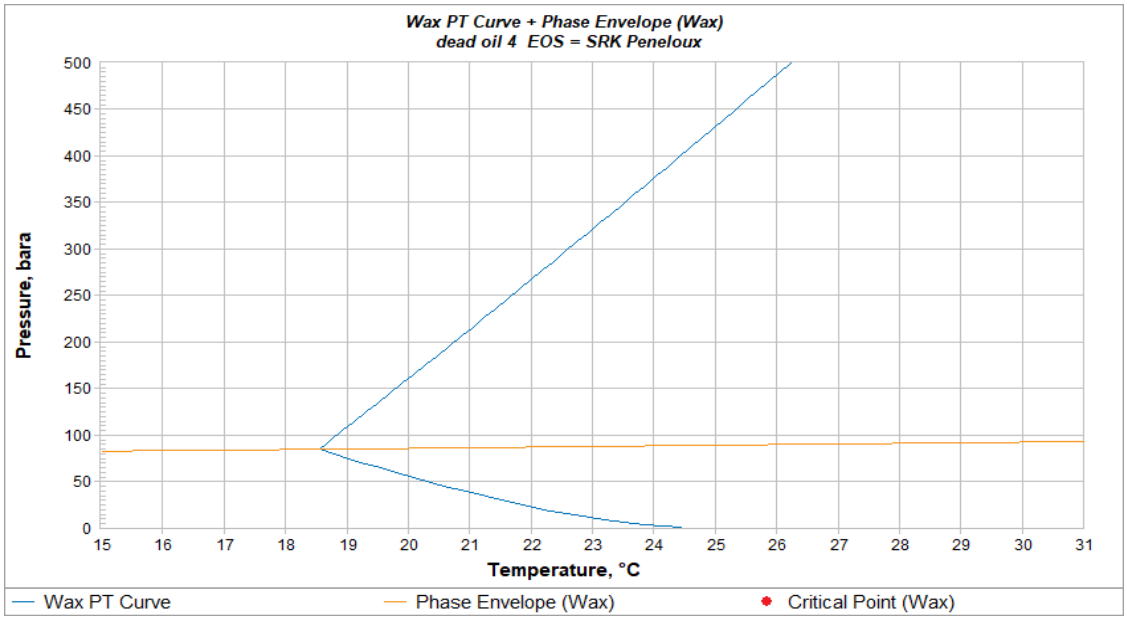

Figure A 6 Wax phase boundary for Fluid 4 calculated by PVTsim

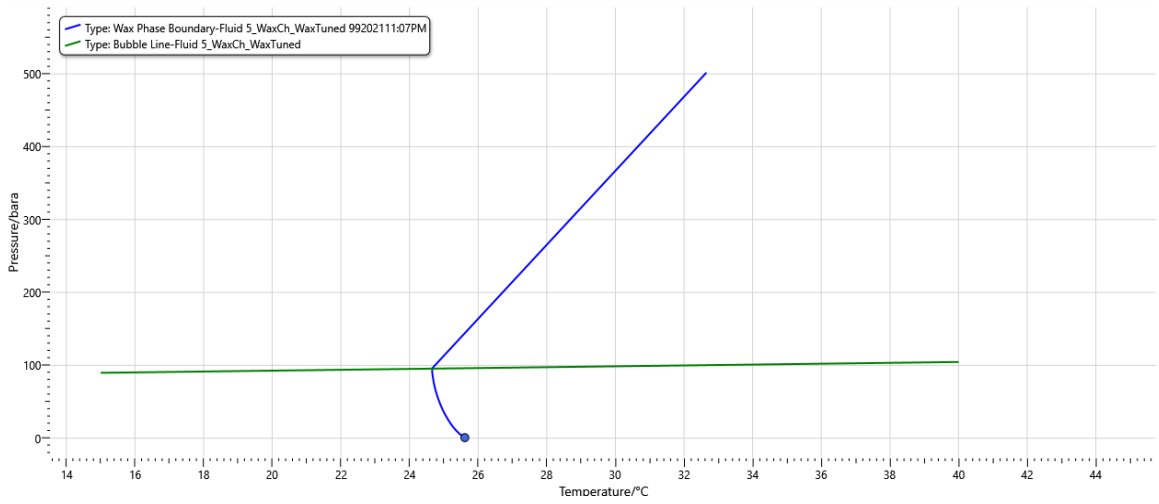

Figure A 7 Wax phase boundary for Fluid 5 calculated by HydraFLASH

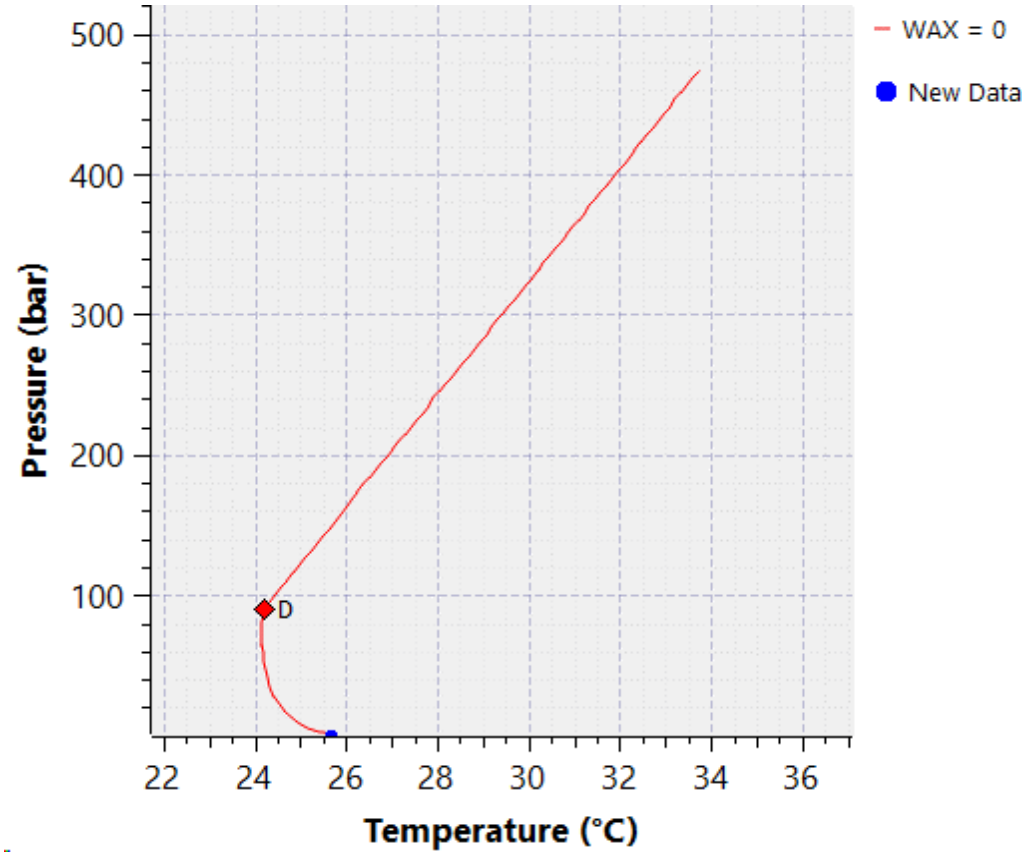

Figure A 8 Wax phase boundary for Fluid 5 calculated by Multiflash

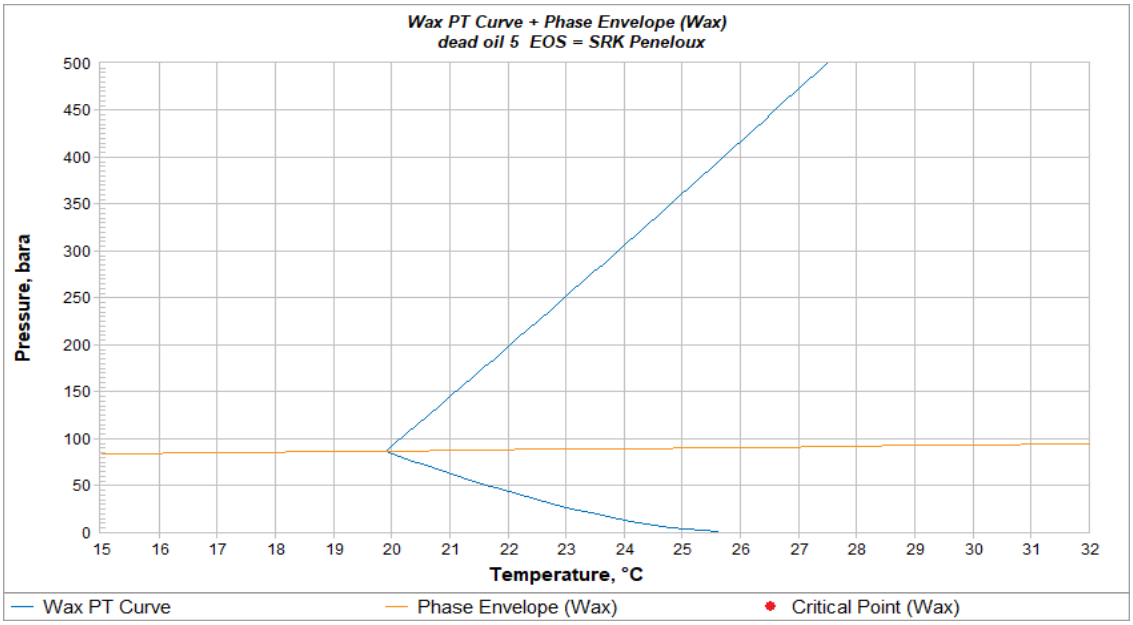

Figure A 9 Wax phase boundary for Fluid 5 calculated by PVTsim

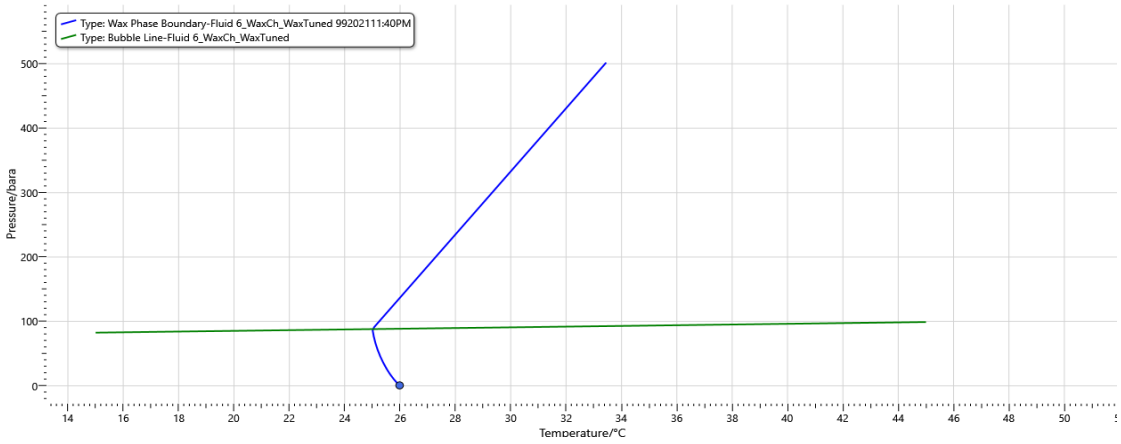

Figure A 10 Wax phase boundary for Fluid 6 calculated by HydraFLASH

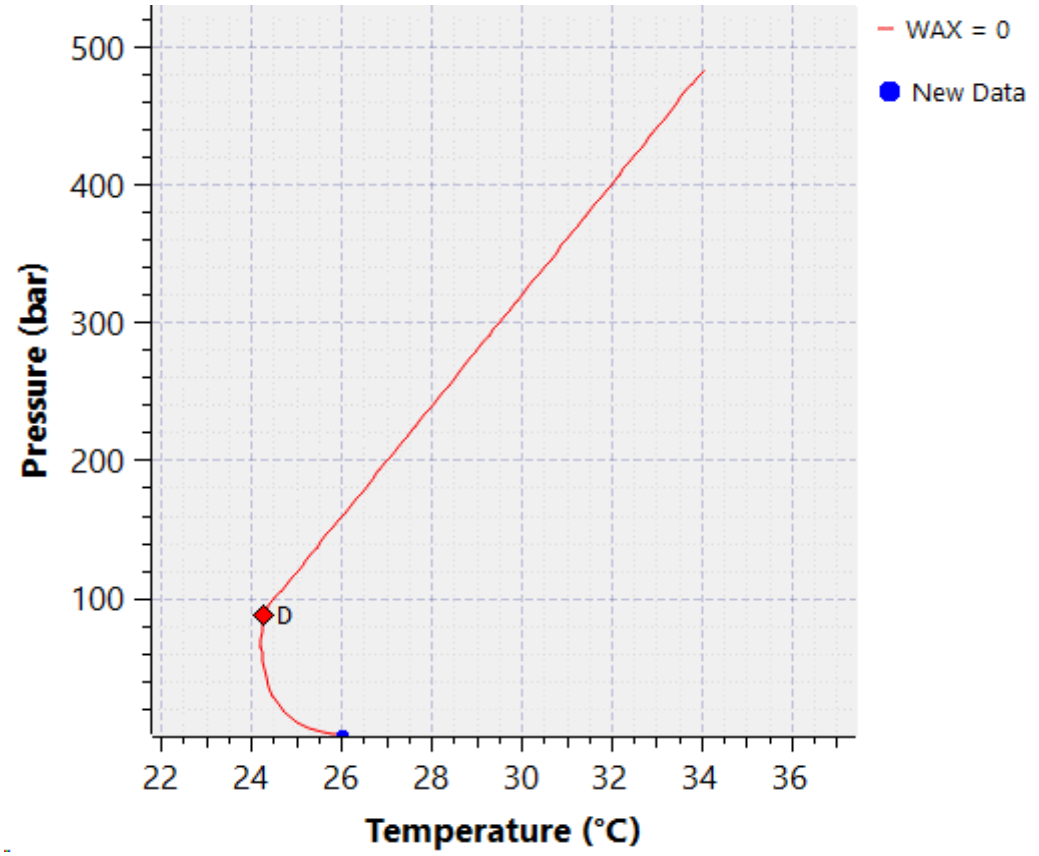

Figure A 11 Wax phase boundary for Fluid 6 calculated by Multiflash

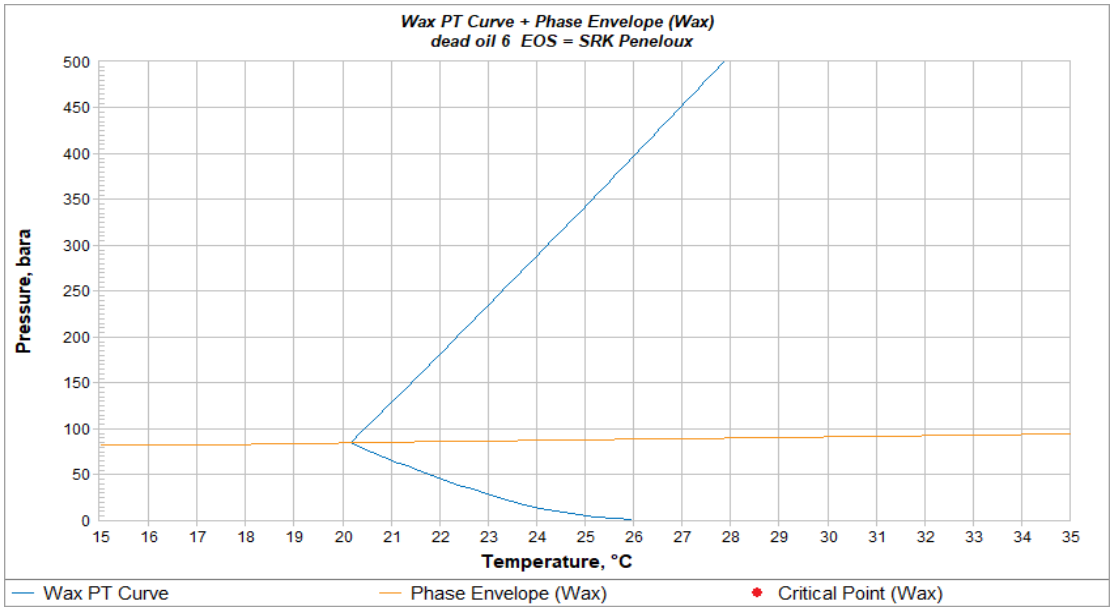

Figure A 12 Wax phase boundary for Fluid 6 calculated by PVTsim

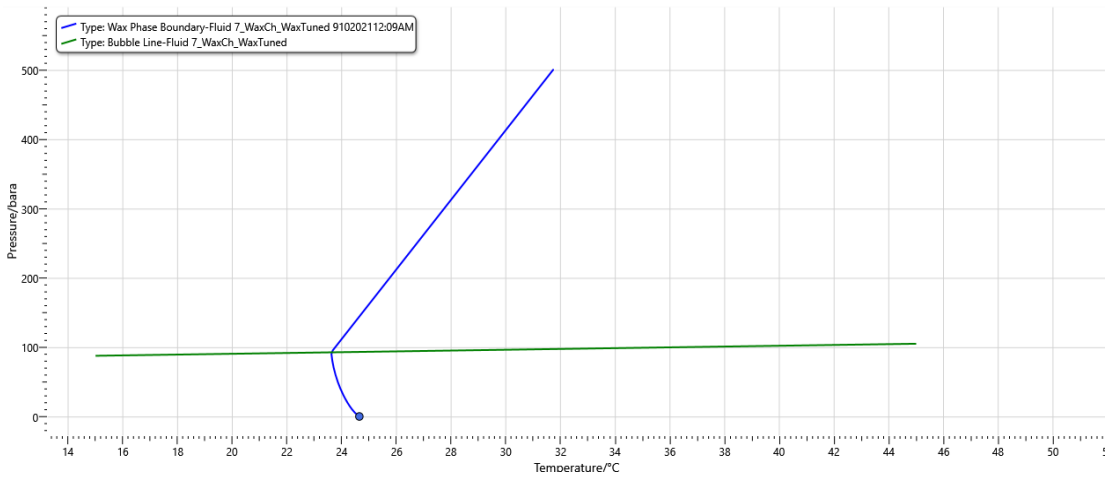

Figure A 13 Wax phase boundary for Fluid 7 calculated by HydraFLASH

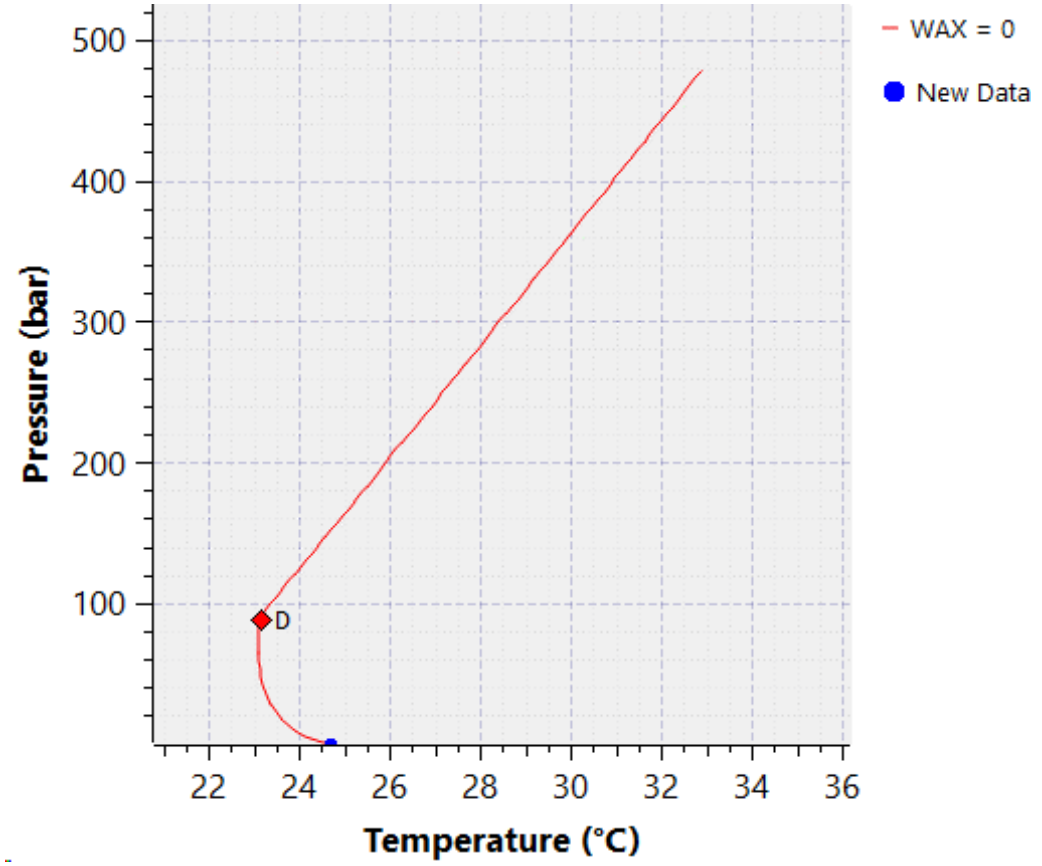

Figure A 14 Wax phase boundary for Fluid 7 calculated by Multiflash

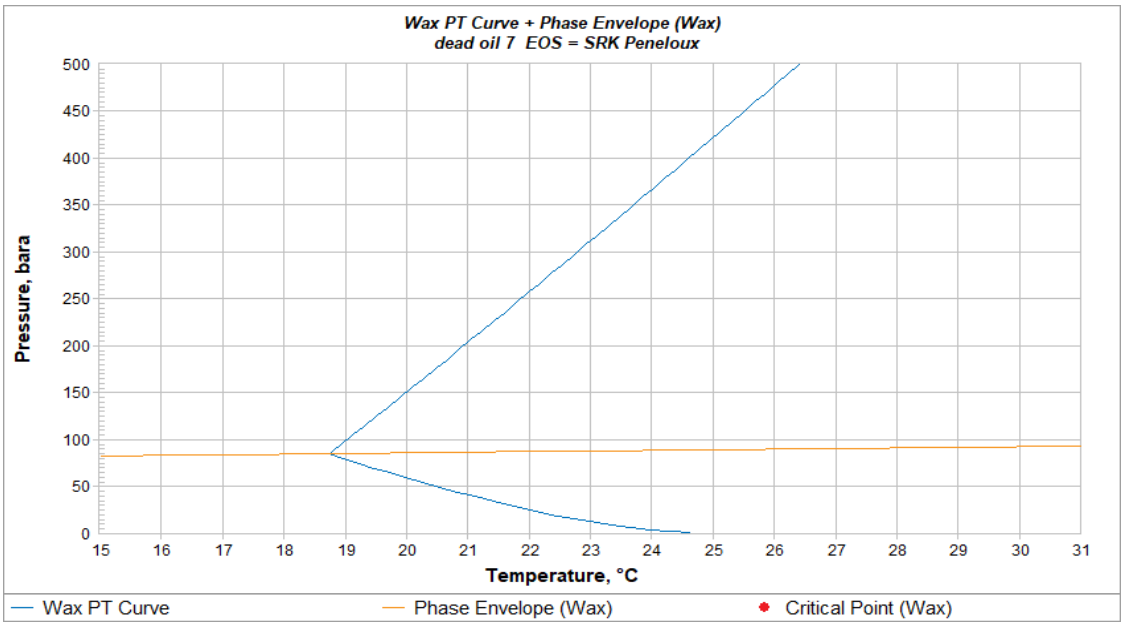

Figure A 15 Wax phase boundary for Fluid 7 calculated by PVTsim

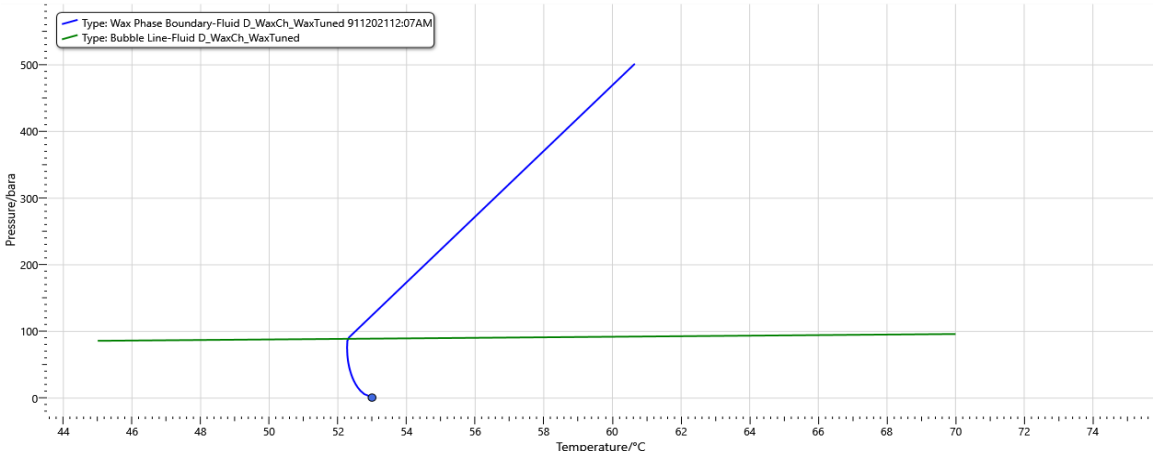

Figure A 16 Wax phase boundary for Fluid 12 calculated by HydraFLASH

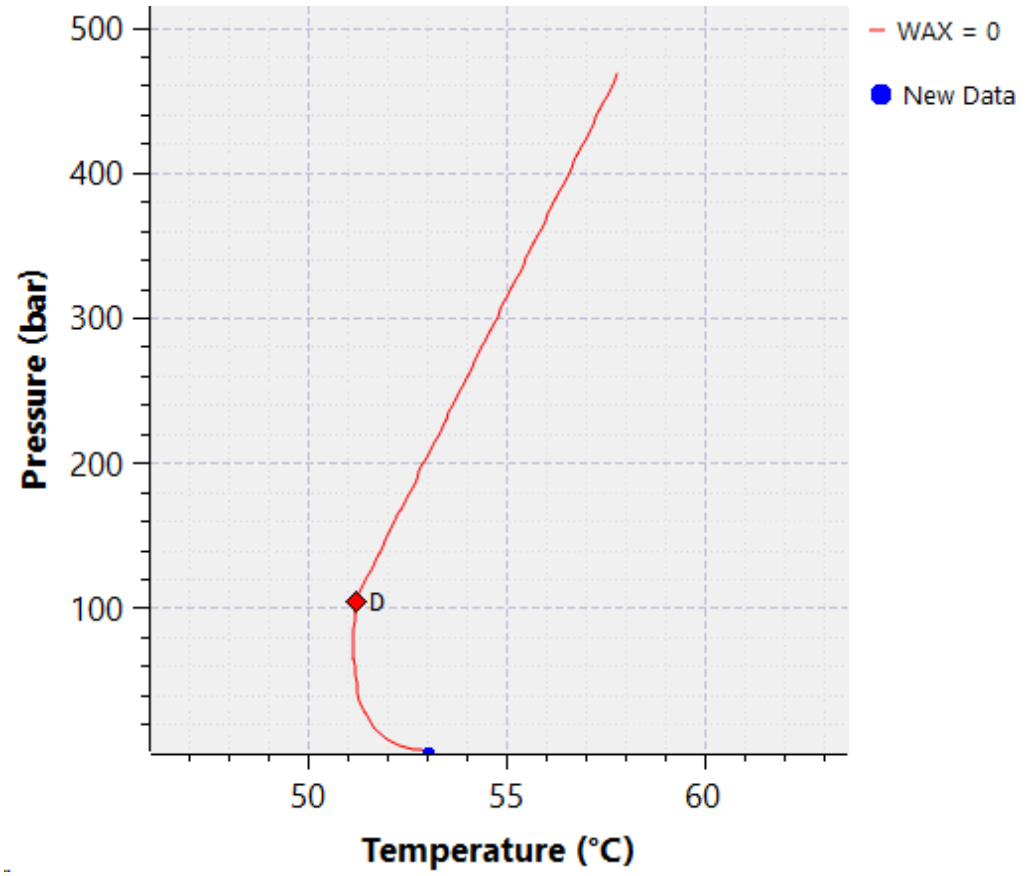

Figure A 17 Wax phase boundary for Fluid 12 calculated by Multiflash

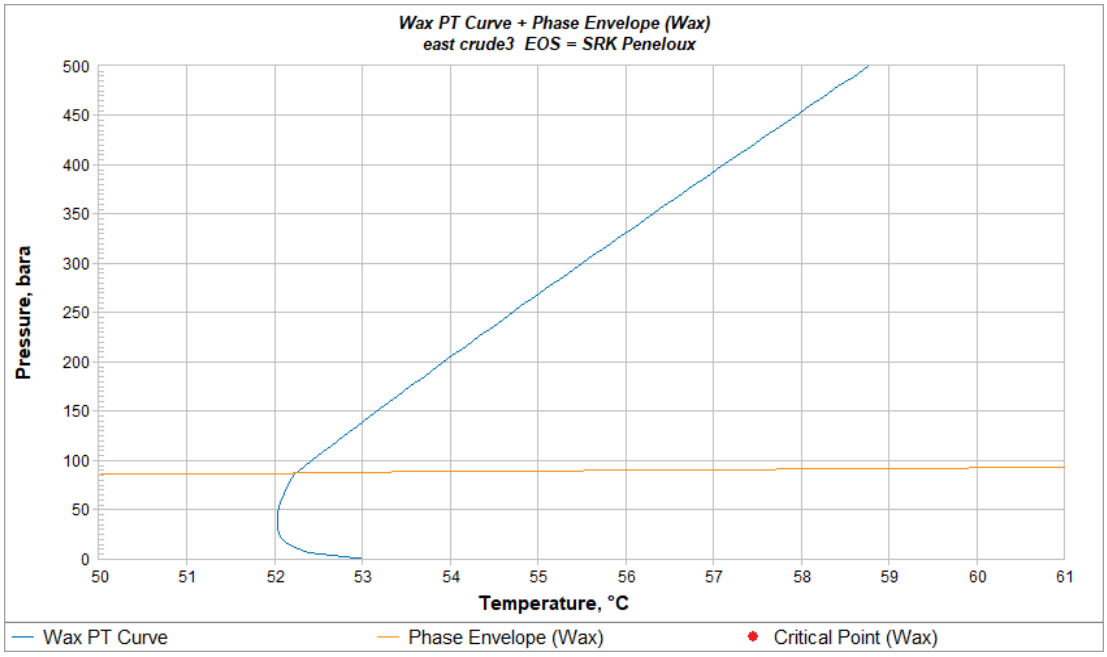

Figure A 18 Wax phase boundary for Fluid 12 calculated by PVTsim

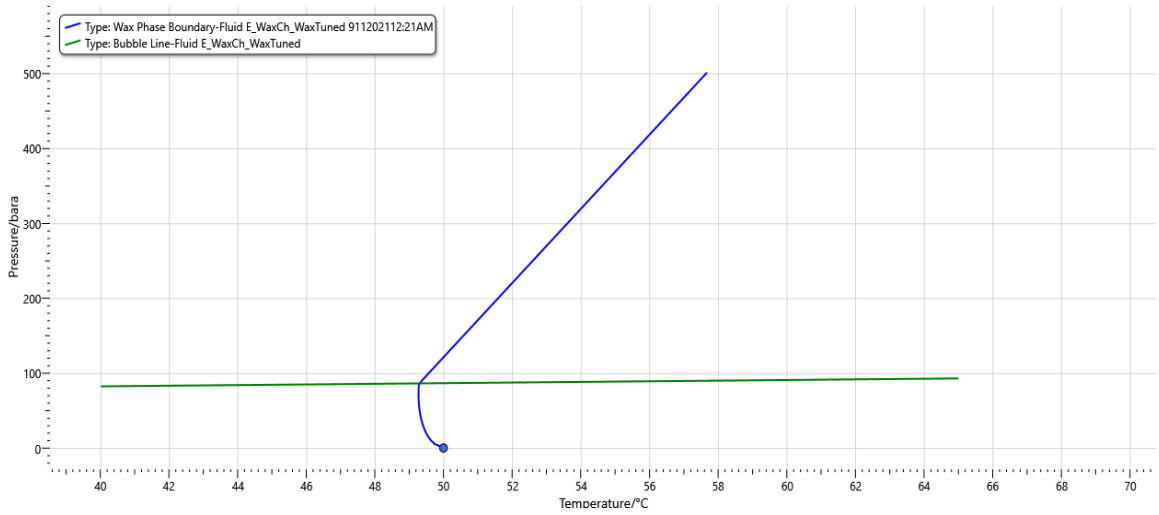

Figure A 19 Wax phase boundary for Fluid 13 calculated by HydraFLASH

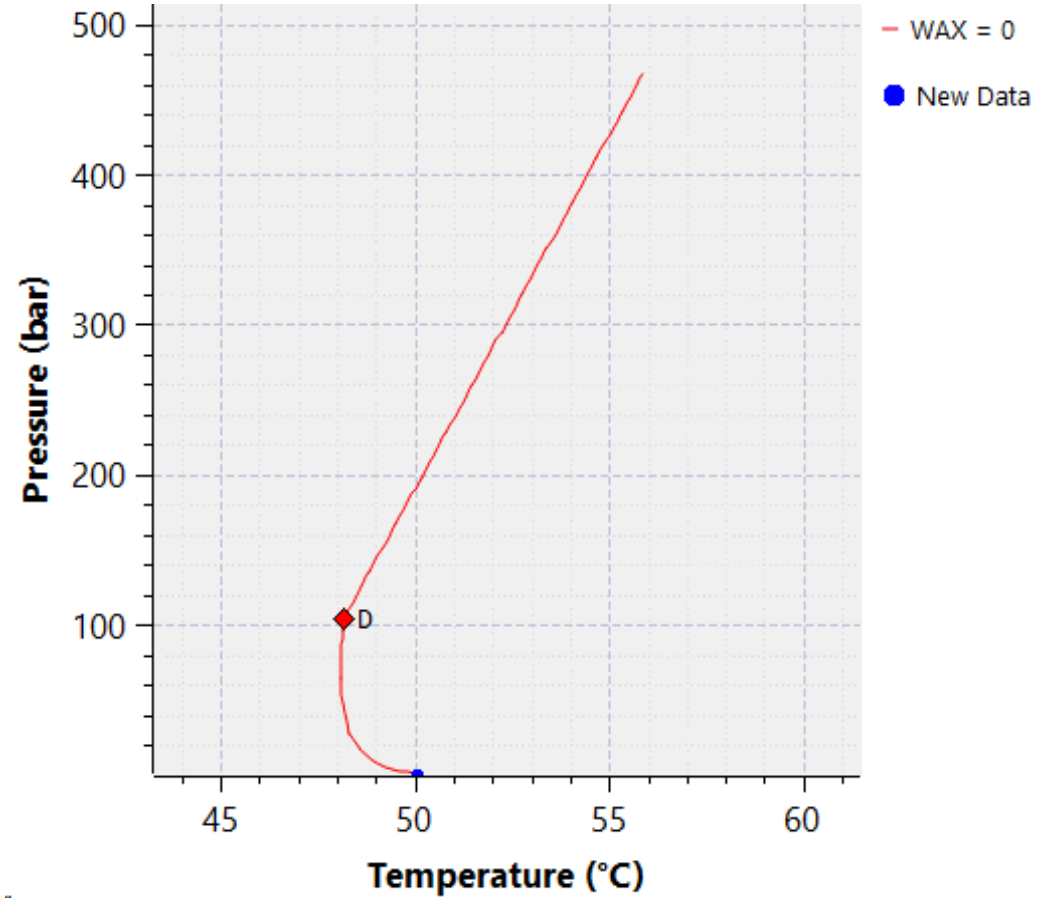

Figure A 20 Wax phase boundary for Fluid 13 calculated by Multiflash

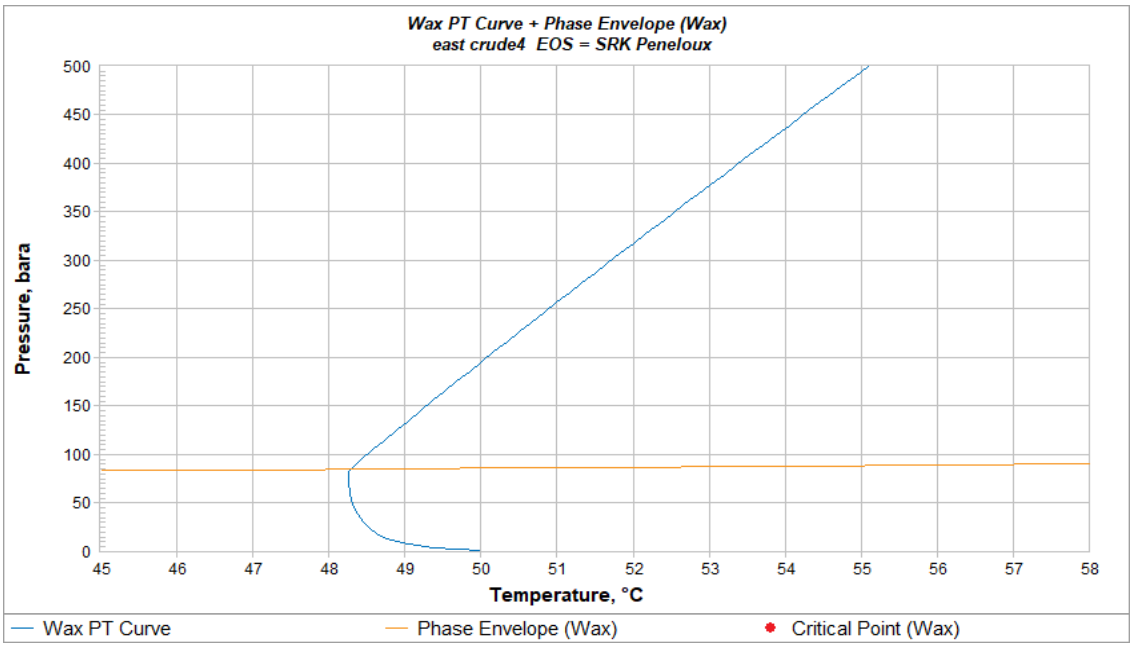

Figure A 21 Wax phase boundary for Fluid 13 calculated by PVTsim

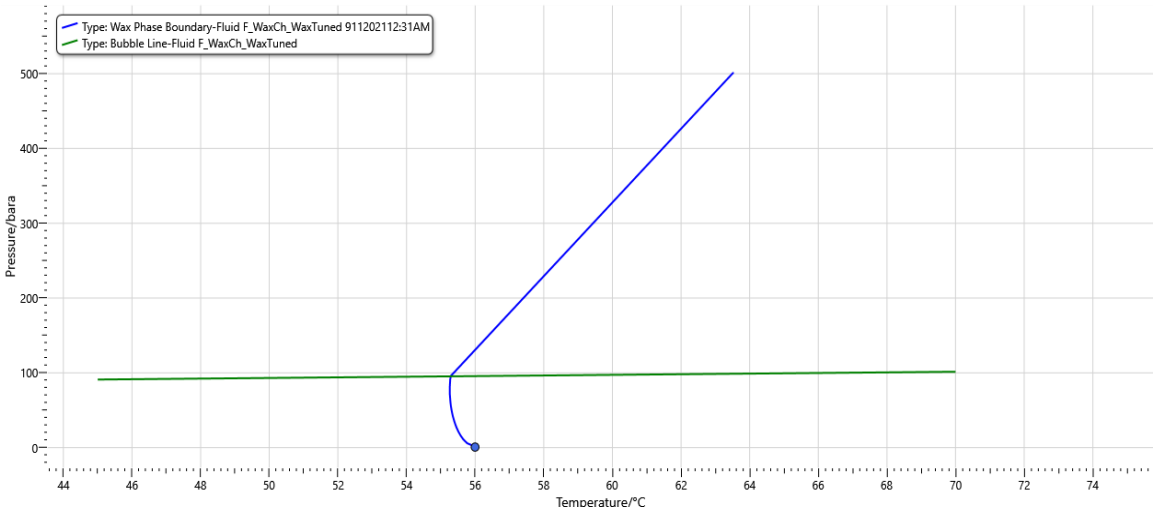

Figure A 22 Wax phase boundary for Fluid 14 calculated by HydraFLASH

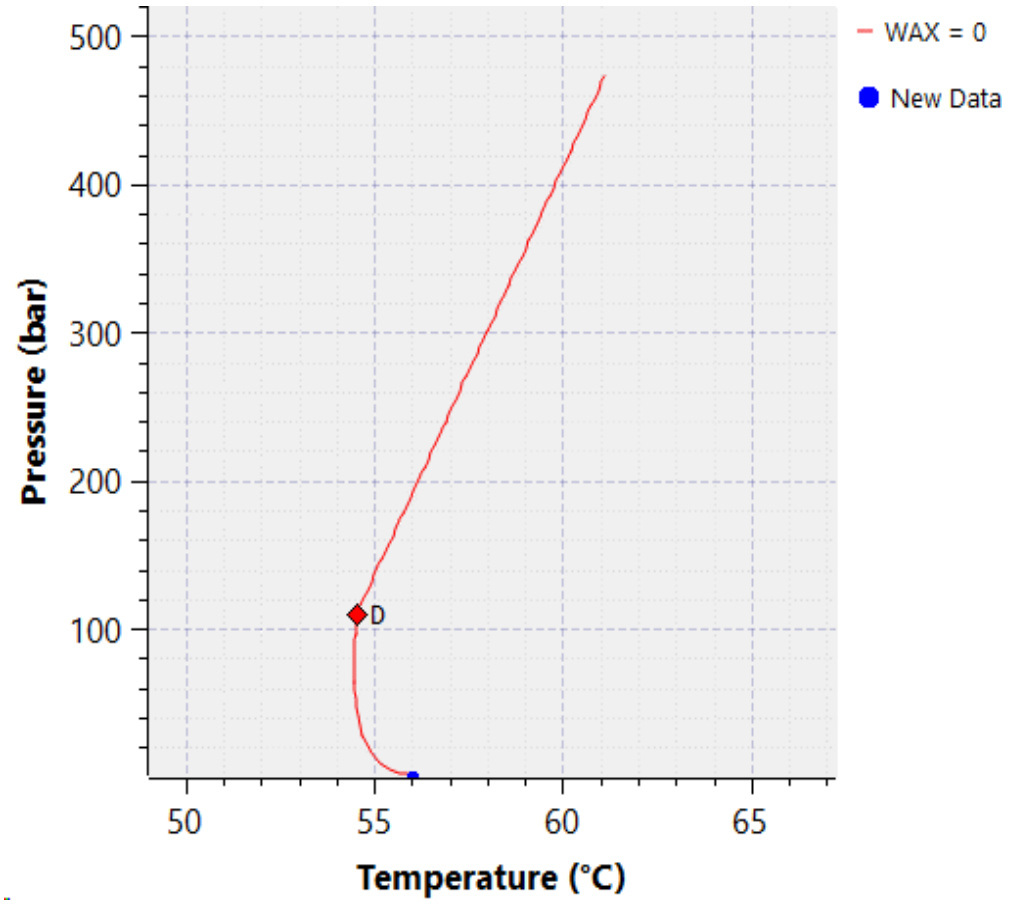

Figure A 23 Wax phase boundary for Fluid 14 calculated by Multiflash

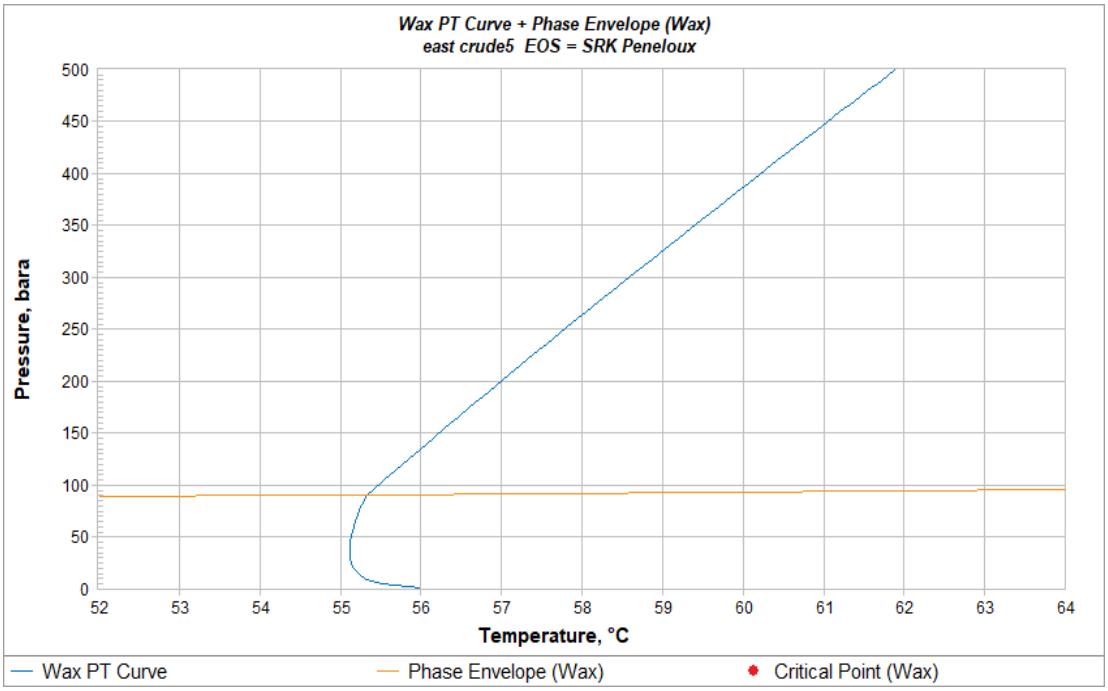

Figure A 24 Wax phase boundary for Fluid 14 calculated by PVTsim

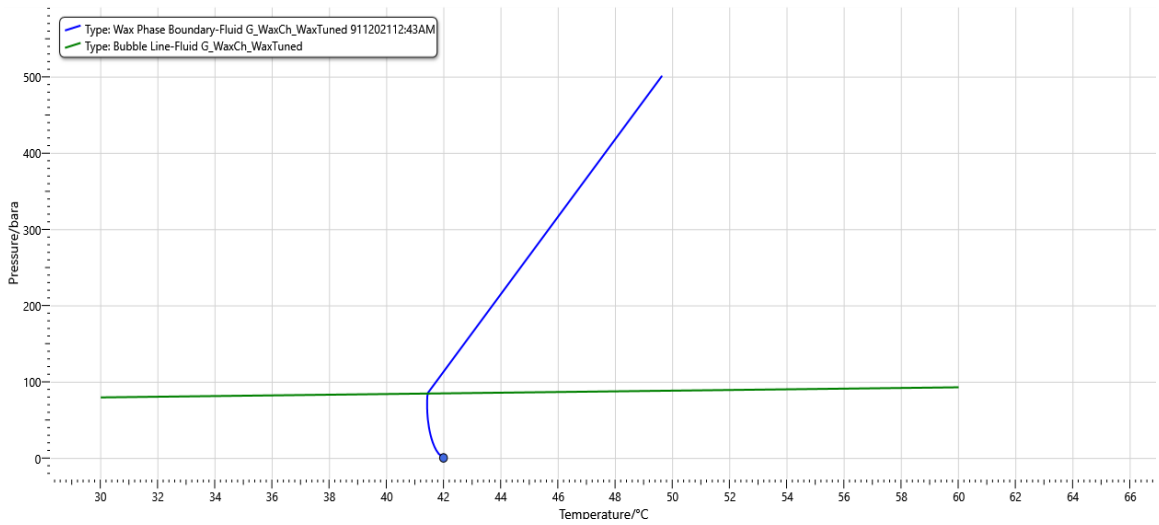

Figure A 25 Wax phase boundary for Fluid 15 calculated by HydraFLASH

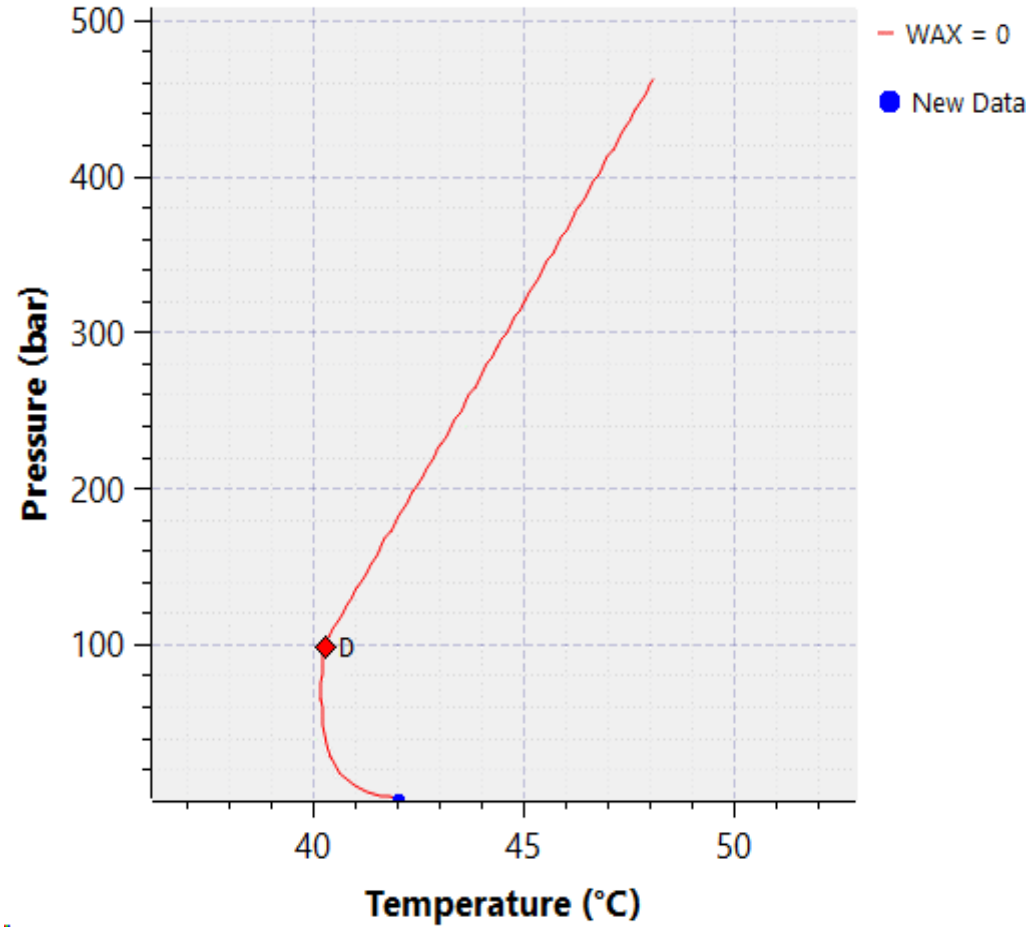

Figure A 26 Wax phase boundary for Fluid 15 calculated by Multiflash

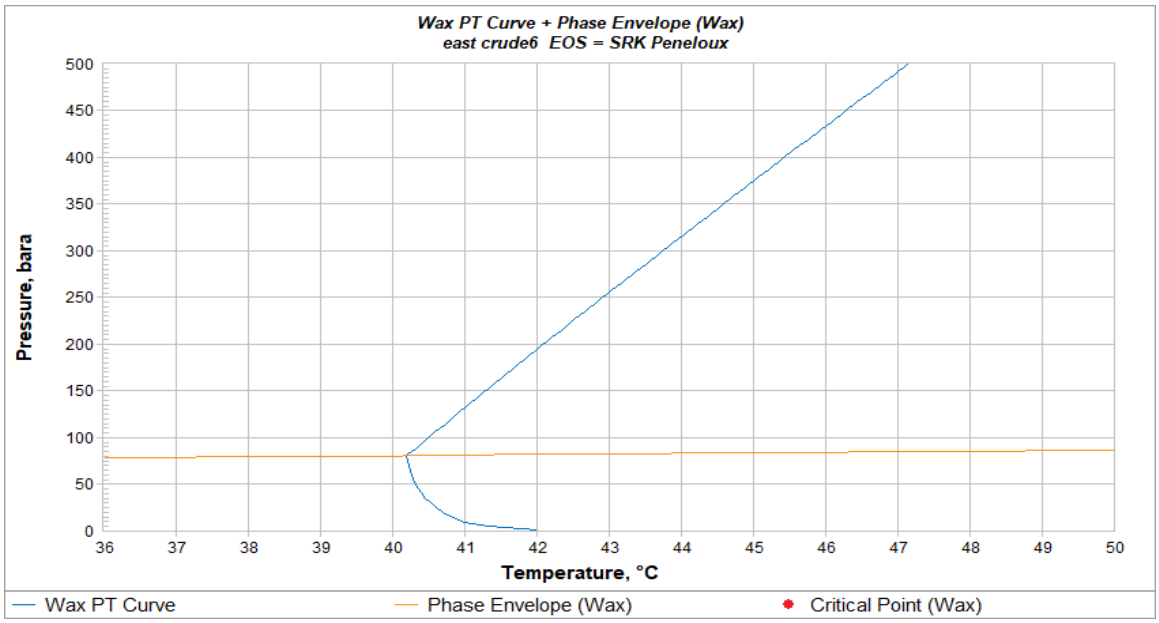

Figure A 27 Wax phase boundary for Fluid 15 calculated by PVTsim

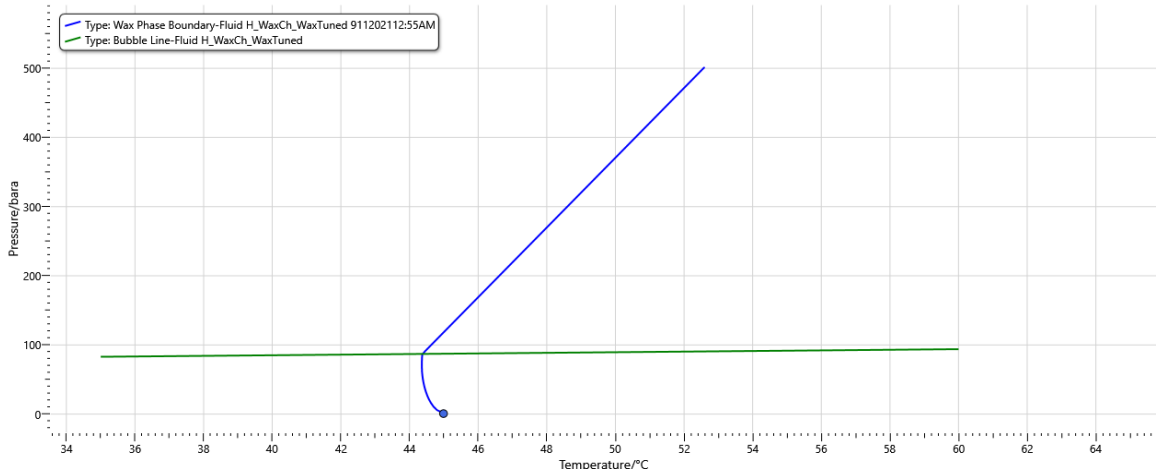

Figure A 28 Wax phase boundary for Fluid 16 calculated by HydraFLASH

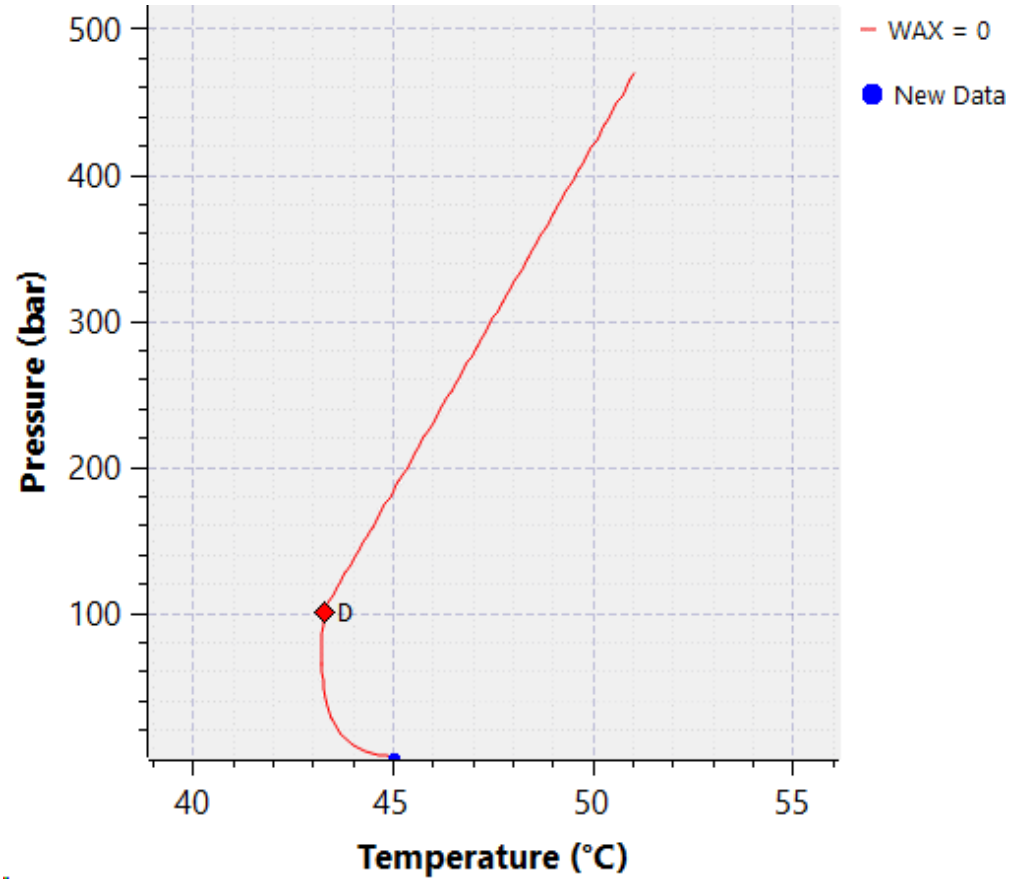

Figure A 29 Wax phase boundary for Fluid 16 calculated by Multiflash

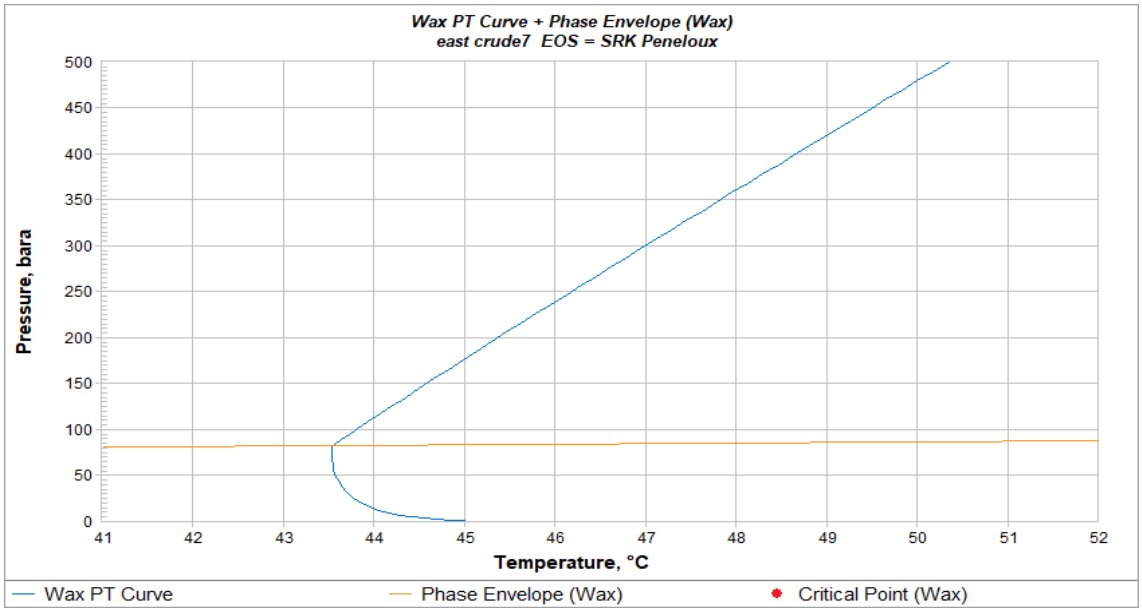

Figure A 30 Wax phase boundary for Fluid 16 calculated by PVTsim